ANNUAL REPORT 2014

理论有机化学与功能分子

教育部重点实验室

工作年报

Key Laboratory of Theoretical Organic Chemistry and Functional Molecule, Ministry of Education

理论有机化学与功能分子
教育部重点实验室工作年报
(2014年)

通讯地址：湖南科技大学理论有机化学与功能分子教育部重点实验室，411201

联系电话：0731-58290097　　传真：58290097

目 录

一、 实验室概况……1

二、 学术交流情况……8

三、 开放基金评审……10

四、 科普传播……11

五、 发表的学术论文……11

1. 主要论文目录……11

2. 部分论文首页……18

一、实验室概况

湖南科技大学理论化学与分子模拟省部共建教育部重点实验室，于 2008 年 11 月经教育部批准立项建设（教育部科技函 [2008]153 号），并以湖南科技大学化学湖南省重点学科和化学（一级学科）、应用化学、化学工艺等硕士点为主要依托进行建设，于 2013 年 7 月通过教育部验收。

实验室主要以《国家中长期科学和技术发展规划纲要》为指导，面向《国家优先发展与重点支持领域》中的环保、新材料与药物等重大战略需求，聚焦环境治理、功能分子材料、药物创制与开发及其分子构效关系的研究，将合成的功能分子材料及药物重点用于环境治理，助推湖南医药产业升级。坚持理论与应用相结合，注重学科交叉，立足地方，瞄准学科前沿，形成四个稳定并具特色的研究方向：分子构效关系，资源环境功能分子材料，光电功能分子材料，生物活性分子与药物。注重微观与宏观相结合、理论与实践相结合，在提升知识创新能力和学术水平的同时，为地方经济建设服务。

通过近5年来的建设与发展，实验室已形成一支结构比较合理、团结协作、具有多学科研究背景的学术队伍。现有研究人员 45 人，其中教授 20 人，副教授 12 人，博士 43 人，博士生导师 4 人，硕士生导师 35 人，国务院政府特殊津贴专家 2 人，教育部新世纪人才 1 人，湖南省“ 杰出青年基金 ”获得者 1 人，湖南省跨世纪学术和技术带头人 1 人，湖南省121人才工程入选者 3 人，湖南省普通高校学科带头人 2 人。外聘湖南科技大学“湘江学者计划”特聘教授 2 人。

5 年来实验室新增科研项目 150 项，其中国家级项目 37 项（国家自科基金项目 35 项、国际合作重点项目 1 项、国家科技支持计划子课题 1 项）、省

部级项目 45 项、横向项目 22 项，新增科研经费累计 3265.6 万元。在 ***Biomaterials, Biosens. Bioelectron., Anal. Chem., Chem. Comm., J. Phys. Chem. B, Org. Lett., J. Org. Chem.***等期刊上共发表论文 500 篇，其中被 SCI 、EI 、ISTP 等收录的论文 270 篇，出版专著 3 部、教材 2 部。获发明专利 40 项（授权），省部级科研奖励 16 项。获湖南省高校科技创新团队 1 个。

实验室面积达 5000 平方米，拥有液质联用仪、核磁共振波谱仪 (500MHz)、X-射线单晶衍射仪、扫描电镜、微量热仪、原子力显微镜、X-粉末衍射仪、圆二色光谱仪、气质联用仪、液相色谱仪等一批先进大型仪器，总值达 4200 余万元。

在实验室的大力支撑下，获批矿业工程博士点和博士后科研流动站。实验室依托化学一级硕士学位授权点、应用化学和化学工艺二级硕士学位授权点进行研究生招生与培养，5 年来共招收硕士研究生 250 人，207 人获得硕士学位。同时还与厦门大学、中南大学、湘潭大学等联合培养研究生， 与中南大学联合博士生 1 人。实验室共有 8 个相关本科专业：化学、无机非金属材料化学、材料化学、应用化学、化工工艺、环境工程、制药工程、能源化工程等，其中化学为国家第一类特色专业，材料化学为省级特色专业。拥有有机化学省级优秀教学团队 1 个，省级精品课程 3 门（有机化学、物理化学和量子化学）。形成了“夯实基础，接触前沿，以培养创新能力为目标” 的人才培模式，确保人才培养质量，获省级教学成果奖 2 项。

1．实验室各研究单元的构成

理论化学与功能分子教育部重点实验室由分子构效关系，生物活性分子与药物，资源环境功能分子材料，光电功能分子材料等 4 个研究单元构成，重点实验室学术带头人和学术骨干名单见下表。

实验室学术带头人和学术骨干一览表

研究方向	姓名	出生年月	获最高学位时间	专业技术职务
分子构效关系	曹晨忠	1957	2004.07(博士)	教授/博士导师
	易平贵	1961	2000.03(博士)	教授/博士导师
	曾荣今	1963	2006.12(硕士)	教授/硕士导师
	周再春	1974	2007.07(博士)	副教授/硕士导师
	袁华	1976	2007.07(博士)	副教授/硕士导师
资源环境功能分子材料	刘立华	1969	2006.07(博士)	教授/硕士导师
	冯涛	1957	1999.07(博士)	教授/博士导师
	戴财胜	1964	2000.07(博士)	教授/硕士导师
	曾坚贤	1970	2008.07(博士)	教授/硕士导师
	周虎	1981	2009.07 (博士)	副教授/硕士导师
光电功能分子材料	黄昊文	1969	2004.08(博士)	教授/硕士导师
	田俐	1973	2009.07 (博士)	教授/硕士导师
	易清风	1963	2001.07(博士)	教授/硕士导师
	龙云飞	1969	2007.12(博士)	教授/硕士导师
	陈建	1980	2009.06 (博士)	副教授/硕士导师
生物活性分子与药物	唐子龙	1967	2004.08(博士)	教授/硕士导师
	谢文林	1967	2003.06(博士)	教授/硕士导师
	李筱芳	1972	2003.06(博士)	教授/硕士导师
	周智华	1973	2007.06(博士)	教授/硕士导师
	于贤勇	1975	2005.07(博士)	副教授/硕士导师

2. 实验室主任及管理人员

实验室主任：曹晨忠

实验室常务副主任：唐子龙

学术秘书：于贤勇，周再春

室务会成员：曹晨忠，易平贵，唐子龙，曾荣今，易清风，曾云龙，于贤勇

3. 实验室学术委员会组成人员

学术委员会主任：郭庆祥

学术委员会副主任：易平贵

学术委员会委员(按姓氏拼音排序)：

曹晨忠，方维海，郭庆祥，胡常伟，黄培强，刘又年，潘远江，唐子龙，吴海龙，吴水珠，肖文精，杨楚罗，杨松，易平贵，易清风，杨新玲，朱晓晴。

4．实验室 2014 年取得成绩

4.1 获得的科研项目

新增各类科研项目 29 项，其中国家自科基金课题 11 项、省部级课题 9 项、横向课题 6 项；累计经费 1187 万元，学校配套经费 389.3 万元，合计 1576.3 万元。

序号	项目编号	项目、课题名称	项目来源	项目起讫时间	科研经费（万元）	负责人
1	21372070	新型 CYP51 抑制剂：硝基苯并噁嗪类化合物的设计合成与构效关系研究	国家自然科学基金项目	2014.01-2017.12	80 (+38)	唐子龙
2	21371054	构型可调的 N-错位卟啉及其手性金属配合物的合成及其与 G-四链体 DNA 的相互作用研究	国家自然科学基金项目	2014.01-2017.12	80 (+38)	李筱芳
3	51378201	功能化有序多孔材料的设计合成及其对重金属离子的吸附性能研究	国家自然科学基金项目	2014.01-2017.12	80 (+38)	刘立华
4	21376070	原位还原法制备碳纳米管负载钯基纳米复合物及其对 C2-C4 醇氧化的电催化活性	国家自然科学基金项目	2014.01-2017.12	80 (+38)	易清风
5	21372069	血红素中 Fe-O2 络合的顺磁性依赖	国家自然科学基金项目	2014.01-2017.12	80 (+38)	周再春
6	51373051	有序纳米孔道交联聚苯乙烯整体材料设计合成与优化	国家自然科学基金项目	2014.01-2017.12	80 (+38)	刘清泉
7	21375036	可控纳米结构表面等离子体共振生物传感器的构建及肝癌早期检测研究	国家自然科学基金项目	2014.01-2017.12	80 (+38)	黄昊文
8	51373002	水分散性荧光聚合物量子点设计合成及多色可调光开关研究	国家自然科学基金项目	2014.01-2017.12	85 (+39)	陈建
9	21301058	光磁双功能纳米晶的可控合成及磁控制发光	国家自然科学基金项目	2014.01-2017.12	24 (+20.3)	刘云新
10	51302080	碳纳米管/磷酸银新型复合光催化剂的制备及在可见光下降解抗生素类污染物的机理研究	国家自然科学基金项目	2014.01-2017.12	25 (+22)	汤建庭

11	51343004	响应性金纳米簇杂化微凝胶的可控制备及性能研究	国家自然科学基金项目	2014.01-2017.12	15 (+18)	廖博
12	NCET-13-0784	稀土钒酸盐纳米材料的调控制备与荧光性能研究	教育部新世纪优秀人才支持计划项目	2014.01-2016.12	50	田俐
13	14JJ5005	利用氟钛酸钾生产含铁废水制备低浓度聚合氯化硫酸铁的关键技术研究	湖南省自然科学基金重点项目	2014.01-2016.12	20 (+5)	曾荣今
14	14JJ5013	印刷电路板微钻孔用功能盖板材料的开发及其应用性能研究	湖南省自然科学基金重点项目	2014.01-2016.12	10 (+5)	周虎
15	14JJ2095	有序纳米孔道交联聚苯乙烯整体材料设计合成优化	湖南省自然科学基金项目	2014.01-2016.12	4 (+2)	刘清泉
16	14JJ3112	嘧啶环 2,5-位取代基交换对嘧啶衍生物物理化学性质的影响规律研究	湖南省自然科学基金项目	2014.01-2016.12	4 (+2)	袁华
17	14JJ3113	高孔隙率 MOFs 的定向构筑与 H_2、CO_2 气体吸附性能研究	湖南省自然科学基金项目	2014.01-2016.12	4 (+2)	郑柏树
18	14JJ2096	用于无膜直接乙醇/空气燃料电池的新型电极材料制备与性能研究	湖南省自然科学基金项目	2014.01-2016.12	4 (+2)	易清风
19	14JJ7054	可控金纳米复合结构表面等离子体共振生物传感器的构建研究	湖南省自然科学基金项目	2014.01-2016.12	1	黄昊文
20	2014FJ3048	重组酶与碳纳米管及石墨烯复合纳米材料界面的制备及传感应用	湖南省科技计划项目	2014.05-2015.05	5 (+2)	邓克勤
21	湘财采计[2014G]0756	氟钛酸钾生产线含铁废水综合利用技术的研发与应用	湖南省环保科技重点招标项目	2014.11-2017.12	50	曾荣今
22	14A052	三维导电网络结构 $LiMnBO_3$/科琴黑复合材料的制备及电化学性能研究	湖南省教育厅重点项目	2014.06-2017.12	8 (+2)	唐安平
23	14B064	PCB 精密钻孔用复合型盖板材料的制备与性能研究	湖南省教育厅优秀青年项目	2014.09-2017.12	5 (+2)	周虎
24	D114D4	低成本、小孔径润滑铝基盖板技术开发	深圳市柳鑫实业有限公司	2014.11-2020.11	100	周虎
25	D11455	聚乙烯醇衍生的光电材料的合成研究	湖南湘维有限公司	2014.10-2016.11	100	陈建
26	D114A1	PCB 微钻孔用吸热与润滑型铝基盖板的生产技术	深圳市柳鑫实业有限公司	2014.10-2033.11	10	周虎
27	D114B9	粉煤灰制备多孔硅酸钙吸附 VOC 技术研究	湖南艾尔希科技发展有限公司	2014.10-2015.06	10	伍泽广

28	D11469	一种以单一乳化剂制备非离子型氧化 聚乙烯乳液的方法	南雄市连邦化工石油科技有限公司	2014.05-2033.04	5	刘清泉
29	D11498	复合型水煤浆添加剂研究	株洲蓝宇环保能源实业有限公司	2014.04-2018.12	80	戴财胜

注：括号内为学校配套经费。

4.2 发表论文

2014 年本实验室共发表SCI论文 60 篇。

4.3 专利

2014年本实验室共申请 8 项发明专利，授权专利 2 项。

序号	专　　利　　名　　称	专利号	专利类型	申请时间	第一完成人
1	一种优化的依达拉奉合成方法	ZL201110282520.2	发明专利	2014-07-23	于贤勇
2	一种钻孔用铝基盖板的制备方法	ZL201110389703.4	发明专利	2014-06-04	周虎
3	一种由聚丙烯、尼龙 6 和氧化石墨烯组成的高性能复合材料及其制备方法	201410753487.0	发明专利	2014-12-11	欧宝立
4	一种石墨烯接枝聚酰胺 6 纳米复合纤维的制备方法	201410733420.0	发明专利	2014-12-06	欧宝立
5	一种硅酸钙/聚烯烃复合材料的制备方法	201410712411.3	发明专利	2014-11-30	周智华
6	一种适于工业生产 3-吗啉酮的制备方法	201410696806.9	发明专利	2014-11-28	伍泽广
7	一种快速制备石墨烯/硫化银量子点纳米复合材料的方法及产品	201410672172.3	发明专利	2014-11-22	易清风
8	一种检测葡萄糖和铜的含量的方法及其应用	201410371264.8	发明专利	2014-07-31	欧宝立
9	一种利用无机膜过滤生产油剂型铝粉颜料的方法及其装置	201410330874.3	发明专利	2014-07-09	黄昊文
10	一种表面皱褶明胶/透明质酸复合微球的制备方法	201410071174.7	发明专利	2014-03-01	曾坚贤

4.4 学科建设与人才培养

2014 年本实验室获批湖湘英才 1 人。共招收 38 名硕士研究生，30 名研究生获得硕士学学位。

4.5 获奖情况

2014获省部级以上科研成果奖 1 项。

序号	项目名称	完成人	单位	获奖时间	获奖名称、等级	发证机关
1	高效水处理材料及新型高级氧化技术研究基础	郑怀礼、李风亭、赵纯、张冰如、张智、吴胜举、张鹏、吴一楠、朱国成	湖南科技大学	2014.09	教育部高等学校自然科学二等奖	教育部

二、学术交流情况

2014 年主办的学术会议。

学术会议名称	时间	参加总人数
湖南省化学化工学会 2014 年学术年会	2014.11.01-2014.11.02	300

2014 年实验室人员参加国内外学术会议统计情况如下。

参会人	时间	地点	会议名称	主（承）办单位
周智华	20141102	湖南师范大学	第四届湖南省高分子科学与技术研讨会	湖南省化学化工学会
刘万强	20141115	湘潭大学	湖南省化学化工学会物理化学专业委员会 2014 年学术研讨会	湖南省化学化工学会

唐安平	20141115	湘潭大学	湖南省化学化工学会物理化学专业委员会 2014 年学术研讨会	湖南省化学化工学会
唐子龙	20140814	南开大学	第二届全国化学键及应用学术会议	中国化学会
李大塘	20140524	长沙学院	2014 湖南省无机化学及应用化学学术暨教学研讨会	湖南省化学化工学会
刘国清	20141101	海口	第六届泛珠三角（“9+2”）化工专业本科教学工作会议	第六届泛珠三角（“9+2”）化工专业本科教学工作会议
刘国清	20141211	汕头	2014 年第三期工程教育专业认证培训研讨会	教育部高等教育教学评估中心
于贤勇	20141016	上海大学	全国第十一届有机合成化学学术研讨会	中国化学会
谢文林	20141016	上海大学	第十一届有机合成化学学术研讨会	中国化学会
焦银春	20141016	上海大学	第十一届有机合成化学学术研讨会	中国化学会
易清风	20140727	海南师范大学	第十四届全国有机电化学与工业学术会议	中国电化学会
唐安平	20140314	上海	2014 Electrochemical Conference on Energy & the Environment	美国电化学会 中国电化会
龙云飞	20141015	重庆	第八届海峡两岸分析化学学术会议	中国化学会
周再春	20140719	南开大学	第二届全国化学键及应用学术研讨会	中国化学会
刘立华	20140821	成都	2014 年中国环境科学学会学术年会	中国环境科学学会
周虎	20140721	成都	第十届全国皮革化学品会议	中国皮革协会

2014 年来访人员学术报告情况

姓名	**职称**	**单位**	**报告题目**	**时间**
吴明姆	教授	中山大学	稀土光电纳米材料的外延和拓扑生长	20140311

陈波	教授	湖南师范大学	敞开式质谱技术研究及应用	20141102
徐昕	教授	复旦大学	NOx storage mechanism on NSR catalysts	20141103
王建秀	教授	中南大学	疾病标志物检测的方法学研究及纳米材料的合成与相关应用	20140530
王平山	教授	中南大学	全共轭三联吡啶金属有机大环分子自组装及其光电转化性能	20140530
唐亮	教授	美国德克萨斯大学	Label free, multiplexed plasmonic biochip	20140619
雷爱文	教授	武汉大学	One or Two Electron Redox - Radical Oxidative Coupling and Mechanism Revealed by Operando XAS, IR	20140505
张海良	教授	湘潭大学	侧链液晶高分子的反思与设计合成	20141102

三、开放基金评审

2014年度理论化学与分子模拟省部共建教育部重点实验室开放基金

编号	姓名	题　　目	经费/万元	申报人所在单位
1	彭洪亮	低温燃料电池碳基催化剂的应用与理论研究	1.5	华南理工大学
2	王宏青	N-（1,3,4-噻二唑基）-苯并噁嗪（硫酮）类化合物的合成及其杀菌活性	2	南华大学
3	方正军	芳基希夫碱分子内二面角对光谱性能的影响	1.5	湖南工程学院
4	汪朝旭	胍盐类离子液体中若干重要离（分）子间相互作用的理论研究	2	湖南科技大学
5	肖秋国	负热膨胀材料 $ZrWMoO_8$ 与改性聚四氟乙烯复合材料的研究	1.5	湖南科技大学
6	邓克勤	碳纳米材料与重组酶构筑有序纳米界面及生物传感研究	1.5	湖南科技大学

四、科普传播

2014.06.05-2014.06.07（3 天)和2014.10.10-2014.10.12（3 天)作为实验室科普固定开放日，共接收 80 余人来实验室参观学习。本年度科普宣讲，累计参与公众 100 余人次；发表科普文章 1 篇。

五、2014年发表的主要研究论文

理论化学与分子模拟省部共建教育部重点实验室 2014 年所发论文目录

1. Bin Liu, Hailin Cong, Xiaofang Li, Bing Yu, Lipiao Bao, Wenting Cai, Yunpeng Xie, Xing Lu. Highly Regioselective 1, 3-Dipolar Cycloaddition of Diphenylnitrilimine to $Sc_3N@/_{h}\text{-}C_{80}$ Affording a Very Stable, Unprecedented Pyrazole-Ring Fused Derivative of Endohedral Metallofullerenes. ***Chemical Communications*** 2014, 50, 12710-12713.
2. Hanwen Liu, Wenchou Pei, Zilong Tang, Yunhui Zhao. Synthesis of Thioureas Containing Thiadiazole. ***Chemical Journal and Chinese Universities-Chinese*** 2014, 35, 511-517.
3. Yunhui Zhao, Xinfang Ren, Hanwen Liu, Zilong Tang. Study on Synthesis and Ortho-Hydroxyl Aromatic N-Tert-Butylsulfinyl Imines Under Microwave Irradiation. ***Chinese Journal and Organic Chemistry*** 2014, 34, 1218-1221.
4. Xiaoyun Yuan, Huiyan Kuang, Lei Feng, Haowen Huang, Chunran Tang, Yunlong Zeng. Determination of Moroxydine Residue in Tomatoes Using CdTe Quantum Dots as Fluorescence Probes. ***Chinese Journal of Analytical Chemistry 2014, 42, 1057-1060.***
5. Jianxian Zeng, Qiannan Guo, Zhenzhong Ou-Yang, Hu Zhou, Huajun Chen. Chromium (VI) Removal from Aqueous Solutions by Polyelectrolyte-Enhanced Ultrafiltration with Polyquaternium. ***Asia-Pacific Journal of Chemical Engineerng*** 2014, 9, 248-255.
6. Wenlin Xie, Shimin Xie, Ying Zhou, Xufu Tang, Jian Liu, Wenqian Yang, Minghua Qiu. Design and Synthesis of Novel 5, 6-Disubstituted Pyridine-2, 3-Dione-3-Thiosemicarbazone Derivatives as Potential Anticancer Agents European Journal of Medicinal Chemistry 2014, 81, 22-27.

7. Bin Liu, Xiaofang Li, Justyna Maciołek. Marcin StępieńPiotr J. Chmielewski. Regioselective internal Carbonylation of the 2 Aza-21- Carbaporphyrin, Access to Configurationally Stable Chiral Porphyrinoids. ***The Journal of Organic Chemistry*** 2014, 797, 3129-3139.
8. Xianyong Yu, Lin Deng, Hongwen Tao, Bingfei Jiang, Xiaofang Li. NMR and Theoretical Study on The Coordination interaction Between Peroxovanadium(V) Complexes and 5-Amino-1, 10-Phenanthroline. ***Journal of Coordination Chemistry*** 2014, 67, 315-322.
9. Qingquan Liu, Zhe Tang, Baoli Ou, Lihua Liu, Zhihua Zhou, Shaohua Shen, Yinxiang Duan. Design, Preparation, and Application of Ordered Porous Polymer Materials. ***Materials Chemistry and Physics*** 2014, 144, 213-225.
10. Chunxiang Li, Xiyang Qiu, Keqin Deng, Zhaohui Hou. Electrochemical Co-Reduction Synthesis of Au/Ferrocene-Graphene Nanocomposites and Their Application in An Electrochemical Immunosensor of a Breast Cancer Biomarker. ***Analytical Methods-Uk*** 2014, 6, 9078-9084.
11. Zhihua Zhou, Liujiao Xiang, Baoli Ou, Tianlong Huang, Hu Zhou, Wennan Zeng, Lihua Liu, Qingquan Liu, Yanmin Zhao, Siliang He, Huihua Huang. Biological Assessment *in vivo* of Gel-HA Scaffold Materials Containing Nano-Bioactive Glass for Tissue Engineering. ***Journal of Macromolecular Science Part A, Pure and Applied Chemistry*** 2014, 51, 572-576.
12. Zhihua Zhou, Jiahui Chen, Cheng Peng, Tianlong Huang, Hu Zhou, Baoli Ou, Jian Chen, Qingquan Liu, Siliang He, Dafu Cao, Huihua Huang, Liujiao Xiang. Fabrication and Physical Properties of Gelatin/Sodium Alginate/Hyaluronic Acid Composite Wound Dressing Hydrogel. ***Journal of Macromolecular Science, Part A, Pure and Applied Chemistry*** 2014, 51, 318-325.
13. Zhihua Zhou, Huihua Huang, Tianlong Huang, Cheng Peng, Baoli Ou, Hu Zhou, Wennan Zeng, Qingquan Liu, Zhongmin yang, Liujiao Xiang, Siliang He. Influences of Molecular Weight and Content of Polyethylene Glycol on Morphology and Size of Nano-Bioactive Glass. ***Journal of Macromolecular Science, Part A, Pure and Applied Chemistry*** 2014, 51, 522-526.
14. Qian Zhao, Shenna Chen, Lingyang Zhang, Haowen Huang, Fengping Liu, Xuanyong Liu. Synthesis of Biocompatible Auags/Ag_2S Nanoclusters and Their Applications in Photocatalysis and Mercury Detection. ***Journal of Nano Research*** 2014, 16, 2793-2803.

15. Qian Zhao, Shenna Chen, Haowen Huang , Fengping Liu, Youtao XieVersatile Sensitive Localized Surface Plasmon Resonance Sensor Based On Core-Shell Gold Nanorods for The Determination of Mercury(II) and Cysteine. ***Analytical Letters*** 2014, 47, 295-308.
16. Baoli Ou, Rao Huang, Wenyun Wang, Hu Zhou, Cong He. Preparation of Conductive Polyaniline Grafted Graphene Hybrid Composites Via Graft Polymerization at Room Temperature. ***RSC Advances*** 2014, 4, 43212-43219.
17. Jianting Tang, Datang Li, Zhaoxia Feng, Zhen Tan, Baoli Ou. A Novel $AgIO_4$ Semiconductor with Ultrahigh Activity in Photodegradation of Organic Dyes, insights into The Photosensitization Mechanism. ***RSC Advances*** 2014, 4, 2151–2154.
18. Qingquan Liu, Zhe Tang, Minda Wu, Zhihua Zhou. Design, Preparation and Application of Conjugated Microporous Polymers. ***Polymer International*** 2014, 63, 381-392.
19. Baoli Ou, Zhihua Zhou, Qingquan Liu, Bo Liao, Yan Xiao, Juncheng Liu, Xin Zhang, Duxin Li, Qiuguo Xiao, Shaohua Shen. Mechanical Properties and Nonisothermal Crystallization Kinetics of Polyamide 6/Functionalized TiO_2 Nanocomposites. ***Polym Composite*** 2014, 35, 294-300.
20. Hexiu Liu, Ruilin Man, Baishu Zheng, Zhaoxu Wang, Pinggui Yi. Insight into Capture of Greenhouse Gas (CO_2) based on Guanidinium Ionic Liquids. ***Chinese Journal of Chemical Physics*** 2014, 27, 144-148.
21. Bo Hou, Pinggui Yi, Zhaoxu Wang, Shuqun Zhang, Jinhua Zhao, Ricardo L. Mancera, Yongxian Cheng, Zhili Zuo Assignment of Aromaticity of the Classic Heterobenzenes by Three Aromatic Criteria. ***Computational and Theoretical Chemistry*** 2014, 1046, 20-24.
22. Kai Liang, Qingquan Liu, Yue Ding Removal of Methyl Violet and Cationic Gold Yellow from Aqueous with Porous Magnetic Polymer Microspheres and its Adsorption. ***Polymers & Polymer Composites*** 2014, 22, 809-816.
23. Lei Feng, Huiyan Kuang, Xiaoyun Yuan, Haowen Huang, Shoujun Yi, Tianlun Wang, Keqin Deng, Chunran Tang, Yunlong Zeng A Novel Method for Aqueous Synthesis of CdTe Duantum Dots. ***Spectrochimica Acta Part a-Molecular and Biomolecular Spectroscopy*** 2014, 123, 298-302.

24. Liting Du, Shilong Yang, Li Xu, Huihua Min, Baishu Zheng. Highly Selective Carbon Dioxide Uptake by a Microporous Kgm-Pillared Metal-Organic Framework with Acylamide Groups. ***Crystengcomm*** 2014, 16, 5520-5523.
25. Qian Zhao, Shenna Chen, Lingyang Zhang, Haowen Huang, Yunlong Zeng, Fengping Liu. Multiplex Sensor for Detection of Different Metal Ions Based on On–Off of Fluorescent Gold Nanoclusters. ***Analytica Chimica Acta*** 2014, 852, 236-243.
26. Anping Tang, Jie Shen, Yongjun Hu, Guorong Xu, Donghua He, Qinfeng Yi, Ronghua Peng. Electrochemical Performance of A-Livopo4/Carbon Composite Material Synthesized by Sol–Gel Method. ***Journal of The Electrochemical Society*** 2014, 161, A10-A13.
27. Hu Zhou, Ruiping Xun, Zhihua Zhou, Qingquan Liu, Peng Wu, Kejian Wu. Preparation of Collagen Fiber/$CaCO_3$ Hybrid Materials and Their Applications in Synthetic Paper. ***Fibers and Polymers*** 2014, 15, 519-524.
28. Qian Zhao, Shenna Chen, Haowen Huang, Lingyang Zhang, Linqian Wang, Fengping Liu, Jian Chen, Yunlong Zeng, Paul K. Chu. Colorimetric and Ultra-Sensitive Fluorescence Resonance Energy Transfer Determination of H_2O_2 and Glucose by Multi-Functional Au Nanoclusters. ***Analyst*** 2014, 139, 1498-1503.
29. Hexiu Liu, Ruilin Man, Zhaoxu Wang, Pinggui Yi, Jingjing Liu. Theoretical Investigation on the Interplay of Hydrogen Bond and Halogen Bond in HX Center Dot Center dot Center Dot(BrCl)(n) (X = F, Cl, Br and n = 1, 2) Complexes. ***Journal of Theoretical & Computational Chemistry*** 2014, 13, 1450001.
30. Xianyong Yu, Zhixi Liao. Bingfei Jiang. Lingyi Zheng, Xiaofang Li. Study on the interaction Between Carbonyl-Fused N-Confused Porphyrin and Bovine Serum Albumin by Spectroscopic Techniques. ***Spectrochimical Acta Part A*** 2014, 133, 372-377.
31. Zhixi Liao, Xianyong Yu, Qing Yao, Pinggui Yi Interaction Between Pirenoxine and Bovine Serum Albumin in Aqueous Solution. ***Spectrochimical Acta Part A*** 2014, 129, 314-319.
32. XinYan Hou, Shu Chen, Jian Tang, Yunfei Long. Visual Determination of Trace Cysteine Based on Promoted Corrosion of Triangular Silver Nanoplates by Sodium Thiosulfate. ***Spectrochimical Acta Part A*** 2014, 125, 285-289.

33. Lihua Liu, Yanhong Li, Xing Liu, Zhihua Zhou Yulin Ling. Chelating Stability of An Amphoteric Chelating Polymer Flocculant With Cu(II), Pb(II), Cd(II). ***Spectrochimical Acta Part A*** 2014, 118, 765-775.
34. Hu Zhou, Bin Yu, Ruiping Xun, Ning Li, Kejian Wu, Hanzhou Sun, Zhihua Zhou. Novel Temperature-Sensitive and Ph-Sensitive Polyurethane Membranes, Preparation and Characterization Asia-Pacific. ***Journal of Chemical Engineering*** 2014, 10, 193-200.
35. Xinyan Hou, Shu Chen, Jian Tang, Yuan Xiong, Yunfei Long. Silver Nanoplates Based Colorimetric Iodide Recognition and Sensing using Sodium Thiosulfate as a Sensitizer. ***Analytica Chimica Acta*** 2014, 825, 57-62.
36. Zhihua Zhou, Siliang He, Baoli Ou, Tianlong Huang, Wennan Zeng, Lihua Liu, Qingquan Liu, Jian Chen, Yanmin Zhao, Zhongmin yang, Dafu Cao. Influence of Nano-Bioactive Glass (NBG) Content on Properties of Gelatin-Hyaluronic Acid/NBG Composite Scaffolds, Journal of Macromolecular Science.***Journal of Macromolecular Science, Part B, Physics*** 2014, 53, 1145-1155.
37. Hu Zhou, Ruiping Xun, Qingquan Liu, Haojun Fan, Yuansen Liu. Preparation of Thermal and pH Dually Sensitive Polyurethane Membranes and Their Properties. ***Journal of Macromolecular Science Part B*** 2014, 53, 398-411.
38. Yunhui Zhao, Hanwen Liu. Asymmetric Synthesis of Novel Vicinal Amino Alcohols via Intramolecular Ketone-N-Sulfinylimine Pinacol-Type Reductive Coupling Promoted by S_mI_2. ***Synthetic Communications*** 2014, 44, 1012-1018.
39. Xianyong Yu, Lin Deng, Baishu Zheng, Birong Zeng, Pinggui Yi, Xin Xu. A Spectroscopic Study on The Coordination and Solution Structures of the interaction Systems Between Biperoxidovanadate Complexes and The Pyrazolylpyridine-Like Ligands. ***Dalton Transactions*** 2014, 43, 1524-1533.
40. Baishu Zheng, Xiu lin, Zhaoxu Wang, Ruirui Yun, Yanpeng Fan, Mingsheng Ding, Xiaolian Hu, Pinggui Yi. Enhanced Water Stability of a Microporous Acylamide-Functionalized Metal-Organic Framework Via interpenetration and Methyl Decoration. ***Crystengcomm*** 2014, 16, 9586-9589.

41. Xianyong Yu, Zhixi Liao, Qing Yao, Heting Liu, Wenlin Xie Spectroscopic Studies on the interaction of Phacolysin and Bovine Serum Albumin. ***Spectrochimical Acta Part A*** 2014, 127, 231-236.
42. Shu Chen, Lin Zhang, Yunfei Long, Feimeng Zhou Electroanalytical Sensors and Methods for Assays and Studies of Neurological Biomarkers. ***Electroanal*** 2014, 26 1236-1248.
43. Xianyong Yu, Zhixi Liao, Heting Liu, Xiaofang Li, Pinggui Yi The investigation of the interaction Between Tropicamide and Bovine Serum Albumin by Spectroscopic Methods. ***Spectrochimical Acta Part A*** 2014, 118, 331-336.
44. Xiaofang Li, Haochong Liu, Aiting Zheng, Zhikui Li, Xianyong Yu, Pinggui Yi. One-Pot Synthesis of Novel Spiro Pyrano[2,3-D][1,3]Thiazolo[3,2-A]Pyrimidine Derivatives. ***Synthetic Communications*** 2014, 44, 1414-1421.
45. Qingquan Liu, Zhe Tang, Zhihua Zhou, Hu Zhou, Baoli Ou, Bo Liao, Shaohua Shen, Lijuan Chen. A Novel Route to Prepare Cationic Polystyrene Latex Particles with Monodispersity. ***Journal of Macromolecular Science Part A*** 2014, 51, 271-278.
46. Junfeng Xiang, Pinggui Yi, Zhiyong Ren, Xianyong Yu, Jian Chen, Wu Liu, Taomei Li. Effect of Supra-Molecular Interaction on the Intramolecular Proton Transfer of 2-(2-Aminophenyl)benzothiazole. ***Acta Physico-Chimica Sinica*** 2014, 32, 624-630.
47. Linyan Wang, ChaoTun Cao, Chenzhong Cao. An Attempt of Molecular Design and Synthesis of 3, 4′4, 3′-Disubstituted Benzylideneanilines With Specified UV–Vis Absorption Maximum Wavelength. ***Journal of Physical Organic Chemistry*** 2014, 27, 818-822.
48. Pinggui Yi, Jin Liu, Jian Chen, Xianyong Yu, Xiaofang Li, Baishu Zheng, Hongwen Tao, Yanlei Hao. Study on Proton Transfer of 2-(2'-Hyhroxyphenyl)imidazo[1,2-a]pyridine with Cucurbit[7]uril by Spectroscopic Methodology Chemical. ***Journal of Chinese Universities*** 2014, 35, 1219-1223.
49. Xiao Dong Xia, HaoWen Huang. Using Unmodified Au Nanoparticles as Colorimetric Probes for TNT Based on Their Competitive Reactions with Melamine. ***Chinese Chemical Letters*** 2014, 25, 1271-1274.
50. 曾坚贤，陈华俊，刘国清，喻谢，钱朝辉. Cu^{2+}印迹壳聚糖/Al_2O_3的制备及动态吸附性能. ***化学工程*** 2014, 42, 22-27.

51. 袁华，卢永志. 分子结构对羧酸酯亲核取代反应速率的定量影响规律. ***湖南科技大学学报*** 2014, 4, 98 -103.

52. 王 恋，唐子龙，王宏清，王岭帅，焦银春. 邻氨基苯甲醇烷基化反应合成2-(2-羟甲基苯基氨基)乙酰芳胺. ***精细化工中间体*** 2014, 4, 35-39.

53. 李春香，邱喜阳，周建红，邓克勤. 电化学法制备电还原的氧化石墨烯-铁氰化镍修饰电极检测亚硝酸根. ***分析试验室*** 2014, 33, 1241-1244.

54. 贺冬华，唐安平，申洁，徐国荣，刘立华，令玉林. 锂离子电池电极材料磷酸氧钒锂的研究进展. ***应用化学*** 2014, 31, 1115-1122.

55. 唐子龙，夏赞稳，陆良秋. $FeCl_3.6H_2O$催化合成2, 3-二取代-1, 3-苯并噁嗪及其杀菌活性. ***华中科技大学学报***（自然科学版）2014, 3, 360-365.

56. 刘立华，李波，唐安平，徐国荣 溶胶－凝胶自蔓延燃烧法制备铜铬黑颜料及表征. ***湖南科技大学学报（自然科学版）***2014, 29, 91-97.

57. 石顺存，龙云飞，邓春凤，喻娟娟，康玉佳. 咪唑啉季铵盐与fsDNA作用的共振光散射光谱及分析应用. ***湖南科技大学学报(自然科学版)*** 2014, 29, 98-102.

58. 徐百元，易平贵，汪朝旭，于贤勇，刘峥军，侯博，郝艳雷. 2-(2－羟苯基)苯并咪唑-碱(土)金属离子π复合物的电子结构及其分子内质子转移. ***湖南科技大学学报(自然科学版)*** 2014, 29, 89-93.

59. 黄富华，陈建，李亚，曾志强，侯庆杨，丁勇，刘胜利. 一步raft聚合法合成两亲性嵌段共聚物PEG-b-P(St-co-VBC). ***湖南科技大学学报(自然科学版）*** 2014, 29, 108-113.

60. 周虎，寻瑞平，吴科建，周智华，余斌，唐友新 温度和pH双重敏感聚氨酯膜材料的制备及其性能. ***功能高分子学报*** 2014, 27, 419- 425.

ChemComm

COMMUNICATION

View Article Online
View Journal | View Issue

Cite this: *Chem. Commun.*, 2014, **50**, 12710

Received 6th August 2014,
Accepted 1st September 2014

DOI: 10.1039/c4cc06134a

www.rsc.org/chemcomm

Highly regioselective 1,3-dipolar cycloaddition of diphenylnitrilimine to $Sc_3N@I_h$-C_{80} affording a very stable, unprecedented pyrazole-ring fused derivative of endohedral metallofullerenes†

Bin Liu,‡[a] Hailin Cong,‡[b] Xiaofang Li,*[a] Bing Yu,[b] Lipiao Bao,[c] Wenting Cai,[c] Yunpeng Xie[c] and Xing Lu*[c]

Formation of a very stable, unprecedented pyrazole-ring fused derivative of endohedral metallofullerenes was achieved by the first 1,3-dipolar cycloaddition reaction of $Sc_3N@C_{80}$ with diphenylnitrilimine in a highly regioselective manner.

Endohedral metallofullerenes (EMFs), a new family of carbon clusters formed by encapsulation of metallic species inside fullerene cages, have attracted considerable attention during recent years due to their unique structures, special electronic properties and potential applications in nanoscience, organic solar cells and biomedicine.[1–3] Chemical functionalization of EMFs has attracted increasing interest because it is not only helpful in understanding the intriguing properties of EMFs but also of practical significance for producing potentially applicable materials.[4] To date, various approaches have been utilized to modify the outer cage of EMFs, such as disilylation, Diels–Alder reaction, 1,3-dipolar cycloaddition, Bingel–Hirsch reaction, [2+2] cycloaddition with benzyne, [2+1] cycloaddition with carbene, free-radical reaction and so on.[4] Among these methods, 1,3-dipolar cycloaddition is rather attractive and has been widely adopted to synthesize the nitrogen-heterocycle derivatives of EMFs because of its versatility. However, 1,3-dipolar cycloaddition of EMFs reported so far produced exclusively the corresponding derivatives with pyrrolidino-ring fused structures.[5–8] Accordingly, it is desirable to get novel derivatives of EMFs with different heterocycle structures, which may bear unexpected properties.

Nitrilimines, a special kind of reactive dipoles with a linear R-CN-NR structure, can readily undergo 1,3-dipolar cycloaddition with different double bonds of dipolarophiles.[9–11] This is also a powerful tool for the synthesis of various fullerene derivatives with pyrazole rings.[12,13] Since pyrazoles are also a major class of five-membered nitrogen heterocycles found in a wide variety of natural products and drug molecules, such structures have received great interest as a result of their broad range of biological activities.[14,15] The reaction of nitrilimines and C_{60} has been investigated previously,[9,16,17] but nitrilimines have never been used to functionalize EMFs. In this context, for the first time we report the highly regioselective 1,3-dipolar cycloaddition reaction of $Sc_3N@I_h$-C_{80} with diphenylnitrilimine (DPNI, **1**), which is generated *in situ* by dehydrohalogenation of *N*-phenylbenzenecarbohydrazonoyl chloride with triethylamine (Scheme 1).

Under an argon atmosphere, $Sc_3N@C_{80}$ reacted with an excess amount of *N*-phenylbenzenecarbohydrazonoyl chloride (*ca.* 5-fold) in the presence of triethylamine in *o*-dichlorobenzene (*o*-DCB) at elevated temperatures (see the ESI† for Experimental details). The reaction progress was monitored by high performance liquid chromatography (HPLC) and the profiles are shown in Fig. 1. Before reaction, a strong peak corresponding to $Sc_3N@C_{80}$ appeared at 40.6 min (Fig. 1a). After 1 hour (Fig. 1b), a new peak appeared at 19.0 min, which was later assigned as the target product (**2**). The intensity of the adduct peak continued to increase with

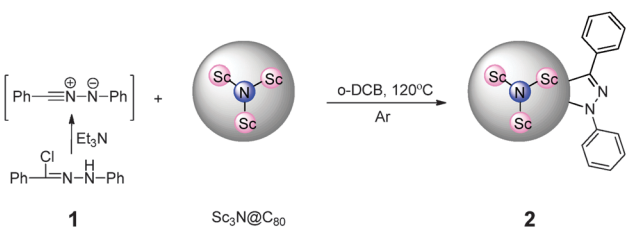

Scheme 1 Reaction between $Sc_3N@C_{80}$ and *N*-phenylbenzenecarbohydrazonoyl chloride in the presence of triethylamine.

[a] *Key Laboratory of Theoretical Chemistry and Molecular Simulation of Ministry of Education, Hunan Province College Key Laboratory of QSAR/QSPR, School of Chemistry and Chemical Engineering, Hunan University of Science and Technology, Xiangtan, Hunan 411201, China. E-mail: lixiaofang@iccas.ac.cn*

[b] *Lab for New Fiber Materials and Modern Textile-Growing Base for State Key Laboratory, College of Chemical and Environmental Engineering, Qingdao University, Qingdao, 266071, China*

[c] *State Key Laboratory of Materials Processing and Die & Mold Technology, School of Materials Science and Engineering, Huazhong University of Science and Technology (HUST), Wuhan 430074, China. E-mail: lux@hust.edu.cn*

† Electronic supplementary information (ESI) available: Experimental procedures, the ^{1}H NMR spectrum and X-ray structures of **2**. CCDC 1014737. For ESI and crystallographic data in CIF or other electronic format see DOI: 10.1039/c4cc06134a

‡ Equal contribution.

Vol.35 高等学校化学学报 No.3
2014 年 3 月 CHEMICAL JOURNAL OF CHINESE UNIVERSITIES 511~517

doi: 10.7503/cjcu20130698

含噻二唑基硫脲类化合物的合成

刘汉文, 裴文丑, 唐子龙, 赵云辉

(湖南科技大学化学化工学院, 理论化学与分子模拟省部共建教育部重点实验室, 湘潭 411201)

摘要 以噻二唑-2-氨甲基酚(**1**)为原料, 与异硫氰酸苯酯反应, 以中等到良好的产率得到噻二唑基 *N*-苯基取代硫脲类化合物(**3**a~**3**i); 而化合物 **1** 与活性较高的 *N*,*N*-二甲胺基硫代甲酰氯反应, 则可以得到—NH 和—OH 同时反应的含有 *N*,*N*-二甲基硫脲和 *N*,*N*-二甲基硫代氨基甲酸芳酯官能团的产物. 利用核磁共振、红外光谱以及高分辨质谱等手段对产物结构进行了表征.

关键词 1,3,4-噻二唑; 硫脲; 异硫氰酸苯酯

中图分类号 O621.3 **文献标志码** A

硫脲类化合物是较早被人们研究的化合物, 其含有 N, S 杂原子的结构特征, 可参与生物体内复杂的反应, 因而普遍具有良好的生物活性. 自 1946 年, Domagk 等[1] 发现苯甲醛缩氨基硫脲具有抗菌活性以来, 关于硫脲的化学和药理学等方面的研究引起人们的关注. 研究表明, 硫脲类化合物具有抗菌、抗肿瘤、抗病毒和抗疟病等多种生物活性[2~6]. 近年文献报道硫脲类衍生物具有抗惊厥、抗脑血管硬化[7,8] 及调节植物生长等功能[9~11]. 1,3,4-噻二唑(又称噻重氮)类化合物含有 "—N═C—S—" 基本骨架[12], 这种结构是构成氢键的良好位点, 也是阴离子的良好作用点, 可与阳离子络合形成配合物, 从而增加药物对生物膜的通透性. 因此, 1,3,4-噻二唑类化合物具有较强的药理活性, 如杀菌和抗肿瘤等[13~17], 它们还具有较好的除草和调节植物生长作用[18,19].

根据生物活性叠加原理[20], 本文将硫脲衍生物结构和 1,3,4-噻二唑五元杂环分子片段叠加, 期望获得具有优良生物活性的化合物.

1 实验部分

1.1 试剂与仪器

异硫氰酸苯酯和 *N*,*N*-二甲胺基硫代甲酰氯(分析纯, Fluka 化学公司); 三乙胺(Et_3N)、氢化钠(NaH)和二甲亚砜(分析纯, 国药试剂公司).

Yanaco MP500 型显微熔点测定仪; Xevo Q-TOF MS 液相色谱-质谱联用仪; Nicolet 5-DX 型傅里叶红外光谱仪(KBr 压片); Bruker AV-II 500 MHz 核磁共振仪.

1.2 实验部分

目标化合物的合成路线如 Scheme 1 所示.

1.2.1 含噻二唑基 *N*-苯基取代硫脲类化合物(**3**)的合成 参照文献[12]方法, 以 2-氨基-5-芳基噻二唑类化合物和 4-羟基苯甲醛为原料, 经加成/脱水、还原两步 "一锅法" 合成噻二唑-2-氨甲基酚 **1**. 将化合物 **1**(10 mmol)和三乙胺(3.03 g, 30 mmol)溶于二甲亚砜(10 mL)中, 室温搅拌下, 缓慢滴加异硫氰酸苯酯(4.05 g, 30 mmol), 10 min 滴加完毕, 升温至 80 ℃搅拌 7 h, 用 TLC 监测反应完毕. 向反应混合物中缓慢加入少量的水淬灭反应, 用乙酸乙酯萃取 3 次, 合并有机相, 用饱和食盐水洗涤, 无水硫酸钠干燥 1 h, 过滤, 浓缩有机溶剂, 粗产物用快速层析柱 [*V*(石油醚) : *V*(乙酸乙酯) = 2 : 1] 提纯, 得

收稿日期: 2013-07-22.

基金项目: 国家科技支撑计划项目子课题(批准号: 2011BAE06B01)和湖南省科学基金(批准号: 11JJ3016)资助.

联系人简介: 刘汉文, 男, 教授, 主要从事有机合成研究. E-mail: hwyliu@126.com

赵云辉, 男, 博士, 讲师, 主要从事有机合成与生物医药材料研究. E-mail: 1060126@hnust.edu.cn

有机化学 DOI: 10.6023/cjoc201401019 研究简报
Chinese Journal of Organic Chemistry NOTE

邻羟基芳香 *N*-叔丁基亚磺酰亚胺的微波合成研究

赵云辉* 任新芳 刘汉文* 唐子龙
([a]湖南科技大学化学化工学院 湘潭 411201)
([b]理论化学与分子模拟省部共建教育部重点实验室 湘潭 411201)

摘要 手性 *N*-叔丁基亚磺酰亚胺是一类非常重要的有机化学合成中间体. 报道以水杨醛类化合物 **1** 和 *N*-叔丁基亚磺酰胺(**2**)为原料, 分别以硫酸氢钾、碳酸铯为促进剂在微波辐射条件下反应, 合成得到 11 种未见文献报道的水杨醛类 *N*-叔丁基亚磺酰亚胺(**3**), 产率中等到良好. 研究发现: 带有强吸电子基的底物在硫酸氢钾的作用下, 产率较高; 而带有强供电子基化合物、取代基位阻大的化合物在碳酸铯的作用下反应效果较好. 所有新化合物均通过红外光谱、核磁共振谱、高分辨质谱对其结构进行了确认.

关键词 微波; 手性亚胺; *N*-叔丁基亚磺酰胺; 水杨醛

Study on Synthesis of *ortho*-Hydroxyl Aromatic *N*-*tert*-Butylsulfinyl Imines under Microwave Irradiation

Zhao, Yunhui* Ren, Xinfang Liu, Hanwen* Tang, Zilong
([a] *School of Chemistry and Chemical Engineering, Hunan University of Science and Technology, Xiangtan 411201, China*)
([b] *Key Laboratory of Theoretical Chemistry and Molecular Simulation of Ministry of Education of China, Human University of Science and Technology, Xiangtan 411201, China*)

Abstract Chiral *N*-*tert*-butanesulfinyl imines have been shown to be important intermediates for asymmetric synthesis in recent years. Eleven new (*R*,*E*)-*N*-(2-hydroxybenzylidene)-*tert*-butyl-sulfinamides (**3**) were synthesized from salicylaldehydes **1** and chiral *tert*-butanesulfinamide **2** under microwave irradiation in moderate to good yields. The reaction could work well in the mixture of $KHSO_4$/PhMe or Cs_2CO_3/CH_2Cl_2. And the results show that the $KHSO_4$/PhMe reaction system is helpful for the salicylaldehydes with electron-donating group; however, the Cs_2CO_3/CH_2Cl_2 reaction system is applicable to the salicylaldehydes with electron-deficient group and steric hindrance group. The structures of these new compounds were determined by ^1H NMR, ^{13}C NMR, IR and HRMS.

Keywords microwave irradiation; chiral imine; (*R*)-*tert*-butylsulfinamide; salicylaldehyde

手性 *N*-叔丁基亚磺酰亚胺是一类非常重要的有机化学中间体. 因该亚胺含有一个手性硫中心和一个潜在的手性碳原子, 而被广泛应用于不对称合成中. 该亚胺其碳氮双键经不对称加成后, 可以合成手性氨[1]、手性支链氨[2,3]、手性氨基酸[4,5]、手性氨基醇[6,7]、手性氨基酮[8,9]、手性氮杂环[10]等小分子化合物; 也可以参与手性生物大分子药物[11~13]的合成. 据报道水杨醛类亚胺是合成苯并呋喃[14,15]、苯并噁嗪[16,17]、苯并恶唑[18]等杂环的重要中间体, 其碳氮双键经不对称还原后形成的邻胺甲基苯酚[19]类化合物是手性金属催化剂的重要配体[20,21].

水杨醛亚胺的传统合成一般在加热条件下进行[22]. 与传统的制备方法相比, 微波法制备有机化合物具有快速、高效、反应条件温和、操作简单易行、能够实现某些用传统方法无法进行的合成反应等优点. 我们拟采用微波的方法, 以水杨醛类化合物 **1** 和手性 *N*-叔丁基亚磺酰胺 **2** 合成一类结构新颖的水杨醛类 *N*-叔丁基亚磺酰亚胺化合物 **3**, 以期其具有更广泛的不对称合成用途.

* E-mail: zhao_yunhui@163.com; hwyliu@126.com
Received January 11, 2014; revised February 12, 2014; published online March 10, 2014.
Project supported by the National Natural Science Foundation of China (No. 21372070), the Science Foundation of Hunan Province (No. 11JJ3016) and the Hunan Provincial Education Office Scientific Research Foundation Project (No. B31314).
国家自然科学基金(No. 21372070)、湖南省科学基金课题(No. 11JJ3016)和湖南省教育厅基金(No. B31314)资助项目.

DOI: 10.11895/j.issn.0253-3820.140054

以碲化镉量子点为荧光探针测定西红柿中残留吗啉胍

元晓云 匡慧艳 冯 磊 黄昊文 唐春然 曾云龙*
(湖南科技大学化学化工学院,理论化学与分子模拟省部共建教育部重点实验室,
分子构效关系湖南省普通高等学校重点实验室,湘潭 411201)

摘 要 利用吗啉胍使 CdTe 量子点荧光增强的特性,建立了西红柿中吗啉胍残留量的检测新方法。研究了影响量子点荧光探针行为的因素,确定最佳工作条件: 量子点浓度为 1×10^{-4} mol/L,pH = 5.6,反应温度为 20 ℃,反应时间为 20 min。在最佳测定条件下,CdTe 量子点荧光探针对吗啉胍响应的线性范围为 1.0×10^{-12} ~ 5.0×10^{-10} mol/L,检出限为 5.2×10^{-13} mol/L,线性相关系数 $R=0.9981$,方法的回收率 97% ~ 106%,常见共存离子、抗生素、维生素等共存物质对吗啉胍的测定不产生干扰。本方法用于西红柿中吗啉胍残留量的测定,结果令人满意。

关键词 吗啉胍; 西红柿; CdTe 量子点; 荧光增强; 荧光探针

1 引 言

吗啉胍 (Moroxydine) 主要用于流感病毒及疱疹病毒感染的治疗,而后吗啉胍又用于防治禽类的禽流感、鸡马立克病等病毒病,并且具有很好的疗效。由于吗啉胍对农作物病害的防治效果也非常好,自 20 世纪 70 年代我国开始用于植物病害的防治以来,吗啉胍用于防治农作物病害的范围越来越广,尤其在蔬菜、水果种植阶段,用量逐渐增大。吗啉胍的广泛大量使用,必然会形成残留。因此,蔬菜水果中吗啉胍残留量的检测已引起人们的高度重视[1]。目前,已有色谱法[2,3]、质谱法[4,5]、滴定法[6]、化学发光法[7]和电化学法[8]等测定吗啉胍的报道。但色谱法灵敏度不够高; 化学发光法的稳定性和重现性较差; 而紫外分光光度法和电化学方法的检测灵敏度和准确度有待提高。因此,需要建立快速测定蔬菜水果中吗啉胍残留量的新方法。量子点优异的光学性质,在分析化学中已得到广泛应用[9~11]。本研究依据吗啉胍增强量子点荧光的性质,建立了测定吗啉胍的新方法。本方法具有灵敏度高、选择性好、操作快速等优点。

2 实验部分

2.1 仪器与试剂

RF-5301 型荧光分光光度计(日本岛津公司); Lambda 35 紫外-可见分光光度计(美国 PerkinElmer 公司)。

TeO_2,$NaBH_4$,氯化隔($CdCl_2\cdot2.5\ H_2O$) CdO,巯基乙酸(TGA),吗啉胍公司(阿拉丁试剂公司); 0.2 mol/L HAc-NaAc 缓冲液,用分析纯醋酸和醋酸钠配制而成; 0.01 mol/L 吗啉胍溶液: 准确称取 0.1038 g 吗啉胍,用水溶解并定容至 50 mL; 其它浓度的吗啉胍溶液均由该浓度稀释而得。所用试剂均为分析纯或优级純; 实验用水均为二次蒸馏水。西红柿购自当地超市。

TGA 修饰的量子点的按照文献[12]方法制备,然后用乙醇沉淀纯化,再超声分散于水中,即得到纯化后的量子点,备用。

2.2 西红柿样品的前处理

西红柿的样品前处理过程参考文献[13]方法并稍作改进: 将新鲜西红柿用组织搅碎机搅碎,于冰柜中冷冻保存备用。称取 25 g 样品(精确至 0.1 g),置于 250 mL 锥形瓶中,加入 50 mL 甲醇,超

2014-01-16 收稿; 2014-03-22 接受
本文系国家自然科学基金(No. 21075035),湖南省高校创新平台开放基金(No. 10k024)资助项目,湖南科技大学优秀硕士学位论文培育项目(No. S130027)和湖南科技大学研究生创新项目(No. S120028)资助
* E-mail: yunlongzeng1955@126.com

ASIA-PACIFIC JOURNAL OF CHEMICAL ENGINEERING
Asia-Pac. J. Chem. Eng. 2014; **9**: 248–255
Published online 28 August 2013 in Wiley Online Library
(wileyonlinelibrary.com) DOI: 10.1002/apj.1764

Research article

Chromium(VI) removal from aqueous solutions by polyelectrolyte-enhanced ultrafiltration with polyquaternium

Jianxian Zeng,[1]* *Qiannan Guo,*[1] *Zhenzhong Ou-Yang,*[1,2] *Hu Zhou*[1] *and Huajun Chen*[1]

[1]*School of Chemistry and Chemical Engineering, Hunan University of Science and Technology, Key Laboratory of Theoretical Chemistry and Molecular Simulation of Ministry of Education, Hunan Province College Key Laboratory of QSAR/QSPR, Xiangtan 411201, China*
[2]*Changsha Environmental Protection College, Changsha 410004, China*

Received 11 May 2013; Revised 25 July 2013; Accepted 2 August 2013

ABSTRACT: Polyelectrolyte-enhanced ultrafiltration was investigated for the removal of chromium(VI) anion from aqueous solutions with the help of cationic polyquaternium-6 (PQ6). The ultrafiltration behavior of Cr(VI) aqueous solutions was studied at pH 6. Owing to an effect of electrostatic repulsion, the membrane with a molecular weight cutoff (MWCO) of 10 000 Da rejected about 30% of Cr(VI). Then, ultrafiltration of aqueous solutions of a Cr(VI)–PQ6 complex was further studied. Factors affecting Cr(VI) rejection coefficient (R_{Cr}) and permeate flux (J) such as pH, polymer metal ratio (PMR), the added salts, temperature, operating pressure and MWCO were investigated. The best operating parameters, such as pH 9 and PMR 10, were obtained in order to achieve high R_{Cr} (>0.97). By increasing the concentrations of the added salts (KCl, KNO_3 and K_2SO_4), R_{Cr} was found to decrease significantly. J decreases slightly in the pH range of 2–5. Cl^- or SO_4^{2-} does not affect J, whereas NO_3^- results in the decrease of J. The binding mechanisms of dichromate, chromate and nitrate with PQ6 were proposed. Finally, the concentration experiment was carried out under the optimal conditions. R_{Cr} was close to 1, and J decreases slightly. Chromium was effectively concentrated by the membrane. © 2013 Curtin University of Technology and John Wiley & Sons, Ltd.

Keywords: polyquaternium; chromium(VI); complexation; polyelectrolyte-enhanced ultrafiltration

INTRODUCTION

Chromium has been widely used in different industrial fields such as leather tanning, chromium electroplating, metallurgy and chemical manufacturing industries, which results in substantial amounts of wastewater containing chromium ions.[1,2] Chromium(VI) is highly toxic and carcinogenic, and its pollution of industrial wastewaters represents a major problem for the environment.[2,3] Thus, it is crucial to find effective methods to reduce the pollution. The removal methods of chromium(VI) in aqueous media include mainly chemical precipitation,[4] ion exchange,[5,6] adsorption,[1] extraction,[7,8] membrane separation processes[2,9–11] and so on.

Polyelectrolyte-enhanced ultrafiltration (PEUF) is a promising method for removing metal ions from wastewaters.[12,13] The PEUF is based on the formation of metal ion–polyelectrolyte complexes. Metal ions, which are bound to the polymer with a larger molecular weight than the molecular weight cutoff (MWCO) of ultrafiltration membranes, are retained and concentrated by the membranes, whereas unbound metal ions pass through the membranes.[14–16] The binding of metal ion with polyelectrolyte is generated by electrostatic attraction or electron coordination, depending on the nature of the polyelectrolyte and metal ion.[17] The choice of the proper water-soluble macroligands is important for developing the PEUF. Some natural macroligands, such as chitosan[18,19] and humic substance,[20] were used to bind heavy metal ions. The synthetic macroligands, such as polyethyleneimine,[21,22] ethoxylated polyethylenimine,[23] poly(acrylic acid),[24,25] poly(acrylic acid) sodium salt,[26] polyvinyl alcohol[27,28] and carboxyl methyl cellulose,[29] were mainly employed. The PEUF has been applied to remove many metal ions, most often Hg(II), Cd(II), Pd(II), Ni(II), Zn(II), Cu(II) and radionuclides. This method was also employed to remove chromium species from aqueous solutions. Korus *et al.*[30] tried to remove Cr(III) and

**Correspondence to*: Jianxian Zeng, School of Chemistry and Chemical Engineering, Hunan University of Science and Technology, Key Laboratory of Theoretical Chemistry and Molecular Simulation of Ministry of Education, Hunan Province College Key Laboratory of QSAR/QSPR, Xiangtan 411201, China. E-mail: zengjianxian@163.com

European Journal of Medicinal Chemistry 81 (2014) 22–27

Contents lists available at ScienceDirect

European Journal of Medicinal Chemistry

journal homepage: http://www.elsevier.com/locate/ejmech

Preliminary communication

Design and synthesis of novel 5,6-disubstituted pyridine-2,3-dione-3-thiosemicarbazone derivatives as potential anticancer agents

Wenlin Xie [a,b,c,*], Shimin Xie [d], Ying Zhou [a,b,c], Xufu Tang [a,b,c], Jian Liu [e], Wenqian Yang [a,b,c], Minghua Qiu [a,b,c]

[a] School of Chemistry and Chemical Engineering, Hunan University of Science and Technology, Xiangtan 411201, China
[b] Key Laboratory of Theoretical Chemistry and Molecular Simulation of Ministry of Education, Hunan University of Science and Technology, China
[c] Hunan Provincial University Key Laboratory of QSAR/QSPR, China
[d] Hunan University of Humanities, Science and Technology, Loudi 417000, China
[e] Shenzhen Hanyu Pharmaceutical Co., Ltd., Shenzhen 518057, China

ARTICLE INFO

Article history:
Received 6 October 2013
Received in revised form
29 April 2014
Accepted 1 May 2014
Available online 4 May 2014

Keywords:
2,3-Dihydroxypyridine
Pyridine-2,3-diones
Anticancer activity
Thiosemicarbazone

ABSTRACT

A series of 5,6-disubstituted pyridine-2,3-dione-3-thiosemicarbazone derivatives(2a-2n) and 5,6-disubstituted pyridine-2,3-dione S-benzyl-3-thiosemicarbazones(3a-3g) were synthesized starting from 2,3-dihydroxypyridine via oxidation-Michael additions, condensations and nucleophilic substitutions. The structures of the compounds were established by IR, ^{1}H NMR, ^{13}C NMR, and HRMS. All newly synthesized compounds were screened for their anticancer activity against Breast cancer (MCF-7), Colon cancer (HCT-116) and hepatocellular cancer (BEL7402) cell lines. Bioassay results indicated that most of the prepared compounds exhibited cytotoxicity against various cancer cells in vitro. Some of the compounds exhibited promising antiproliferative activity, which were comparable to the positive control (5-fluorouracil). The structure–activity relationship was discussed.

1. Introduction

Following cardiovascular disease, cancer is the second leading cause of death in both developed and developing countries [1,2], the treatment of cancer still remains an important and challenging problem. For the majority of cancers, chemotherapy has become one of the methods that are being adopted to treat cancer. Many compounds have been synthesized with this aim, but their clinical use has been limited by their relatively high risk of toxicity, because they lack specificity and produce adverse effects related to the impact on rapidly dividing noncancerous cells [2,3]. Therefore, to improve efficacy and decrease the adverse effect potential is one of the goals in developing new anticancer drugs. Another major goal for developing new anticancer agents is to overcome cancer resistance to drug treatment that has made many of the currently available chemotherapeutic agents ineffective [4]. Nitrogen-containing heterocycles have always constituted a subject of great interest due to their ubiquity in nature and extensive presence as part of the skeletal backbone of many therapeutic agents. Of these heterocycles, pyridinone derivatives possess important biological activity such as anti-tumor activity [5], leukemia activity [6], anti-inflammatory activity [7], antimicrobial activity [8], HIV Reverse Transcriptase inhibitor [9] and antimalarial activity [10], pyridinone also is found applications in the preparation of deferiprone [11]. pyridinone-fused heterocycles including 4-(phenylthio)-2(1*H*)-pyridinones [12], [2R-trans,5Z(E,E)]-1,4-dihydroxy-5-phenyl-3-[tetrahydro-3-methyl-5-(6-methyl-2,4-octadienylidene)-2H-pyran-2-yl]-2(1H)-pyridinone(TMC-69) [13], and 3-amino-4-(pyridine-4-yl)-2(1*H*)- pyridinone (Amrinone) [14](Fig. 1) have attracted considerable attention.

On the other hand, thiosemicarbazide also exhibits various biological activities and have attracted considerable pharmaceutical interest [15]. They have been evaluated as antiviral [16], antibacterial [17], anti-inflammatory [18], antimalarial [19], anti-leukemic [20] and anticancer [21–23] activities, therefore, the thiosemicarbazide is a highly efficient pharmacophore in drug molecular design. Recently, several kinds of thiosemicarbazone derivatives have been synthesized and their antitumor activities were also reported [15]. In order to find novel potent pyridinone antitumor agents, we focused on designing and synthesizing some new pyridinone derivatives, wherein the active pharmacophores

* Corresponding author. School of Chemistry and Chemical Engineering, Hunan University of Science and Technology, Xiangtan 411201, China.
E-mail address: xwl2000zsu@163.com (W. Xie).

http://dx.doi.org/10.1016/j.ejmech.2014.05.001
0223-5234/

JOC The Journal of Organic Chemistry

Article

pubs.acs.org/joc

Regioselective Internal Carbonylation of the 2-Aza-21-carbaporphyrin: Access to Configurationally Stable Chiral Porphyrinoids

Bin Liu,[†] Xiaofang Li,*[,†] Justyna Maciołek,[‡] Marcin Stępień,[‡] and Piotr J. Chmielewski*[,‡]

[†]Key Laboratory of Theoretical Chemistry and Molecular Simulation of Ministry of Education, Hunan Province College Key Laboratory of QSAR/QSPR, School of Chemistry and Chemical Engineering, Hunan University of Science and Technology, Xiangtan, Hunan 411201, China

[‡]Department of Chemistry, University of Wrocław, 14 F. Joliot-Curie Street, 50 383 Wrocław, Poland

Supporting Information

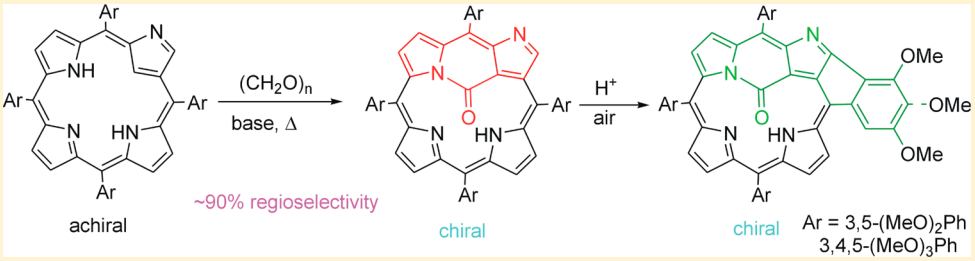

ABSTRACT: Reaction of paraformaldehyde with *meso*-tetraaryl-2-aza-21-carbaporphyrins (NCP) in the presence of a basic catalyst afforded fused lactam derivatives comprising a >C═O bridge linking the internal carbon C21 with one of the internal nitrogens. The isomer **2** with C21−C(O)−N24 bridge is formed with about 9-fold molar excess over that with C21−C(O)−N22 bridge (**3**). The ^{1}H NMR and UV−vis spectral characteristics indicate aromatic character of the derivatives. For *meso*-tetrakis(3′,5′-dimethoxy)- and *meso*-tetrakis(3′,4′,5′-trimethoxy)-21,24-carbonyl-NCP an efficient external ring fusion by linking C3, i.e., the external carbon of the *confused* pyrrole, with an ortho carbon of the adjacent aryl was observed under acidic conditions, yielding derivatives **4c** and **4d**, comprising a linear system of five fused rings. The chirality and configurational stability of these carbonylated systems were established by a chiral stationary phase HPLC and circular dichroism. The interaction of **2** with chiral acids and alcohols leading to the formation of diastereomers was observed by ^{1}H NMR. Slow racemization of **2** under acidic conditions was established by HPLC and ^{1}H NMR and a mechanism for this process was proposed.

INTRODUCTION

Porphyrinoids, the oligopyrrolic aromatic macrocycles, are ubiquitous in basic and applied chemistry owing to their versatile redox, acid−base, optical, and coordination properties.[1−9] Their reactivity is also attractive, allowing fine-tuning of the properties of the system or profound modification of the structure without destruction of the macrocyclic ring. 2-Aza-21-carbaporphyrin[10−12] **1**, also known as N-confused porphyrin (NCP), takes a special part among porphyrin derivatives, analogues, and homologues;[13−17] since its synthesis is facile, and further modifications of the preformed macrocycle are relatively simple by virtue of the *confused* pyrrole that possesses three sites of different reactivity (2-N, 3-C, and 21-C), and each of them can be a target of substitution or addition reactions. In our search for new chiral macrocyclic systems based on the NCP ring,[18−26] we have turned our attention to the reaction that takes place between **1** and formaldehyde under basic conditions that leads to the macrocycle with the interior fused by a carbonyl group. There are several derivatives known already comprising a bridge between atoms of the internal porphyrin core of NCP[27−31] that were obtained as products of multistep processes. The present system can be obtained by one-pot regioselective synthesis gaining configurational stability of the chiral porphyrin ring and retaining its macrocyclic aromaticity.

RESULT AND DISCUSSION

Synthesis and Characterization. The reaction was conducted at elevated temperatures under nitrogen atmosphere with a 10-fold molar excess of paraformaldehyde over NCP (Scheme 1) in the presence of various bases, though only a relatively strong organic proton scavenger resulted in the formation of **2** (see Supporting Information, Table S1). The best results were obtained for triethylamine as a base in refluxing toluene as a solvent. Under these conditions, about 60% conversion after 20 h of the reaction time and more than 40% of overall yield of **2** upon isolation were observed. The effectiveness of the reaction is thus relatively low, but the porphyrin reactant does not undergo decomposition to a considerable degree and the product is easily separable from

Received: February 4, 2014
Published: March 6, 2014

Journal of Coordination Chemistry, 2014
Vol. 67, No. 2, 315–322, http://dx.doi.org/10.1080/00958972.2014.880783

NMR and theoretical study on the coordination interaction between peroxovanadium(V) complexes and 5-amino-1,10-phenanthroline

XIANYONG YU*†‡§, LIN DENG†, HONGWEN TAO†, BINGFEI JIANG† and XIAOFANG LI*†

†Key Laboratory of Theoretical Chemistry and Molecular Simulation of Ministry of Education, Hunan Province College Key Laboratory of QSAR/QSPR, School of Chemistry and Chemical Engineering, Hunan University of Science and Technology, Xiangtan, China
‡State Key Laboratory of Physical Chemistry of Solid Surfaces, Xiamen University, Xiamen, PR China
§Key Laboratory of Computational Physical Sciences, Fudan University, Ministry of Education, Shanghai, PR China

(*Received 4 October 2013; accepted 16 December 2013*)

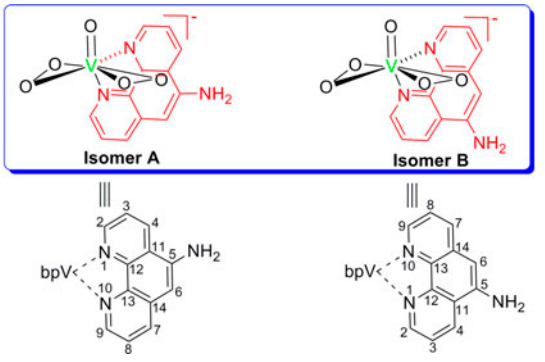

To understand the coordination modes and the solution structure of 5-amino-1,10-phenanthroline (5-NH_2-phen), the coordination reaction between peroxovanadium(V) complex $[OV(O_2)_2(D_2O)]^-$/$[OV(O_2)_2(HOD)]^-$ and 5-NH_2-phen has been investigated by multinuclear (^1H, ^{13}C, and ^{51}V) magnetic resonance with variable temperature NMR, COSY, and HSQC. The experimental results indicate a pair of isomers in solution, which are attributed to different coordination modes between vanadium and 5-NH_2-phen. The solution structures of these newly formed peroxovanadate species were proposed based on experimental NMR information and confirmed by theoretical calculations. Moreover, the results of density functional calculations indicate that solvation plays an important role in these interactions.

Keywords: Peroxovanadate; 5-Amino-1,10-phenanthroline; Coordination reaction; NMR; DFT-calculation

*Corresponding authors. Email: yu_xianyong@163.com (X. Yu); lixiaofang@iccas.ac.cn (X. Li)

Materials Chemistry and Physics 144 (2014) 213–225

Contents lists available at ScienceDirect

Materials Chemistry and Physics

journal homepage: www.elsevier.com/locate/matchemphys

Review

Design, preparation, and application of ordered porous polymer materials

Qingquan Liu*, Zhe Tang, Baoli Ou, Lihua Liu, Zhihua Zhou*, Shaohua Shen, Yinxiang Duan

School of Chemistry and Chemical Engineering, Key Laboratory of Theoretical Chemistry and Molecular Simulation of Ministry of Education, Hunan University of Science and Technology, Xiangtan 411201, China

HIGHLIGHTS

- Breath figures involve polymer casting under moist ambience.
- Hard template employs monodisperse colloidal spheres as a template.
- Soft template utilizes the etched block in copolymers as template.

ARTICLE INFO

Article history:
Received 10 August 2013
Received in revised form
6 January 2014
Accepted 10 January 2014

Keywords:
Microporous materials
Polymers
Etching
Adsorption
Microstructure

ABSTRACT

Ordered porous polymer (OPP) materials have extensively application prospects in the field of separation and purification, biomembrane, solid supports for sensors catalysts, scaffolds for tissue engineering, photonic band gap materials owing to ordered pore arrays, uniform and tunable pore size, high specific surface area, great adsorption capacity, and light weight. The present paper reviewed the preparation techniques of OPP materials like breath figures, hard template, and soft template. Finally, the applications of OPP materials in the field of separation, sensors, and biomedicine are introduced, respectively.

1. Introduction

Ordered porous materials, which were developed rapidly in 1990s, are a kind of materials with ordered nano-structure. Emergence of ordered porous materials attracted a great deal of attention from the field of physics, chemistry, and materials, at the same time, ordered porous materials developed rapidly into one hot research focus [1]. Generally, ordered porous materials can be classified into ordered porous inorganic (OPI) materials and ordered porous polymer (OPP) materials. The preparation and application of OPI materials are becoming mature, whereas OPP materials still have huge development space in the preparation techniques and application fields.

OPP materials have a series of advantages like light weight, ordered alignment of pores, high specific surface area, great adsorption capacity, uniform pore size, and tunable pore size, and this type of materials have great application prospects in the field of biomedicine [2–4], biological film [5,6], bioreactor [7], adsorption [8,9], catalyst supports [10,11], separation [12,13], and growth templates of nanomaterials with specific shapes [14]. Therefore, preparation and application of OPP materials have has drawn much interest of researchers and scientists in the field of polymer materials. Up to now, OPP materials can be classified into two types: OPP membrane and OPP monoliths. The term “monolith” refers to unibody structures composed of interconnected repeating cells or channels [15]. Since Nakahama et al. firstly prepared ordered porous polystyrene (PS) membranes via microphase separation of polystyrene-*b*-polyisoprene and ozonolysis, the last two decades have witnessed the great progress of OPP membrane in the synthetic routes, and in selective separation and photonic application [16].

The development of etching techniques made the preparation of OPP monoliths with thickness of a few millimeters possible. Compared to traditional polymer materials with continuous pore size distribution, OPP monoliths have uniform pores with large aspect ratio. Buchmeiser think this type of materials possess

* Corresponding authors. Fax: +86 731 5829 0045.
E-mail addresses: qqliu@hnust.edu.cn (Q. Liu), zhou7381@126.com (Z. Zhou).

0254-0584/$ – see front matter © 2014 Elsevier B.V. All rights reserved.
http://dx.doi.org/10.1016/j.matchemphys.2014.01.013

Analytical Methods

PAPER

View Article Online
View Journal | View Issue

Cite this: *Anal. Methods*, 2014, **6**, 9078

Electrochemical co-reduction synthesis of Au/ferrocene–graphene nanocomposites and their application in an electrochemical immunosensor of a breast cancer biomarker

Chunxiang Li,[a] Xiyang Qiu,[a] keqin Deng*[a] and Zhaohui Hou*[b]

Received 4th August 2014
Accepted 16th September 2014

DOI: 10.1039/c4ay01838a

www.rsc.org/methods

The nanocomposites (Fc–GO) of ferrocene (Fc) hybridized graphene oxide (GO) were prepared by π–π stacking interactions. Fc–GO and Au(III) are electrochemically co-reduced to obtain Au nanoparticles (AuNPs) and Fc hybridized electrochemically reduced graphene oxide (Fc–ERGO) nanocomposites (AuNPs/Fc–ERGO). Scanning electron microscopy reveals that Au particles are about 10 nm and are dispersed uniformly on Fc–ERGO. The electrochemical behavior of AuNPs/Fc–ERGO demonstrates great electrochemical activity and stability. The AuNPs/Fc–ERGO was applied in a highly sensitive immunosensor of the biomarker carbohydrate antigen 15-3 (CA 15-3). This unique immunosensor, with AuNPs/Fc–ERGO as the immobilization platform and signal probe, exhibited significant sensitivity toward CA 15-3. Under optimal conditions, the peak current of differential pulse voltammetry (DPV) of the immunosensor decreased with increasing CA 15-3 concentration, showing two linear ranges of 2.0–25.0 U mL^{-1} and 0.05–2.0 U mL^{-1} with a low detection limit of 0.015 U mL^{-1}. The strategy developed for this immunosensor provides a promising approach for clinical research and diagnostic applications.

1. Introduction

Graphene has attracted much research attention due to its unique thermal, mechanical, and electrical properties.[1–5] However, because of van der Waals interactions between graphene sheets, graphene is prone to form irreversible agglomerates and even restacking.[6–8] Thus, the preparation of well-dispersed graphene sheets has become a crucial issue. Although there exist strong interlayer interactions from the strong π-stacking, this unique π-stacking system does offer new opportunities to prepare novel hybrid functional structures by introducing advanced materials to graphene sheets.[9–13] Graphene sheets can be noncovalently functionalized with tryptophan (Tryp) through π–π stacking. The Tryp–graphene complex can be stably dispersed in water for several months.[9] Gao *et al.* prepared a hybrid material consisting of metallocene and graphene.[10] The hybrid exhibited excellent electrocatalytic properties. In previous work we constructed a nanohybrid of ferrocene hybridized chemically reduced graphene oxide (CRGO) through π–π stacking interactions, which exhibited a dramatically enhanced dispersibility and stability.[11]

Recently, graphene–metal composites such as graphene/Cu nanoparticles,[14] graphene/Pd nanohybrids,[15] graphene/Au nanocomposites,[16] *etc.* have already been reported. Graphene–metal nanocomposites can display a synergic effect of electrocatalytic characters of both graphene and metal nanoparticles. The metal nanoparticles in graphene sheets can inhibit the aggregation of graphene sheets.[7,17] Several methods were used to prepare graphene–metal composites.[18–20] Among them, the electrochemical method is fast, clean, and nondestructive.[21,22] Fu *et al.* proposed the electrochemical co-reduction of graphene oxide (GO) and chloroauric acid ($HAuCl_4$) by the potentiostatic method.[22] Electrochemical co-reduction synthesis of graphene and Au nanocomposites through cyclic voltammetry was also studied.[23–25] This method was efficient and the resulting graphene–Au nanocomposites showed excellent electrochemical properties. The synergistic effect of graphene and nano-Au could promote the electrocatalysis.[23–25]

In this work, we prepared ferrocene (Fc) hybridized graphene oxide (GO) nanocomposites (Fc–GO) through π–π stacking interactions. Chronoamperometry was adopted to simultaneously reduce $HAuCl_4$ and Fc–GO for synthesizing a novel nanocomposite (AuNPs/Fc–ERGO) consisting of Au nanoparticles (AuNPs) and Fc hybridized electrochemically reduced graphene oxide (Fc–ERGO). This method was simple and green. The obtained nanohybrids (AuNPs/Fc–ERGO) were characterized by scanning electron microscopy (SEM) and electrochemical methods. Based on the excellent properties of

[a]*Key Laboratory of Theoretical Organic Chemistry and Function Molecule, Ministry of Education, Hunan University of Science and Technology, Xiangtan 411201, P. R. China. E-mail: keqindeng@hnust.edu.cn; Tel: +86-731-58290045*

[b]*School of Chemistry and Chemical Engineering, Hunan Institute of Science and Technology, Yueyang 414006, P. R. China. E-mail: zhqh96@163.com*

Journal of Macromolecular Science, Part A: Pure and Applied Chemistry (2014) **51**, 572–576

ISSN: 1060-1325 print / 1520-5738 online
DOI: 10.1080/10601325.2014.916178

Biological Assessment *In-Vivo* of Gel-HA Scaffold Materials Containing Nano-Bioactive Glass for Tissue Engineering

ZHIHUA ZHOU[1,2,3]*, LIUJIAO XIANG[1], BAOLI OU[3], TIANLONG HUANG[4], HU ZHOU[3], WENNAN ZENG[3], LIHUA LIU[3], QINGQUAN LIU[3], YANMIN ZHAO[3], SILIANG HE[3], and HUIHUA HUANG[3]

[1]*Key Laboratory of Theoretical Chemistry and Molecular Simulation of Ministry of Education, Hunan University of Science and Technology, Xiangtan, P. R. China*
[2]*Hunan Province College Key Laboratory of QSAR/QSPR, Hunan University of Science and Technology, Xiangtan, P. R. China*
[3]*School of Chemistry and Chemical Engineering, Hunan University of Science and Technology, Xiangtan, P. R. China*
[4]*Department of Orthopedics, the Second Xiangya Hospital, Central South University, Changsha, P. R. China*

Received and Accepted February 2014

To evaluate the biological safety of the composite materials based on gelatin (Gel), hyaluronic acid (HA), and nano-bioactive glass (NBG), which has a potential application in tissue engineering, the *in-vivo* biological properties were investigated by hemolysis behavior, micronucleus, skin irritation and acute toxicity test. Scanning electron microscopy (SEM) morphology demonstrated that the Gel-HA/NBG composite scaffolds had interconnected pores with mean diameters of 50–500 μm. The hemolysis test suggested that the Gel-HA/NBG composite scaffold, with a hemolysis ratio of 1.11%, showed no obvious hemolysis reaction. The micronucleus frequency of the Gel-HA/NBG was (3.1 $\pm$ 0.52) %; this indicated that it shows no genotoxic effect. The skin irritation result showed no systemic signs of toxicity in the integrity skin of the animals. The Gel-HA/NBG scaffolds showed no acute systemic toxicity and the liver, heart, lung, and kidney samples also showed no remarkable change in the morphology. Therefore, Gel-HA/NBG composite scaffold would be a suitable candidate of biomedical materials for tissue engineering.

Keywords: Gelatin, hyaluronic acid, nano-bioactive glass, composite scaffold, *in-vivo* biological properties

1 Introduction

Biodegradable polymers have been widely used to fabricate 3D porous scaffolds in tissue engineering, which can guide cell/tissue to grow, synthesize extracellular matrix (ECM) or other biological molecules, and facilitate the formation of functional tissues and organs (1, 2).

As scaffolding materials, various natural biodegradable polymers have been widely used. Gelatin (Gel) is known to be the most promising natural polymer and has found diverse applications in tissue engineering due to its excellent biocompatibility and biodegradability (3). Gelatin contains a large number of arginyl-glycyl-l-aspartic acid (RGD) motifs, glycine, proline, and 4-hydroxyproline residues that enhance the cell adhesion since these moieties attach with integrin of the cell's surface, leading to a higher number of cell attachments to the matrix (4, 5). Hyaluronic acid (HA) is a linear anionic polysaccharide composed of repeating disaccharide units of D-glucuronic acid and *N*-acetyl-D-glucosamine (6–8). HA and its derivatives have already found wide-ranging uses in various research fields, including tissue engineering, drug delivery and gene therapy (9–11). However, HA hydrogels cannot provide sufficient mechanical support when used in the body.

In the past few years, increasing attention has been paid to nanocomposites made of biopolymers and nano-bioactive materials for application in tissue engineering. Many kind of nano-bioactive materials including bioactive glasses (BG), bioactive glass–ceramics, and calcium phosphate ceramics, have been developed and some of them are now applied to repair and reconstruct diseased or damaged bones or tissues (12, 13). Among bioactive materials, nano-bioactive glasses (NBG) have gained much attention because they are biocompatible, bioactive, osteoconductive and osteoproductive (14–17.) Also, when NBG is implanted in human body, the apatite layer can be formed on the surface, which chemically bonds with living bone.

For tissue engineering scaffolds, the selection of a material to be employed as a biomaterial for a specific end use must meet several criteria such as physicochemical

*Address correspondence to Zhihua Zhou, Key Laboratory of Theoretical Chemistry and Molecular Simulation of Ministry of Education, Hunan University of Science and Technology, Xiangtan 411201, P. R. China. E-mail: zhou7381@126.com

Color versions of one or more figures in this article can be found online at www.tandfonline.com/lmsa.

Journal of Macromolecular Science, Part A: Pure and Applied Chemistry (2014) **51**, 318–325

ISSN: 1060-1325 print / 1520-5738 online
DOI: 10.1080/10601325.2014.882693

Fabrication and Physical Properties of Gelatin/Sodium Alginate/Hyaluronic Acid Composite Wound Dressing Hydrogel

ZHIHUA ZHOU[1,2,3]*, JIAHUI CHEN[1], CHENG PENG[4], TIANLONG HUANG[5], HU ZHOU[1], BAOLI OU[1], JIAN CHEN[1], QINGQUAN LIU[1], SILIANG HE[1], DAFU CAO[1], HUIHUA HUANG[1], and LIUJIAO XIANG[1]

[1]*School of Chemistry and Chemical Engineering, Hunan University of Science and Technology, Xiangtan, P. R. China*
[2]*Key Laboratory of Theoretical Chemistry and Molecular Simulation of Ministry of Education, Hunan University of Science and Technology, Xiangtan, P. R. China*
[3]*Hunan Province College Key Laboratory of QSAR/QSPR, Hunan University of Science and Technology, Xiangtan, P. R. China*
[4]*Department of Burns and Plastic Surgery, the Third Xiangya Hospital, Central South University, Changsha, P. R. China*
[5]*Department of Orthopedics, the Second Xiangya Hospital, Central South University, Changsha, P. R. China*

Received October 2013, Accepted November 2013

Gelatin (Gel), sodium alginate (SA) and hyaluronic acid (HA) based various hydrogels for biomedical applications were prepared by freezing-drying method using 1-ethyl-3-(3-dimethyl aminopropyl) carbodiimide (EDC) as a crosslinker. The physical properties including morphology, water vapor transmission rate and hydrophilicity were investigated. The result showed the Gel/SA/HA composite hydrogels were successfully crosslinked by the crosslinking agent. All the Gel/SA/HA composite hydrogels with different compositions had highly homogeneous and interconnected pores, and the compositions had no significant effect on the surface and cross-section morphologies of the Gel/SA/HA hydrogels. The incorporation of sodium alginate enhanced the water vapor transmission capacity of the hydrogel; however, there were no significant differences between the water vapor transmission rates of all the Gel/SA/HA hydrogels. Gelatin had a low hydrophilic behavior, while sodium alginate exhibited relatively high hydrophilic behavior. The results indicate that the Gel/SA/HA hydrogel cross-linked via EDC is a potential wound dressing material capable of the adequate provision of moist environment for comfortable wound healing.

Keywords: gelatin, hyaluronic acid, sodium alginate, wound dressing hydrogel, physicochemical property

1 Introduction

Various types of wound dressings and cultured skin substitutes have been developed and used to provide effective therapy for skin wounds. Hydrogels are drawing more attention to be used for the healing of skin lesions in the form of bandages, adhesives, and burn wound dressings (1, 2). A hydrogel dressing prevents the wound from microbial contamination, inhibits the loss of body fluids, provides free flow of oxygen to the wound, and generally accelerates the healing process. Natural based wound dressing hydrogels are considered as promising and potential wound covering options because of their non-toxicity, biocompatibility, biodegradability but also insolubility, hydrophilicity, and excellent swelling behavior. While, they have a form of flexible and durable covering materials permeable to water vapor and metabolites, they protect the wound again bacterial infection. (3–5).

Gelatin (Gel) is obtained by the thermal denaturation of collagen from animal skin and bones. It contains mainly the residues of three amino acids-glycine (arranged every third residue), proline, and 4-hydroxyproline in its structure. Gel exhibits readily accessible cell-adhesive motifs and matrix metalloproteinase-sensitive degradation sites that are essential for cell–matrix interactions (6). The presence of positively charged residues in Gel, such as lysine and arginine, allows for the complexation of various growth factors and ECM components. With the gelling property, adhesive property, solubility and other excellent features, it is widely used in the pharmaceutical material (7–10).

Hyaluronic acid (HA) is a naturally occurring linear polysaccharide with a high molecular weight. It has a

*Address correspondence to: Zhihua Zhou, Key Laboratory of Theoretical Chemistry and Molecular Simulation of Ministry of Education, Hunan University of Science and Technology, Xiangtan 411201 P. R. China. E-mail: zhou7381@126.com

Color versions of one or more of the figures in the article can be found online at www.tandfonline.com/lmsa.

Journal of Macromolecular Science, Part A: Pure and Applied Chemistry (2014) **51**, 522–526

ISSN: 1060-1325 print / 1520-5738 online
DOI: 10.1080/10601325.2014.906268

Influences of Molecular Weight and Content of Polyethylene Glycol on Morphology and Size of Nano-Bioactive Glass

ZHIHUA ZHOU[1,2,3*], HUIHUA HUANG[1], TIANLONG HUANG[4], CHENG PENG[5], BAOLI OU[1], HU ZHOU[1], WENNAN ZENG[1], QINGQUAN LIU[1], ZHONGMIN YANG[1], LIUJIAO XIANG[1], and SILIANG HE[1]

[1]*School of Chemistry and Chemical Engineering, Hunan University of Science and Technology, Xiangtan, P. R. China*
[2]*Key Laboratory of Theoretical Chemistry and Molecular Simulation of Ministry of Education, Hunan University of Science and Technology, Xiangtan, P. R. China*
[3]*Hunan Province College Key Laboratory of QSAR/QSPR, Hunan University of Science and Technology, Xiangtan, P. R. China*
[4]*Department of Orthopedics, the Second Xiangya Hospital, Central South University, Changsha, P. R. China*
[5]*Department of Burns and Plastic Surgery, the Third Xiangya Hospital, Central South University, Changsha, P. R. China*

Received December 2013, Accepted January 2014

Nano-bioactive glass (NBG) was prepared via sol-gel method and freeze-dried technique using polyethylene glycol (PEG) as templates. The influences of molecular weight and content of polyethylene glycol on the morphology and the size NBG particles were investigated. The optimal sintering temperature of NBG was determined by using thermal gravimetric (TG) and differential thermal analysis (DTA), and the NBG particles were characterized by Fourier-transformed infrared (FTIR) spectroscopy, transmission electron microscopy (TEM) and X-ray diffraction (XRD). The XRD pattern of NBG sintered at 650°C in air confirmed that the calcined glass existed in amorphous state. The results indicated that the PEG molecular weight and PEG content have obvious effects on the morphology and size of the NBG particles. The size of NBG particle prepared with PEG-200 was beyond 1μm and the aggregation was obvious. The size of obtained NBG particle with PEG-10000 was between 50 nm and 80 nm, with a hollow spherical shape; while the morphology of the NBG with PEG-20000 was needle-shaped, with an average width of 20 nm and length of 100 nm. The particle size of the NBG particles decreased with the increase of PEG concentration.

Keywords: Nano-bioactive glass, polyethylene glycol, molecular weight, content, morphology, size

1 Introduction

Recently, remarkable advances in the field of biomaterials have led to the development of various types of bioceramics and bioactive glass (BG) for bone repair and prosthesis. (1, 2) BG has been studied for more than thirty years since Hench first invented bioglass 45S5 (3). Because of the good bioactivity, osteoconductivity and biodegradability, bioactive glasses have been used in clinic for more than ten years (4–6). In addition, BG is the only one, which could bond to hard and soft tissue (7, 8). Recent studies showed that the degradation products of bioactive glasses could stimulate the production of growth factors, cell proliferation and activate the gene expression of osteoblast (9–14).

Recent studies showed that increasing specific surface area and pore volume of BG may greatly accelerate the deposition process of hydroxyapatite (6). Researchers revealed that the biomaterials in nano-scale could stimulate the reaction between materials and cells (15–17). Recently, nano-bioactive glasses (NBG) particles were prepared by Brunner et al using flame synthesis, (18) but the flame synthesis needs high temperature environment. On the contrary, the sol-gel technology and lyophilization are low temperature preparation method, and the glasses prepared by sol-gel method have porous structure with high specific surface area. However, the particle-size of the traditional sol-gel-derived bioactive glasses was bigger than 1 μm (19, 20). In addition, the time of the synthesis of bioactive glasses by traditional sol-gel process is quite long because of the long gelation and aging time (21). This work reports the preparation of the nano-bioactive glasses (NBG) by a quick sol-gel and lyophilization methods, and we demonstrated that, using PEG as a dispersant, the size of NBG could be controlled by adjusting the molecular weight and amount of PEG.

*Address correspondence to: Zhihua Zhou, School of Chemistry and Chemical Engineering, Hunan University of Science and Technology, Xiangtan 411201, P. R. China; E-mail: zhou7381@126.com

Color versions of one or more of the figures in the article can be found online at www.tandfonline.com/lmsa.

J Nanopart Res (2014) 16:2793
DOI 10.1007/s11051-014-2793-4

RESEARCH PAPER

Synthesis of biocompatible AuAgS/Ag_2S nanoclusters and their applications in photocatalysis and mercury detection

Qian Zhao · Shenna Chen · Lingyang Zhang · Haowen Huang · Fengping Liu · Xuanyong Liu

Received: 16 September 2014 / Accepted: 2 December 2014 / Published online: 11 December 2014

Abstract In this paper, a facile approach for preparation of AuAgS/Ag_2S nanoclusters was developed. The unique AuAgS/Ag_2S nanoclusters capped with biomolecules exhibit interesting excellent optical and catalytic properties. The fluorescent AuAgS/Ag_2S nanoclusters show tunable luminescence depending on the nanocluster size. The apoptosis assay demonstrated that the AuAgS/Ag_2S nanoclusters showed low cytotoxicity and good biocompatibility. Therefore, the nanoclusters can be used not only as a probe for labeling cells but also for their photocatalytic activity for photodegradation of organic dye. Moreover, a highly selective and sensitive assay for detection of mercury including Hg^{2+} and undissociated mercury complexes was developed based on the quenching fluorescent AuAgS/Ag_2S nanoclusters, which provides a promising approach for determining various forms of Hg in the mercury-based compounds in environment. These unique nanoclusters may have potential applications in biological labeling, sensing mercury, and photodegradation of various organic pollutants in waste water.

Keywords AuAgS/Ag_2S nanoclusters · Hg^{2+} · Photodegradation · Biocompatibility · Sensors

Introduction

As exciting new materials, noble metal-derived quantum clusters exhibit unique properties due to the confinement of electrons in discrete energy levels (Shang et al. 2011; Zheng et al. 2007; Díez and Ras 2011). These subnanometer particles have a core of only a few metal atoms that can be considered as the monolayer-protected clusters, which show molecule-like electronic transitions within the conduction band strong fluorescence. These clusters have found potential application in single-molecule optoelectronic nanodevices (Reichel et al. 2006), biological labeling (Ma et al. 2011), optical (Qiao et al. 2013; Zhang et al. 2012), ensing (Dai et al. 2014; MacLean et al. 2013), alysis (Zhu et al. 2011; Qian et al. 2012), se-enhanced Raman spectroscopy (SERS) (Silva et al. 2011; Fleger et al. 2009). Study on the synthesis and

Electronic supplementary material The online version of this article (doi:10.1007/s11051-014-2793-4) contains supplementary material, which is available to authorized users.

Q. Zhao · S. Chen · L. Zhang · H. Huang (✉) · F. Liu
Key Laboratory of Theoretical Organic Chemistry and Function Molecule, Ministry of Education, Hunan Provincial University Key Laboratory of QSAR/QSPR, School of Chemistry and Chemical Engineering, Hunan University of Science and Technology, Xiangtan, China
e-mail: hhwn09@163.com

S. Chen · X. Liu (✉)
State Key Laboratory of High Performance Ceramics and Superfine Microstructure, Shanghai Institute of Ceramics, Chinese Academy of Sciences, Shanghai 200050, China
e-mail: xyliu@mail.sic.ac.cn

Analytical Letters, 47: 295–308, 2014

ISSN: 0003-2719 print/1532-236X online
DOI: 10.1080/00032719.2013.832272

Taylor & Francis
Taylor & Francis Group

Sensors

VERSATILE SENSITIVE LOCALIZED SURFACE PLASMON RESONANCE SENSOR BASED ON CORE-SHELL GOLD NANORODS FOR THE DETERMINATION OF MERCURY(II) AND CYSTEINE

Qian Zhao,[1] Shenna Chen,[1] Haowen Huang,[1,2] Fengping Liu,[1] and Youtao Xie[2]

[1]*Key Laboratory of Theoretical Chemistry and Molecular Simulation of Ministry of Education, School of Chemistry and Chemical Engineering, Hunan University of Science and Technology, Xiangtan, China*

[2]*Key Laboratory of Inorganic Coating Materials, Chinese Academy of Sciences, Shanghai, China*

A versatile sensitive localized surface plasmon resonance sensor was fabricated for the determination of mercury(II) and cysteine. The determination of mercury(II) was performed by taking advantage of the affinity between core-shell nanostructure and mercury to form a nanocomposite, leading to significant changes of localized surface plasmon resonance properties. The outstanding selectivity and sensitivity of the method provide a unique way to determine mercury(II) to concentrations as low as 5.00×10^{-8} M in aqueous solution. In addition, a strategy of orientation axially (end-to-end) assembly of core-shell gold nanorods at acidic medium was been developed that resulted in coupling of the plasmon band of core-shell gold nanorods, and was the basis of determining cysteine. An ultra-sensitive assay for the determination of cysteine was subsequently developed and levels of cysteine as low as 10^{-12} M can be determined. Compared with other gold nanorods-based sensors requiring molecular modification, these two approaches are simple in aqueous solution because of the unmodified design.

Keywords: Assembly; Core-shell gold nanorods; Cysteine; Localized surface plasmon resonance; Mercury; Sensor

INTRODUCTION

Gold nanorods have gained widespread attention with their excellent physical and chemical properties and biocompatibility (Mayer and Hafner 2011; Yang and Cui 2008; Vigderman, Khanal, and Zubarev 2012). They exhibit unique surface

Received 6 June 2013; accepted 28 July 2013.

This work was supported by Natural Science Foundation of China (21075035) and the Key Laboratory of Inorganic Coating Materials, Chinese Academy of Sciences.

Address correspondence to Haowen Huang, Key Laboratory of Theoretical Chemistry and Molecular Simulation of Ministry of Education, School of Chemistry and Chemical Engineering, Hunan University of Science and Technology, Xiangtan, China. E-mail: hhwn09@163.com

RSC Advances

PAPER

View Article Online
View Journal | View Issue

Cite this: *RSC Adv.*, 2014, **4**, 43212

Preparation of conductive polyaniline grafted graphene hybrid composites *via* graft polymerization at room temperature

Baoli Ou,*[abd] Rao Huang,[a] Wenyun Wang,[c] Hu Zhou[a] and Cong He[a]

Received 17th July 2014
Accepted 4th August 2014

DOI: 10.1039/c4ra07247b

www.rsc.org/advances

Graphene was covalently functionalized with phenol groups *via* a 1,3-dipolar cycloaddition reaction without degrading its electronic properties. The most important thing is that two hydroxyl groups can be covalently attached to the graphene sides in a single step. Here, the phenols on the functionalized graphene have been further derivatized with γ-aminopropyltriethoxysilane to form a dense aminopropylsilane self assembled monolayer with active sites for the graft polymerization of aniline. The conductive polyaniline layer was chemically grafted on the surface of the self assembled monolayer coated graphene by *in situ* polymerization of the aniline monomer in the presence of ammonium peroxodisulfate under acidic conditions. This reaction was found to be extremely efficient for producing conductive polyaniline–graphene hybrid composites, even at room temperature and short reaction times (24 h), and was usually performed using graphene oxide. The chemical grafting of PANI was confirmed using Fourier transform infrared spectroscopy. Thermogravimetric analysis indicated that the polymer functionalized graphene consisted of 24.5 wt% polymer. The morphologies of the polyaniline grafted graphene hybrid composites and hydroxyl functionalized graphene were examined by scanning electron microscopy and transmission electron microscopy, showing relatively uniform polymer coatings on the sides of graphene.

1. Introduction

Ever-increasing attention has been paid to the field of graphene-based materials since graphene was isolated by K. S. Novoselov *et al.* in 2004[1] because it is a single-atom-thick, two-dimensional sheet of sp^2-hybrized carbon atoms arranged in a honeycomb crystal structure with exceptionally high strength, surface area, thermal conductivity, and electronic conductivity.[2,3] These superior properties make graphene a very promising candidate in many potential applications such as energy conversion and storage devices,[4] catalysts,[5] optoelectronics,[6] chemical sensors, flash memory storage devices, transparent conductors, distributed ignition, and supercapacitors.[7]

Laith Al-Mashat *et al.*[8] synthesized graphene–polyaniline (PANI) nanocomposites, which were applied in the development of a hydrogen (H_2) gas sensor. The sensing performance of the synthesized nanocomposites was considerably better than that of the sensors based on only graphene sheets and PANI nanofibers. Recently, because of increasing air pollution, global warming and the depletion of traditional energy resources, the development of renewable energy production and hybrid electric vehicles with low CO_2 emissions has stimulated intense research on energy storage and the use of alternative energy sources.[9] Graphene has attracted considerable attention and has proven to be an outstanding candidate for the preparation of graphene/conductive polymer based hybrids as supercapacitor electrode materials. Among the conducting polymers, PANI is considered to be the most promising electrode material for supercapacitors because of its excellent capacity for energy storage, easy synthesis, high conductivity and low cost.[10]

For example, graphene–PANI composite films that could be directly used as the supercapacitor electrode were synthesized *via* an electrochemical process.[11] Wei Fan *et al.*[12] used a solution-based coassembly process to prepare polyaniline hollow spheres (PANI-HS)@electrochemical reduced graphene oxide (ERGO) hybrids, which indicates good cycling stability. Other supercapacitor devices based on self-assembled hierarchical graphene@polyaniline nanoworm composites also showed high electrochemical capacitance and effectively improved electrochemical stability and rate performances.[13] It must be pointed out that in these composites, the interactions between graphene and the conductive polymer, such as PANI, are van der Waals forces. It is well-known that the large surface area of graphene and strong van der Waals forces would result

[a]*School of Chemistry and Chemical Engineering, Hunan University of Science and Technology, Key Laboratory of Theoretical Organic Chemistry and Function Molecule, Ministry of Education, Xiangtan 411201, China. E-mail: oubaoli@163.com; Fax: +86 731 58290880; Tel: +86 731 58290880*

[b]*Hunan Province Key Laboratory of Coal Resources Clean-utilization and Mine Environment Protection, Xiangtan 411201, China*

[c]*Hunan Provincial Key Laboratory of Health Maintenance for Mechanical Equipment, Hunan University of Science and Technology, Xiangtan 411201, China*

[d]*State Key Laboratory of Powder Metallurgy, Central South University, Changsha 410083, China*

RSC Advances

COMMUNICATION

View Article Online
View Journal | View Issue

Cite this: *RSC Adv.*, 2014, **4**, 2151

A novel $AgIO_4$ semiconductor with ultrahigh activity in photodegradation of organic dyes: insights into the photosensitization mechanism†

Received 11th September 2013
Accepted 13th November 2013

DOI: 10.1039/c3ra45003a

www.rsc.org/advances

Jianting Tang,* Datang Li,* Zhaoxia Feng, Zhen Tan and Baoli Ou

A novel $AgIO_4$ semiconductor has been prepared *via* a facile precipitation method. It exhibited much higher activity than Ag_3PO_4 or Ag_3AsO_4 in photodegradation of rhodamine B under visible-light irradiation. The ultrahigh activity of $AgIO_4$ is attributed to the photosensitization mechanism of the photodegradation process.

Development of semiconductor photocatalysts for sunlight utilization is increasingly becoming an important research topic owing to the global energy shortage. Solar energy conversion through photocatalysis needs to maximize the utilization of visible light, and the dye-sensitized semiconductors have been widely studied for this purpose. Many dye-sensitized semiconductors, such as dye-sensitized TiO_2 and carbon nitride, have been successfully applied to visible-light-induced hydrogen production[1] and pollutant degradation[2] in aqueous solution, photoelectric conversion in solar cells,[3] or photocatalytic organic synthesis.[4] Although success has been achieved in the study of dye-sensitized semiconductors, the obtained photosensitization efficiency is still low and the insight for the important factors influencing photosensitization is deficient. Therefore, it is still highly desirable to develop novel semiconductor materials for efficient photosensitization-based utilization of solar energy and to research the relevant photosensitization mechanism.

As a highly efficient visible-light-responsive photocatalyst, Ag_3PO_4 semiconductor has attracted much attention because it showed higher photocatalytic activity than the currently known photocatalysts including $BiVO_4$, N-doped TiO_2, *etc.*, in water oxidation and photodegration of organic compounds.[5] Very recently, we reported a novel photocatalyst, Ag_3AsO_4, which achieved higher photodegradation activity than Ag_3PO_4 in degradation of rhodamine B (RhB) or methyl orange under irradiation of visible light.[6] In this work, we developed another new semiconductor, $AgIO_4$, through a facile precipitation process (see ESI for experiment details†). Notably, its activity is much higher than Ag_3PO_4 or Ag_3AsO_4 in photodegradation of RhB under visible-light irradiation. It was found that the ultrahigh photogradation activity of $AgIO_4$ is closely related to the self-sensitization of RhB. In addition, the key factor influencing photosensitization efficiency was proposed based on the study of the photodegradation mechanism of $AgIO_4$ in degradation.

Silver and iodine contents of the $AgIO_4$ sample were measured to be 35.2 wt% and 43.6 wt%, respectively, by ICP-MS technique. The contents are quite close to the corresponding theoretical values of pure $AgIO_4$ compound, confirming the successful preparation of $AgIO_4$. Fig. 1a displays the photo and SEM image of the $AgIO_4$ sample. It is yellow and mostly has rhombic shape with particle size of 3–15 μm. The XRD pattern of $AgIO_4$ is shown

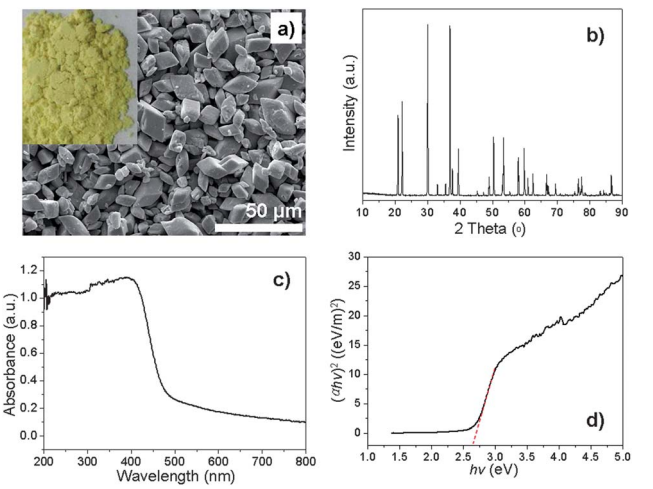

Fig. 1 (a) SEM image, (b) XRD pattern, (c) UV-vis DRS and (d) the corresponding plot of $(\alpha h\nu)^2$ *versus* $h\nu$ of $AgIO_4$. The inset in (a) shows the photo of $AgIO_4$.

Key Laboratory of Theoretical Chemistry, Molecular Simulation of Ministry of Education, School of Chemistry and Chemical Engineering, Hunan University of Science and Technology, Xiangtan 411201, China. E-mail: jttang1103@126.com; dtlhx@163.com; Tel: +86-731-58290045

† Electronic supplementary information (ESI) available. See DOI: 10.1039/c3ra45003a

Received: 11 August 2013 Revised: 24 September 2013 Accepted article published: 23 October 2013 Published online in Wiley Online Library: 18 November 2013

(wileyonlinelibrary.com) DOI 10.1002/pi.4640

Design, preparation and application of conjugated microporous polymers

Qingquan Liu,* Zhe Tang, Minda Wu and Zhihua Zhou**

Abstract

Conjugated microporous polymers (CMPs) are of great interest because these types of materials have high specific surface area and pore diameters less than 2 nm. CMPs have found applications in the fields of hydrogen storage, heterogeneous catalysts, gas-permeable membranes and light-emitting organics. A large number of recent reports have demonstrated that CMPs can be prepared using several approaches like noble metal-mediated ethynyl, Sonogashira–Hagihara coupling, Suzuki coupling and Yamamoto coupling reactions. In this review, the synthetic routes, functionalization and potential applications of CMPs are systematically introduced.

Keywords: conjugated microporous polymers; specific surface area; Sonogashira–Hagihara; Yamamoto coupling

INTRODUCTION

Recently, a new series of microporous crystalline zeolite analogues with small pores (<2 nm) and very high apparent Brunauer–Emmett–Teller surface areas (S_{BET})[1] have found widespread applications in diverse potential technological areas, such as separations,[2] gas storage,[3–7] catalysis,[2–5] removal of dyes from wastewater,[8] photocatalysts for water splitting[9] and heterogeneous catalysts for chemical synthesis.[10]

Metal–organic frameworks (MOFs) are the result of copolymerization of larger organic linkers with metal ions to yield new classes of designed crystalline materials.[11] Having high levels of porosity, MOFs offer considerable control over pore size and composition.[12] Unfortunately, MOFs with high surface area general suffer from low thermal and hydrothermal stabilities, which severely limit their applications, particularly in industry.[13]

Covalent organic frameworks (COFs) are constructed solely from light elements (H, B, C, N and O) known to form strong covalent bonds.[14] The highest S_{BET} of COFs was up to 4210 $m^2 g^{-1}$. COFs have good thermal stability but are relatively moisture-sensitive.[15]

Hyper-crosslinked polymers have high S_{BET} in the range 330–2090 $m^2 g^{-1}$,[7] but strong Lewis acids such as $FeCl_3$ and hydrochloric acid have been involved in their synthesis.[16] In this case, the incorporation of certain chemical functionalities may be precluded as a result of harsh synthesis conditions, which limits the potential synthetic diversity.

Polymers of intrinsic microporosity (PIMs) have rigid twisted structures preventing the polymer chains packing efficiently, creating S_{BET} ranging from 500 to 750 $m^2 g^{-1}$. Uniquely, linear PIM networks, S_{BET} of which is up to 1064 $m^2 g^{-1}$, have the unique advantage of being solution processable. They can be cast from solution to form good mechanical porous films.[17,18]

The new class of materials dubbed 'conjugated microporous polymers' (CMPs) in 2007 are typically prepared via metal-catalyzed cross-coupling of di- or trihalo aromatics with di- or triethynyl aromatics, and are porous poly(arylene ethynylene)s.[19–22] CMPs have stable, excellent S_{BET} and interesting optoelectronic properties, and consequently attract much attention in the fields of holes, hosts for chromophores and electron conductors. Furthermore, CMPs might invoke synergism effects of applications in organic devices.[23] Indeed, CMPs have been largely used as suitable compounds for devices of aggregation and excimer formation in the field of hyperbranched, dendritic or star-shaped conjugated polymers.[24–27] A large number of conjugated crosslinking bonds in CMPs provide the high accessible S_{BET} and porosities. Thus most CMPs are absolutely insoluble in any solvent. However, there are limited examples of soluble CMPs, first reported by the Cooper research group in 2012.[28–30] The Morisaki group have synthesized a kind of CMP consisting of tetrasubstituted [2.2]paracyclophane junctions, which had a relatively uniform morphology and diameters of about 0.2 μm, and was readily dispersed in common organic solvents.[31] The remarkable features of CMPs are their microporosity, high S_{BET} and extended conjugation. To date, S_{BET} of CMPs has been reported as high as 5640 $m^2 g^{-1}$.[32]

In this review, we firstly summarize the preparation routes to CMPs. The potential applications of various types of CMPs are then discussed.

PREPARATION ROUTES TO CMPS

Here, the progress in the syntheses of CMPs is summarized.[33–38] Due to the inherent rigidity of most conjugated π-systems leading to permanent microporosity, the average pore diameter is

* *Correspondence to: Qingquan Liu; Zhihua Zhou, School of Chemistry and Chemical Engineering, Key Laboratory of Theoretical Chemistry and Molecular Simulation of Ministry of Education, Hunan University of Science and Technology, Xiangtan 411201, China. qqliu@hnust.edu.cn, zhou7381@126.com*

School of Chemistry and Chemical Engineering, Key Laboratory of Theoretical Chemistry and Molecular Simulation of Ministry of Education, Hunan University of Science and Technology, Xiangtan 411201, China

Mechanical Properties and Nonisothermal Crystallization Kinetics of Polyamide 6/Functionalized TiO_2 Nanocomposites

Baoli Ou,[1,2] Zhihua Zhou,[1] Qingquan Liu,[1] Bo Liao,[1] Yan Xiao,[1] Juncheng Liu,[1] Xin Zhang,[3] Duxin Li,[2] Qiuguo Xiao,[1] Shaohua Shen[1]

[1]*School of Chemistry and Chemical Engineering, Hunan University of Science and Technology, Key Laboratory of Theoretical Chemistry and Molecular Simulation of Ministry of Education, Hunan Province College Key Laboratory of QSAR/QSPR, Xiangtan 411201, People's Republic of China*

[2]*State Key Laboratory of Powder Metallurgy, Central South University, Changsha 410083, People's Republic of China*

[3]*Hunan Province Key Laboratory of Coal Resources Clean-utilization and Mine Environment Protection, Xiangtan 411201, People's Republic of China*

Titanium dioxide (TiO_2) nanoparticles were pretreated with excessive toluene-2,4-diisocyanate (TDI) to synthesize TDI-functionalized TiO_2 (TiO_2-NCO), and then polymeric nanocomposites consisting of polyamide 6 (PA6) and functionalized-TiO_2 nanoparticles were prepared via a melt compounding method. The interfacial interaction between TiO_2 nanoparticles and polymeric matrix has been greatly improved due to the isocyanate (—NCO) groups at the surface of the functionalized-TiO_2 nanoparticles reacted with amino groups (—NH_2) or carboxyl (—COOH) groups of PA6 during the melt compounding and resulted in higher tensile and impact strength than that of pure PA6. The nonisothermal crystallization kinetics of PA6/functionalized TiO_2 nanocomposites was investigated by differential scanning calorimetry (DSC). The nonisothermal crystallization DSC data were analyzed by the modified-Avrami (Jeziorny) methods. The results showed that the functionalized-TiO_2 nanoparticles in the PA6 matrix acted as effective nucleation agents. The crystallization rate of the nanocomposites obtained was faster than that of the pure PA6. Thus, the presence of functionalized-TiO_2 nanoparticles influenced the mechanism of nucleation and accelerated the growth of PA6 crystallites. POLYM. COMPOS., 35:294–300, 2014. © 2013 Society of Plastics Engineers

Correspondence to: B. Ou; e-mail: oubaoli@163.com

Contract grant sponsor: Hunan Provincial Natural Science Foundation of China; contract grant number: 13JJA004; contract grant sponsor: Fund of State Key Laboratory of Powder Metallurgy, People's Republic of China.

DOI 10.1002/pc.22661

Published online in Wiley Online Library (wileyonlinelibrary.com).

INTRODUCTION

In recent years there has been a great deal of interest in the development of polymer based nanocomposites with low-level loadings of reinforcing materials due to their significant improvements in mechanical strength and stiffness, enhanced gas barrier behavior, reduced linear thermal expansion coefficients, and increased solvent resistance in comparison with pure polymers [1, 2]. Polyamide 6 (PA6) is a typical semicrystalline thermoplastic with a wide range of engineering applications. Up to now, numerous researchers have described nanocomposites based on PA6 matrices. The inorganic materials used to modify the PA6 were usually montmorillonite (clay) [1, 3, 4], carbon [2], nano calcium carbonate ($CaCO_3$) [5], or graphite oxide [6]. However, other cheap nanoparticles, especially those having certain functional properties, such as TiO_2 nanoparticles, have been less involved in studies according to the open Ref. 7]. TiO_2 nanoparticles have strong antibacterial and antioxidation properties. Adding TiO_2 into polymer matrix might produce nanocomposites with excellent mechanical and high antimicrobial and antioxidation properties [8]. In addition, it is well known that the physical, chemical, and mechanical properties of semicrystalline polymers depend greatly on the crystalline structure and degree of crystallinity. To control the rate of the crystallization and the degree of crystallinity and to obtain the desired properties, a great deal of effort has been devoted to studying the crystallization kinetics and its connection with material properties of PA6 and other polymers [6, 9]. The crystallization behavior of thermoplastic polymers during nonisothermal

ARTICLE

Insight into Capture of Greenhouse Gas (CO_2) based on Guanidinium Ionic Liquids

He-xiu Liu[a,b], Rui-lin Man[a*], Bai-shu Zheng[b], Zhao-xu Wang[b], Ping-gui Yi[b]

a. School of Chemistry and Chemical Engineering, Central South University, Changsha 410083, China
b. Key Laboratory of Theoretical Chemistry and Molecular Simulation of Ministry of Education, Hunan University of Science and Technology, Xiangtan 411201, China

(Dated: Received on September 24, 2013; Accepted on February 10, 2014)

Quantum mechanics and molecular dynamics are used to simulate guanidinium ionic liquids. Results show that the stronger interaction exists between guanidine cation and chlorine anion with interaction energy about 109.216 kcal/mol. There are two types of spatial distribution for the title system: middle and top. Middle mode is a more stable conformation according to energy and geometric distribution. It is also verified by radial distribution function. The continuous increase of carbon dioxide (CO_2) does not affect the structure of ionic liquids, but CO_2 molecules are always captured by the cavity of ionic liquids.

Key words: Ionic liquids, Quantum chemical calculation, Molecular dynamics simulation, Interaction energy, Radial distribution

I. INTRODUCTION

Ionic liquid is a new type of liquid compound with low melting point, low vapor pressure, high solubility, and high heat stability [1−4]. Green ionic liquid is the ionic liquid made up of recycled cations and anions, which has less volatile, recycled characteristics and is in line with the green chemistry. Over the past twenty years, synthesis of green medium and functional materials has received extensive attention from the domestic and international academic and industrial fields. The "programmable" feature of ionic liquids makes it possible to adjust its physical and chemical properties by changing the type and size of cations or anions and to design the ionic liquid with special function according to specific applications and needs. Great progress has been made in the application and research of ionic liquids so far, which has been widely used as a solvent, reaction medium, catalyst and functional material in the synthesis and catalysis, extraction and separation, electrochemistry, biological chemistry and other fields [5].

In recent years, the climate warming caused by CO_2 has become one of the focuses on environmental issues in the world. It is urgent to solve the problem of CO_2 greenhouse effect. But the CO_2 is a safe and abundant carbon resource from a point of recycling. The gaseous CO_2 can be used as a fertilizer and sterilization, *etc.* Supercritical CO_2 can also be used for food, pharmaceutical and other industries. Solid CO_2 can be used for artificial rainfall, concrete production and environmental protection, *etc.* Therefore, there is important scientific significance in fixing and recovering CO_2 industrially. Existing CO_2 fixation technologies such as biological method, physical method and chemical method have some limitations that carbon resource waste and organic solvent volatilization can lead to the problems of environment pollution, the equipment corrosion and post-processing complexity. Because of the features of low vapor pressure and strong dissolving ability of the ionic liquid, to fix CO_2 using ionic liquids has attracted great attentions. There are the following advantages in applying ionic liquid to fix CO_2. The CO_2 recycling use takes the place of the direct abandon of traditional method. Nature of the ionic liquid is stable, non-volatile and recycled. It is shown that ionic liquids have good abilities to absorb and dissolve CO_2 and show effective catalytic or sub-catalytic performances in the CO_2 conversion reaction under certain conditions [6−10].

Compared with imidazoles and phosphonium salt, guanidinium ionic liquid has more significant thermal and chemical stability, better catalytic activity and stronger biological activity *etc.* [11−13]. In addition, the charge dispersion degree is high in guanidine salt cation. Moreover, the different substituent on the three nitrogen atoms and the counter anions can be directionally designed and chosen in order to make the ionic liquid own some excellent physical or chemical properties. For example, Wang *et al.* studied the force field of the TMGL ionic liquid and the solubility of SO_2 and CO_2 from molecular danymics simulation [14]. Zhang *et al.* investigated the microscopic structure, interactions, and properties of pure ionic liquid [ppg][BF_4]

*Author to whom correspondence should be addressed. E-mail: rlman@mail.csu.edu.cn, hxliu12@hnust.edu.cn

DOI:10.1063/1674-0068/27/02/144-148

Computational and Theoretical Chemistry 1046 (2014) 20–24

Contents lists available at ScienceDirect

Computational and Theoretical Chemistry

journal homepage: www.elsevier.com/locate/comptc

Assignment of aromaticity of the classic heterobenzenes by three aromatic criteria

Bo Hou [a,b], Pinggui Yi [b,*], Zhaoxu Wang [b], Shuqun Zhang [a], Jinhua Zhao [a], Ricardo L. Mancera [c], Yongxian Cheng [a,*], Zhili Zuo [a,*]

[a] State Key Laboratory of Phytochemistry and Plant Resources in West China, Kunming Institute of Botany, Chinese Academy of Sciences, Kunming 650201, People's Republic of China
[b] Key Laboratory of Theoretical Chemistry and Molecular Simulation of Ministry of Education, Hunan University of Science and Technology, Xiangtan 411201, People's Republic of China
[c] School of Biomedical Sciences, CHIRI Biosciences, Curtin University, GPO Box U1987, Perth, WA 6845, Australia

ARTICLE INFO

Article history:
Received 21 May 2014
Received in revised form 14 July 2014
Accepted 19 July 2014
Available online 29 July 2014

Keywords:
NICS
ELF
Heterobenzenes
Global Aromaticity
π Aromaticity
σ Aromaticity

ABSTRACT

Aromaticity is a key concept in physical organic chemistry. The aromatic order of the classic heterobenzenes was reported in experiment early. However, the unambiguous criteria used to validate the aromaticity of that were controversial or inadequate in theory. In this work, the global aromaticity of the compounds has been studied using the ELF, NICS and ISE. $NICS(max)_{zz}$ was calculated based on the maximum NICS contribution to the out-of-plane zz tensor component. Two types of bonds are observed. The correlations between $NICS(max)_{\sigma zz}$ and $NICS(max)_{\pi zz}$ with respect to aromaticity are demonstrated, specifically between $NICS(max)_{\pi zz}$ and ELF_{π} (cc = 0.98) for π bonds. For σ bonds, the different electron delocalization of σ bonds out of the plane of the ring predicted well the discrepancies between $NICS(max)_{\sigma zz}$ and ELF_{σ}. The σ aromatic order of the classic heterobenzenes ($C_5H_5N > C_6H_6 > C_5H_5P > C_5H_5As > C_5H_5Bi$, C_5H_5Sb) was proved *via* the level of electronic delocalization.

1. Introduction

A variety of chemical aromaticity indices have been developed on the basis of structural criteria, the harmonic oscillator model of aromaticity (HOMA) [1–3] and ^1H NMR chemical shifts [4], among others. The aromaticity or anti-aromaticity of a chemical compound defined using these indices is usually controversial [5–7]. To have general applicability, the well-established definition of these concepts needs to be presented in a quantitative way [8–14]. Aromaticity scales based on energy considerations have been developed, such as the aromatic stabilization energies (ASEs) [15–18], which aims to measure the total stabilization energy of an aromatic ring by considering ring strain, hyperconjugation, differences in types of bonds, hybridization and the stabilization present in conjugated, non-aromatic systems. Ring strain and the presence of heteroatoms complicate the evaluation of ASEs and so the "isomerization method" was developed to consider the differences between the total energies of the methyl derivative of the aromatic system and its nonaromatic exocyclic methylene isomer, resulting in isomerisation stabilization energies (ISEs, correction = 0 kcal/mol, Scheme 1) [19]. Although analogs of heterobenzens have been synthesized since the mid-16th century, the correspondence between aromatic character and electrons has not been fully characterized theoretically. In 2010, the Ring Critical Points, the magnetic susceptibility exaltation and different NICS types were studies for hetero-benzenes of the group by Ebrahimi et al. Their observations confirmed magnetic and energetic criteria aromaticity were parallel in the present species [20]. To further confirm the above conclusion, we also presented our investigation of the aromaticity of the classic heterobenzenes C_5H_5X (X = N, P, As, Sb and Bi) using the $NICS(max)_{zz}$ and the "isomerization method") [21]. Currently, however, the lack of correlation between σ bonds and π bonds was used for evaluation of aromaticity and has not been proved by other methods. We present here a solution to this problem, via analysis of the Electron Localization Function (ELF) used for studying on the inherent laws of different types of bonds, and comparison of their trend curves with the reported data.

The Electron Localization Function approach, based on properties of the electron delocalization defined by the ELF of Becke and Edgecombe [22,23], has been introduced to explain aromaticity [24,25]. A separation of the ELF into σ and π components was shown to provide a useful scheme to discuss σ and π character

* Corresponding authors. Tel./fax: +86 871 65227196 (Z. Zuo).
E-mail address: zuozhili@mail.kib.ac.cn (Z. Zuo).

http://dx.doi.org/10.1016/j.comptc.2014.07.012
2210-271X/

Removal of Methyl Violet and Cationic Gold Yellow From Aqueous With Porous Magnetic Polymer Microspheres and its Adsorption Kinetics

Kai Liang[1], Qingquan Liu[2*], and Yue Ding[2]
[1]Department of Environmental Engineering, Shaoguan College, Shaoguan 512000, China
[2]Key Laboratory of Theoretical Chemistry and Molecular Simulation of Ministry of Education, School of Chemistry and Chemical Engineering, Hunan University of Science and Technology, Xiangtan 411201, China

Received: 30 August 2013, Accepted: 23 September 2013

SUMMARY

Porous magnetic polymer microspheres (PMPMs) were used as an adsorbent to removal of methyl violet (MV) from wastewater. Ethanol/water co-solvent mixtures in combination with various inorganic salts were used as eluents to regenerate PMPMs. The desorption capacity of the eluents were systematically investigated. The results showed that when ethanol/water co-solvents were used as the eluent, the desorption efficiency increased with the ethanol concentration. Incorporation of inorganic salts into the co-solvents greatly improved the desorption efficiency of the eluents. Among the eluents, a mixture of ethanol/water (8/2, v/v) in combination with 0.1M KCl exhibited excellent ability for recovering cationic dyes and regenerating PMPMs, which was again demonstrated during treatment of wastewater containing cationic golden yellow. Furthermore, the adsorption kinetics of methyl violet by PMPMs was also studied. It was found that the adsorption capacity depended on the initial concentration of dyes, and the pseudo-second-order model was more suitable to describe adsorption kinetics of methyl violet than the pseudo-first-order model.

Keywords: Porous magnetic microspheres; Cationic dye; Regeneration; Adsorption kinetics

1. INTRODUCTION

Cationic dyes have widely used in industries such as textiles, pulp mills, leather, paper, wool and cotton[1]. Since many organic dyes are harmful to human beings and toxic to microorganisms, removal of dyes from wastewater has received considerable attention over the past decades. Up to now, various treatment techniques such as chemical oxidation[2], biological treatment[3], coagulation[4,5], electrochemical degradation[6], membrane separation[7], and adsorption[8-13] were explored for the removal of cationic dyes from industrial dyeing wastewater. Among them, chemical or physical adsorption is generally recognized as a simple, efficient and economical technique. In this regard, many adsorbents like cyclodextrin polymer[14], ion exchange membranes[7], activated carbon[8], clay[9,10], zeolite[11], and other natural materials[12,13] have been employed for lowering concentration of cationic dyes in wastewater. However, there are still some problems in adsorption of cationic dyes by chemical or physical adsorbents, such as the high cost of regeneration[7], low flow rate[8], and difficult separation of absorbent from wastewater[12]. Hence, attempts to explore novel adsorption media and treatment processes for removal of cationic dyes from wastewater would be valuable.

In the previous publication, our research group prepared porous magnetic polystyrene microspheres (PMPMs) with functional groups, which were successfully employed as an adsorbent to remove methyl violet and basic fuchsin from wastewater[15]. In that treatment process, magnetic property of PMPMs enabled separation quite easy and simple. Regeneration was carried out by extracting PMPMs with ethanol at least twice; nevertheless, the adsorption efficiency of PMPMs declined slowly with increasing adsorption/desorption batches. Recently, our work indicated that methanol/water co-solvent in combination with KCl could effectively remove basic fuchsin and methyl violet from PMPMs[16]. Thus, in that manuscript, PMPMs exhibited excellent adsorption efficiency in adsorption/desorption batches. However, methanol is a toxic and inflammable chemical material, and long-term exposure often poses a threat to human health. Thus, in order

*Corresponding Author. E-mail: qqliu@hnust.edu.cn (QQ Liu), Tel: (86-731)5829-0045

Spectrochimica Acta Part A: Molecular and Biomolecular Spectroscopy 123 (2014) 298–302

Contents lists available at ScienceDirect

Spectrochimica Acta Part A: Molecular and Biomolecular Spectroscopy

journal homepage: www.elsevier.com/locate/saa

A novel method for aqueous synthesis of CdTe duantum dots

Lei Feng, Huiyan Kuang, Xiaoyun Yuan, Haowen Huang, Shoujun Yi, Tianlun Wang, Keqin Deng, Chunran Tang, Yunlong Zeng *

School of Chemistry and Chemical Engineering, Hunan University of Science and Technology, Xiangtan 411201, PR China
Key Laboratory of Theoretical Chemistry and Molecular Simulation of Ministry of Education of China, Hunan University of Science and Technology, Xiangtan 411201, PR China

HIGHLIGHTS

- A one-pot method to prepare CdTe QDs was developed using $NH_2OH{\cdot}HCl$ as a reduction.
- CdTe QDs were synthesized in an aqueous solution without supernumerary protection.
- The maximum photoluminescence quantum yields of the QDs can achieve to 47%.

GRAPHICAL ABSTRACT

High quality of CdTe quantum dots have been synthesized by using hydroxylamine hydrochloride as reduction. $NH_2OH{\cdot}HCl$ can play a role of supplying a protective surrounding to avoid the oxidation of Te^{2-} during QD growth without *supernumerary* N_2 protection.

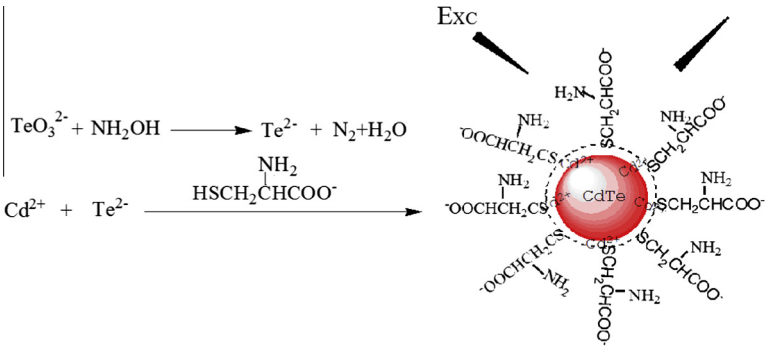

ARTICLE INFO

Article history:
Received 18 October 2013
Received in revised form 7 December 2013
Accepted 11 December 2013
Available online 21 December 2013

Keywords:
A novel method
Cadmium telluride quantum dots
Hydroxylamine hydrochloride
A new reduction
One-pot synthesis method

ABSTRACT

We have developed a simple and an economical one-pot method to synthesize water-soluble CdTe quantum dots (QDs) using hydroxylamine hydrochloride (HAH) as reduction and L-cysteine (CYS) as the ligand. The size of the CdTe QDs could easily be controlled by the duration of reflux and monitored by absorption and photoluminescence spectra. The factors influencing the photoluminescence quantum yields (PL QYs) on the QYs of CdTe NCs were investigated and the optimum conditions were determined. Under the optimum conditions (pH = 11.0, the concentration of Cd^{2+} was 1.0 mmol L^{-1} and the molar ratio of Cd^{2+}:Te^{2-}:CYS:HAH was 1:0.05:2.4:5), photoluminescence quantum yields of the CdTe QDs have been improved significantly and the maximum QYs of the QDs can achieve to 47%. The QDs were characterized by Fourier transform infrared spectrometry (FTIR), transmission-electron microscopy (TEM) and X-ray powder diffraction (XRD). The XRD patterns indicated that CdS was formed in the preparation process of CdTe QDs. This CdS shell could effectively passivate the surface trap states, and enhance the PL QY and stability of the CdTe QDs.

Introduction

Over the past two decades CdTe quantum dots, as a typical semiconductor nanomaterial, have been widely applied to nanosensors [1–3], biological labels [4,5] and electronic [6] due to their unique optical, electronic properties. For their practical application in biological systems or environmental monitoring, several strategies have been explored to make QDs water dispersible and biocompatible [7–9]. Among them, the aqueous synthesis of QDs proved to be the most effective and fascinating. Generally, an atmosphere was necessary removed during the synthesis process of thiol-CdTe QDs owing to the sensitivity of the tellurium

* Corresponding author at: School of Chemistry and Chemical Engineering, Hunan University of Science and Technology, Xiangtan 411201, PR China. Tel.: +86 13787423309.
E-mail address: yunlongzeng1955@126.com (Y. Zeng).

1386-1425/$ - see front matter © 2014 Elsevier B.V. All rights reserved.
http://dx.doi.org/10.1016/j.saa.2013.12.085

CrystEngComm

COMMUNICATION

View Article Online
View Journal | View Issue

Highly selective carbon dioxide uptake by a microporous kgm-pillared metal–organic framework with acylamide groups†

Cite this: *CrystEngComm*, 2014, **16**, 5520

Received 14th March 2014,
Accepted 27th April 2014

DOI: 10.1039/c4ce00530a

www.rsc.org/crystengcomm

Liting Du,[a] Shilong Yang,[e] Li Xu,*[abc] Huihua Min[a] and Baishu Zheng*[d]

A microporous acylamide-functionalized metal–organic framework with a kgm-pillared structure, $[Cu(NAIP^{2-})]_n$, has been designed by self-assembling $[Cu_2(COO)_4]$ paddlewheel SBUs and a novel trigonal heterofunctional ligand with a linking acylamide group. $[Cu(NAIP^{2-})]_n$ exhibits a moderate BET surface area of 1060 $m^2\ g^{-1}$, high CO_2 uptake (4.5 wt% at 0.15 bar and 298 K; 201.8 $cm^3\ g^{-1}$ at 20 bar and 298 K) and high selectivity for CO_2 over CH_4 (8.34) and N_2 (38.3) at 273 K.

Metal–organic frameworks (MOFs) assembled from metal ions or clusters (nodes) and organic building units[1] have emerged as a new type of crystalline porous materials for potential application in greenhouse gas CO_2 capture and separation (CCS) due to their high specific surface areas, tunable pore sizes and designable surface properties.[2] Compared with other classes of porous materials (*e.g.*, zeolite and active carbon), MOFs currently hold the highest record for CO_2 uptake based on physical adsorption.[3] It has been well documented that besides large porosity, high gas affinity of materials involving strong host–guest interactions is also crucial for determining the gas-uptake capacity. Thus, to obtain high-performance porous MOF materials for CCS, great efforts have been devoted to optimize framework–gas interactions by various strategies including tuning the pore size and shape,[4] catenation,[5] introducing open metal sites,[6] some specific functionalizations[7] (*e.g.*, $-NH_2$, $-NO_2$, $-OH$), *etc.* We are especially interested in the decoration of porous MOFs with polar acylamide-bridging groups, and our recent work has demonstrated that inserting polar acylamide groups into frameworks not only can effectively improve the porosity of materials but also can significantly enhance the CO_2 binding ability and selectivity of MOFs.[8]

Linking 2D layers using auxiliary pillars to assemble 3D frameworks is an attractive method to obtain highly porous MOFs, because the porosity of such layer-pillared structures can be readily fine-tuned by altering the length of pillars.[9] With this consideration in mind, we have recently synthesized a microporous MOF, NJU-Bai7,[8b] through pillaring the 2D square lattice (sql)[10] with the internal auxiliary interlinking pyridyl unit of the ligand (5-(pyridin-3-yl)isophthalic acid). NJU-Bai7 exhibits excellent CO_2 adsorption properties. To further expand the framework for CO_2 uptake, herein, we present a novel acylamide-functionalized microporous MOF with a kgm (kagomé lattice)[11]-pillared structure, termed NJFU-1‡ (NJFU denotes Nanjing Forestry University), designed from a flexible trigonal heterofunctional ligand 5-(nicotinamido)isophthalic acid (H_2NAIP).[12] NJFU-1 exhibits a moderate BET surface area of 1060 $m^2\ g^{-1}$, high CO_2 uptake (4.5 wt% at 0.15 bar and 298 K; 201.8 $cm^3\ g^{-1}$ at 20 bar and 298 K) and high selectivity for CO_2/CH_4 (8.34) and CO_2/N_2 (38.3) at 273 K.

The solvothermal reaction of H_2NAIP and $Cu(NO_3)_2{\cdot}3H_2O$ in DMF–ethanol–H_2O (3 : 3 : 0.5 in volume) at 65 °C for 48 hours afforded hexagonal crystals of NJFU-1 in high yields (Fig. S2, ESI†). The single crystal X-ray structure reveals that NJFU-1 crystallizes in the hexagonal system space group $R\bar{3}c$. In the asymmetric unit, there are one copper(II) cation and one $NAIP^{2-}$ ligand. The Cu(II) ions adopt the $Cu_2(COO)_4$ paddlewheel motif, and each Cu(II) ion is five-coordinated with four oxygen atoms and one pyridyl N-donor from five different $NAIP^{2-}$ ligands. In the structure of NJFU-1, the isophthalate moieties with a 120° angle are involved in the

[a] *Advanced Analysis and Testing Center, Nanjing Forestry University, Nanjing 210037, China. E-mail: xuliqby@njfu.edu.cn; Tel: +86 25 68257501*
[b] *College of Science, Nanjing Forestry University, Nanjing 210037, China*
[c] *Jiangsu Key Lab of Biomass-Based Green Fuels and Chemicals, Nanjing 210037, China*
[d] *Key Laboratory of Theoretical Chemistry and Molecular Simulation of Ministry of Education, School of Chemistry and Chemical Engineering, Hunan University of Science and Technology, Xiangtan 411201, China. E-mail: zbaishu@163.com; Tel: +86 731 58290045*
[e] *College of Chemistry and Chemical Engineering, Nanjing Forestry University, Nanjing 210037, China*

† Electronic supplementary information (ESI) available: Experimental details, TGA plots, PXRD patterns, heat of adsorption of CO_2 and CH_4, sorption selectivity calculations. CCDC 981374. For ESI and crystallographic data in CIF or other electronic format see DOI: 10.1039/c4ce00530a

Analytica Chimica Acta 852 (2014) 236–243

Contents lists available at ScienceDirect

Analytica Chimica Acta

journal homepage: www.elsevier.com/locate/aca

Multiplex sensor for detection of different metal ions based on on–off of fluorescent gold nanoclusters

Qian Zhao, Shenna Chen, Lingyang Zhang, Haowen Huang *, Yunlong Zeng, Fengping Liu

Key Laboratory of Theoretical Organic Chemistry and Function Molecule, Ministry of Education, Hunan Provincial University Key Laboratory of QSAR/QSPR, School of Chemistry and Chemical Engineering, Hunan University of Science and Technology, Xiangtan, China

HIGHLIGHTS

- A multiplex sensor for detection of Fe^{3+}, Cu^{2+} and Hg^{2+} ions was developed.
- This sensor provides highly selective detection for the three kinds of metal ions.
- Sensitive detection of Fe^{3+}, Cu^{2+} and Hg^{2+} in real sample of fish was achieved.

GRAPHICAL ABSTRACT

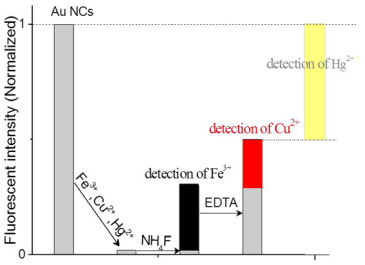

ARTICLE INFO

Article history:
Received 4 July 2014
Received in revised form 13 September 2014
Accepted 19 September 2014
Available online 23 September 2014

Keywords:
Multiplex sensor
Gold nanoclusters
Fluorescence
Metal ions
Fish

ABSTRACT

In this study, a multiplex fluorescence sensor for successive detection of Fe^{3+}, Cu^{2+} and Hg^{2+} ions based on "on–off" of fluorescence of a single type of gold nanoclusters (Au NCs) is described. Any of the Fe^{3+}, Cu^{2+} and Hg^{2+} ions can cause quenching fluorescence of Au NCs, which established a sensitive sensor for detection of these ions respectively. With the introduction of ethylene diamine tetraacetic acid (EDTA) to the system of Au NCs and metal ions, a restoration of fluorescence may be found with the exception of Hg^{2+}. A highly selective detection of Hg^{2+} ion is, thus, achieved by masking Fe^{3+} and Cu^{2+}. On the other hand, the masking of Fe^{3+} and Cu^{2+} leads to the enhancement of fluorescence of Au NCs, which in turn provides an approach for successive determination of Fe^{3+} and Cu^{2+} based on "on–off" of fluorescence of Au NCs. Moreover, this assay was applied to the successful detection of Fe^{3+}, Cu^{2+} and Hg^{2+} in fish, a good linear relationship was found between these metal ions and the degree of quenched fluorescent intensity. The dynamic ranges of Hg^{2+}, Fe^{3+} and Cu^{2+} were 1.96×10^{-10}–1.01×10^{-9}, 1.28×10^{-7}–1.27×10^{-6} and 1.2×10^{-7}–1.2×10^{-6} M with high sensitivity (the limit of detection of Fe^{3+} 2.0×10^{-8} M, Cu^{2+} 1.9×10^{-8} M and Hg^{2+} 2×10^{-10} M). These results indicate that the assay is suitable for sensitive detection of these metal ions even under the coexistence, which can not only determine all three kinds of metal ions successively but also of detecting any or several kinds of metal ions.

1. Introduction

Fluorescent nanomaterials have shown great potential applications in sensing [1,2], imaging [3,4], photovoltaics [5], catalysis [6] and light emitting devices [7]. Among these nanomaterials, noble metal nanoclusters, such as gold nanoclusters and silver nanoclusters, have received much attention recently owing to the ultra-small size, non-toxicity and highly fluorescent properties [8–11]. Their fundamental physicochemical properties are much dependent on the sub-nanometer structure. The size of the nanoclusters is comparable to the Fermi wavelength of an electron, and these nanoclusters exhibit molecule-like properties in the absorption and fluorescence feature.

In recent years, highly luminescent and stable nanoclusters have been extensively reported as fluorescence probes for a wide range of targets, including small ions [12,13], small molecules such

* Corresponding author. Tel.: +86 731 58290045.
E-mail address: hhw@hnust.edu.cn (H. Huang).

http://dx.doi.org/10.1016/j.aca.2014.09.029
0003-2670/

Journal of The Electrochemical Society, **161** (1) A10-A13 (2014)
0013-4651/2014/161(1)/A10/4/$31.00 © The Electrochemical Society

Electrochemical Performance of α-$LiVOPO_4$/Carbon Composite Material Synthesized by Sol–Gel Method

Anping Tang,[a,b,z] Jie Shen,[a] Yongjun Hu,[c] Guorong Xu,[a,b] Donghua He,[a] Qingfeng Yi,[a,b] and Ronghua Peng[a,b]

[a]*School of Chemistry and Chemical Engineering, Hunan University of Science and Technology, Xiangtan 411201, China*
[b]*Key Laboratory of Theoretical Chemistry and Molecular Simulation of Ministry of Education, Hunan University of Science and Technology, Xiangtan 411201, China*
[c]*Department of Chemistry, Hunan City University, Yiyang 413000, China*

$LiVOPO_4$/carbon composite materials were prepared at a moderate temperature of 400°C by oxalic acid assisted sol-gel technique and acetylene black acting as a carbon source. The as synthesized composite materials were characterized by XRD, SEM, galvanostatic charge–discharge and CV measurements. When tested at 0.1 C rate for Li ion insertion properties, α-$LiVOPO_4$/ carbon composite material exhibits good cycle capability with an average capacity degradation of just 0.05 mAh/g per cycle. Additionally, when the various discharge rates were applied progressively for each of ten cycles, it shows excellent rate capability with initial discharge capacities of 138 mAh/g (0.1 C), 134 mAh/g (0.2 C), 108 mAh/g (0.5 C) and 83 mAh/g (1 C), respectively, indicating that carbon modification could enhance the electronic conductivity of $LiVOPO_4$.
 [DOI: 10.1149/2.005401jes]

Manuscript submitted August 12, 2013; revised manuscript received October 7, 2013. Published October 30, 2013.

Since olivine structure $LiFePO_4$ phosphates were first reported as cathode materials for lithium-ion batteries by Padhi et al.,[1] a series of polyanion-based cathode materials have recently been identified as potential electroactive materials for lithium-ion battery applications.[2–12] In the continuing hunt for perfect polyanion insertion hosts, the lithium vanadyl phosphate ($LiVOPO_4$) system has also received some recent attention.[11–18] $LiVOPO_4$ occurs in different crystallographic phases such as triclinic α-$LiVOPO_4$ and orthorhombic β-$LiVOPO_4$, and it has a theoretical capacity of ∼159 mAh/g, which is slightly lower than $LiFePO_4$ (170 mAh/g). In addition to this, it shows a higher lithium intercalation potential (∼3.9 V vs Li/Li^+). The high theoretical energy density (158 mAh/g × 3.9 V = 616 Wh/kg), which is larger than the 578 Wh/kg for $LiFePO_4$, makes it to be a fascinating.

Although the insertion properties of $LiVOPO_4$ phases are relatively encouraging, phosphate cathode materials have low electrical conductivity due to localization of electrons; for example, diffuse reflectance spectra analysis, AC impedance and density functional theory calculation by Yang et al.[19] demonstrated that triclinic α-$LiVOPO_4$ is a wide bandgap semiconductor with an extremely low conductivity. Therefore, it is necessary to improve their conductivity to make them useful in practical applications. Recently, enhanced Li-storage capacities in these cathodes were demonstrated by strategies of mixing conductive additives and morphology tailoring.[11–16,20]

In light of these aspects, we demonstrated the sol-gel synthesis of α-$LiVOPO_4$/carbon composite material using oxalic acid that serve as a chelating agent and acetylene black that affords an electrical conduction network which ultimately enhances α-$LiVOPO_4$ cathode performance.

Experimental

$LiVOPO_4$/carbon composite material was synthesized through a sol-gel route. Starting materials were lithium hydroxide monohydrate ($LiOH \cdot H_2O$, purity 95%), vanadium pentoxide (V_2O_5, purity 98%), ammonium dihydrogen phosphate ($NH_4H_2PO_4$, purity 99.99%), oxalic acid dihydrate ($H_2C_2O_4 \cdot 2H_2O$, purity 99.5%), acetylene black and carbowax 2000 (namely polyethylene glycol 2000, purity 99%) as a nonionic surfactant. All chemicals are of analytical grade from Kemiou Chemical Reagent Company (Tianjin, China) except acetylene black. 4.342 g Oxalic acid dihydrate was first dissolved in 40 mL distilled water, which was employed as both a reductant and a chelating reagent. 1.252 g V_2O_5 powder was slowly added into the oxalic acid solution with magnetic stirring at 70°C for about 30 min. The redox reaction may proceed through the following reaction:

$$V_2O_5 + 3H_2C_2O_4 \rightarrow 2VOC_2O_4 + 3H_2O + 2CO_2$$

After a clear blue solution formed, stoichiometric $LiOH \cdot H_2O$, $NH_4H_2PO_4$ and an appropriate amount of carbowax were added to the solution. Then a certain amount of acetylene black was introduced into the solution. The obtained mixture was dried at 90°C in air to get a gel. Finally, the $LiVOPO_4$/carbon composite materials were obtained by pyrolysis of the precursor at 400°C for 12 h in air.

The CHN Elemental analyzer was used to measure the amount of residual carbon in the $LiVOPO_4$/carbon composite material. X-ray diffraction (XRD) pattern of the sample was recorded using a D/Max III diffractometer with Cu Kα radiation. The XRD patterns were analyzed with MDI Jade 5.0 software to identify phase and calculate Lattice parameters. The surface morphology of the sample was observed using a JSM-6380 scanning electron microscopy (SEM).

For electrochemical studies, composite electrodes were fabricated with the active material, acetylene black and binder (polyvinylidene fluoride) in the weight ratio 75:20:5 using N-methyl pyrrolidone as solvent. Electrodes were prepared using an etched aluminum foil as a current collector using the doctor-blade technique. Lithium metal foil, 1 M $LiPF_6$ in ethylene carbonate and dimethyl carbonate (1:1, v/v) and Celgard 2502 membrane were used as counter electrode, electrolyte and separator respectively to assemble coin-type cells (size 2025) in an Ar-filled glove box (Mikrouna). The active material content in the electrode was around 4∼6 mg. Charge–discharge cycling at a constant current mode was carried out using a computer controlled Neware battery tester (China) at different current rates between 3.0 and 4.5 V at room temperature. Cyclic voltammetry (CV) tests were carried out at room temperature using a computer controlled CHI660C electrochemical analyzer.

Results and Discussion

The XRD pattern of α-$LiVOPO_4$/carbon samples is shown in Figure 1. The structural refinement of the XRD pattern was done based on a triclinic structure using *P*-1 space group. The XRD results of α-$LiVOPO_4$, analyzed with MDI Jade 5.0 software, were shown in Table I, which are much closer to the previous report (ICSD #20537). It can be seen from the XRD pattern that a majority of the XRD peaks of the sample synthesized at 400°C corresponds to triclinic-$LiVOPO_4$ with a trace impurity peak of $VOPO_4$ at an angle of 28.80°, which is denoted by the symbol #. No other common impurities such as VO_2, V_2O_5, Li_3PO_4 and Li_2VPO_6 have been observed. In general, sol-gel synthesis of phase-pure α-$LiVOPO_4$ requires sintering at elevated temperatures (≥ 500°C),[19,20] however in the present case, combustion

[z]E-mail: anpingxt@126.com

Fibers and Polymers 2014, Vol.15, No.3, 519-524 DOI 10.1007/s12221-014-0519-y

Preparation of Collagen Fiber/$CaCO_3$ Hybrid Materials and Their Applications in Synthetic Paper

Hu Zhou*, Ruiping Xun, Zhihua Zhou*, Qingquan Liu, Peng Wu, and Kejian Wu

Key Laboratory of Theoretical Chemistry and Molecular Simulation of Ministry of Education, School of Chemistry and Chemical Engineering, Hunan University of Science and Technology, Xiangtan City 411201, China

(Received June 15, 2013; Revised August 16, 2013; Accepted August 24, 2013)

Abstract: The collagen fiber/$CaCO_3$ hybrid materials were successfully prepared via *in situ* organic-inorganic hybrid technique. The surface morphology, hybrid mechanism, thermal and hydrothermal stability of these materials were investigated, respectively. Scanning electron microscopy (SEM) analysis showed that the size scale and distribution of $CaCO_3$ particles in collagen fiber relied on the concentration of $CaCl_2$. When the $CaCl_2$ was at low concentration, for example 6 wt%, the in-situ produced $CaCO_3$ particles were distributed evenly around the collagen fiber, the particle size could be controlled in the range of 2-4 μm and no apparent coagulation of $CaCO_3$ particles was found. Fourier transform infrared spectroscopy (FTIR) study revealed the interactions between the collagen fiber and $CaCO_3$ particles. The water solubility test and TGA analysis indicated that the solubility of collagen fiber in hot water decreased significantly after hybridization with $CaCO_3$ particles, whereas, the decomposition temperature was improved with increasing of the production of $CaCO_3$ particles. Moreover, the hybrid materials were used in conjunction with polyurethane and $CaCO_3$ powder to fabricate a novel synthetic paper. The result showed that the synthetic paper had good writing and printing.

Keywords: Collagen fiber, $CaCO_3$, Organic-inorganic hybrid, Thermal and hydrothermal stability, Synthetic paper

Introduction

Leather industry has been categorized as one of the highly polluting industries because of generation of huge amount liquid and solid wastes. Solid wastes are mainly skin trimmings, keratin wastes, fleshing wastes, chrome shaving wastes and buffing wastes [1,2]. According to research, these solid wastes are mainly made of collagen fiber, accounting for more than 80 % of the total content [3]. Collagen fiber, as a natural macromolecular material, has a wide variety of applications owing to its cell attachment capabilities, excellent biocompatibility and biodegradability and weak antigenicity [4-7]. So if we could extract collagen fiber from the large quantities of leather solid wastes and make good use of it, we could not only decrease environmental pollution but also increase economic benefits of leather industry.

The synthetic paper is a kind of plastic modification composite material gathering the synthetic resin, inorganic filler and chemical additives [8-10]. Recently, the synthetic paper has been widely applied in many fields due to its some excellent performances such as high specific strength, good shading, tear and wear resistance, etc. [11]. But despite these superior performances, there are still some problems to be improved and perfected in production of synthetic paper. For example, the synthetic resin, one of the key components of the synthetic paper, are typically some of hydrophobic polyolefins (such as polyethylene, polypropylene, polystyrene, etc.), while the ink used for writing and printing is the aqueous dispersion of ink molecules, so obviously this difference causes an exclusion effect between the synthetic paper and printing ink and it discourages the writing and printing of paper [12,13]. On the basis of principles of leather processing, collagen fiber contains abundant functional groups like -OH, -COOH, and -NH_2, and has good hydrophilicity and adsorbability [14]. Therefore, it gives us an inspiration to fabricate a synthetic paper with good writing and printing by using collagen fiber as raw materials. Nevertheless, collagen fiber, as a natural macromolecular material, often has some intrinsic shortcomings when used alone, such as fragility, low molecular weight, low mechanical strength, hard to process into film, soluble in water and bad thermal stability [15]. Thus, improvements must to be done in collagen fiber to make it be better used for synthetic paper.

In recent years, polymer-based organic-inorganic hybrid materials have attracted great interest from researchers since they frequently exhibit excellent properties synergistically derived from two components. The frequently-used inorganic particles used in polymer modification include SiO_2 [16-18], TiO_2 [6,19,20], $CaCO_3$ [21,22], etc. Among the various kinds of inorganic particles, $CaCO_3$ is widely used because of its advantages of no toxicity, structural stability, flame resistance, and ecological friendliness [21]. It is also widely used as inorganic filler in production of synthetic paper for its high whiteness, good oil absorbency, low cost and natural bio-degradability [9,10]. Up to now, a number of study about collagen fiber/SiO_2 [17,18] and /TiO_2 [6,20] hybrid materials have been reported, but there is few report on the collagen fiber/$CaCO_3$ hybrid materials.

In this study, a collagen fiber/$CaCO_3$ hybrid material was prepared via *in situ* organic-inorganic hybrid technique.

*Corresponding author: hnustchem@163.com
*Corresponding author: zhouzhihuawy@163.com

Analyst

PAPER

View Article Online
View Journal | View Issue

Cite this: *Analyst*, 2014, **139**, 1498

Colorimetric and ultra-sensitive fluorescence resonance energy transfer determination of H_2O_2 and glucose by multi-functional Au nanoclusters†

Qian Zhao,[a] Shenna Chen,[a] Haowen Huang,*[a] Lingyang Zhang,[a] Linqian Wang,[b] Fengping Liu,[a] Jian Chen,[a] Yunlong Zeng[a] and Paul K. Chu*[c]

Received 9th October 2013
Accepted 5th December 2013

DOI: 10.1039/c3an01906c

www.rsc.org/analyst

Ultra-sensitive colorimetric determination of H_2O_2 is accomplished based on the intrinsic peroxidase-like activity of Au nanoclusters (AuNCs) stabilized by glutathione (GSH). The color change of 3,3,5,5-tetramethylbenzidine (TMB) catalyzed by AuNCs offers an indirect method to measure glucose. This sensing platform makes use of a dual optical signal change, including the color change in an aqueous solution under visible light illumination and an ultra-sensitive fluorescent assay arising from efficient fluorescence resonance energy transfer (FRET) between the AuNCs and oxidized TMB. The detection limits of H_2O_2 and glucose are 4.9×10^{-13} M and 1.0×10^{-11} M, respectively. In addition, enhanced fluorescence is observed from the AuNCs due to the use of ethanol which produces clear changes in the quantum yield and lifetime of the AuNCs. The quantum yield of AuNCs is enhanced from ~12.5% as an isolated fluorophore to 38.9% in an AuNCs–ethanol complex. The enhanced fluorescence lowers the detection limits of H_2O_2 and glucose by 2 orders of magnitude compared to those attained from the original AuNCs.

Introduction

Noble metal nanoclusters comprising several to tens of atoms possess distinct electronic structures and properties that are fundamentally different from those of larger nanoparticles.[1–5] Their unique physicochemical properties have been exploited in molecular electronics,[6] image markers,[7,8] sensors,[9,10] and catalysts.[11,12] In particular, fluorescent Au and Ag nanoclusters have been used in biological imaging,[13,14] ion sensors,[15,16] and biosensors[17] due to their low toxicity, excellent biocompatibility and stability, good solubility, and desirable luminescence properties.

Catalysis is another promising application of noble metal nanoclusters. Gold was initially thought to be catalytically inert, but nano-scale gold has been demonstrated to exhibit excellent catalytic activity in many chemical reactions.[18,19] An important application of Au nanoclusters (AuNCs) is as artificial enzymes.[20,21] Enzyme mimetics receives much interest because natural enzymes have some intrinsic drawbacks. For example, the catalytic activity is sensitive to environmental conditions and the stability is poor due to denaturation.[22,23] Most research activities focus on the fluorescent properties of metal nanoclusters, but their catalytic properties and potential applications in biological or chemical sensing are also quite important. An Au-nanoparticle-based nano-energy-transfer probe has been developed recently for the rapid and ultra-sensitive determination of mercury.[24] The good stability of AuNCs arises from the chemical inertness of the Au core which is completely encapsulated by ligands, thereby rendering their use in fluorescence resonance energy transfer (FRET) possible. As reported in this paper, AuNCs stabilized by GSH are found to possess intrinsic peroxidase-like activity, which catalyzes oxidation of the peroxidase substrate 3,3,5,5-tetramethylbenzidine (TMB) in the presence of H_2O_2, and ultra-sensitive determination of H_2O_2 and glucose is demonstrated.

Experimental

Chemicals

TMB, GSH, $HAuCl_4 \cdot 3H_2O$, 30% H_2O_2, anhydrous ethanol, glucose, glucose oxidase, cupric chloride ($CuCl_2$), ferric chloride ($FeCl_3$), and mercuric chloride ($HgCl_2$) were purchased from Sinopharm Chemical Reagent Co., Ltd. (Shanghai, China). All of the chemicals, unless mentioned otherwise, were of analytical

[a]*Laboratory of Theoretical Chemistry and Molecular Simulation of Ministry of Education, Hunan Provincial University Key Laboratory of QSAR/QSPR, School of Chemistry and Chemical Engineering, Hunan University of Science and Technology, Xiangtan, China. E-mail: hhwn09@163.com; Tel: +86-731-58290045*

[b]*Department of Laboratory, Hunan Provincial Tumor Hospital, The Affiliated Tumor Hospital of Xiangya Medical School of Central South University, Changsha, Hunan Province, China*

[c]*Department of Physics & Materials Science, City University of Hong Kong, Tat Chee Avenue, Kowloon, Hong Kong, China. E-mail: paul.chu@cityu.edu.hk; Fax: +86-852-34420542; Tel: +86-852-34427724*

† Electronic supplementary information (ESI) available. See DOI: 10.1039/c3an01906c

Journal of Theoretical and Computational Chemistry
Vol. 13, No. 1 (2014) 1450001 (22 pages)

DOI: 10.1142/S0219633614500011

World Scientific
www.worldscientific.com

Theoretical investigation on the interplay of hydrogen bond and halogen bond in $HX\cdots(BrCl)_n$ (X = F, Cl, Br and $n = 1, 2$) complexes

Hexiu Liu[*,†,‡], Ruilin Man[*,§], Zhaoxu Wang[†], Pinggui Yi[†] and Jingjing Liu[*]

[*]*School of Chemistry and Chemical Engineering*
Central South University
Changsha 410083, P. R. China

[†]*Key Laboratory of Theoretical Chemistry and Molecular Simulation of Ministry of Education*
Hunan University of Science and Technology
Xiangtan 411201, P. R. China
[‡]*hxliu12@hnust.edu.cn*
[§]*rlman@mail.csu.edu.cn*

Received 14 September 2013
Accepted 11 October 2013
Published 2 January 2014

Quantum chemical calculations at the MP2 level with the aug-cc-pVTZ basis set were used to investigate the $HX\cdots(BrCl)_n$ (X = F, Cl, Br and $n = 1, 2$) complexes. They are connected via hydrogen bond or halogen bond in dimers and together in trimers. Molecular geometries, interaction energies, cooperative energies and atomic charge of dyads and triads have been studied at the Mp2/aug-cc-pVTZ computational level. All studied trimers show cooperativity with the simultaneous presence of a hydrogen and one or two halogen bond. The molecular electrostatic potential has been employed to explore the formation mechanisms of these molecular complexes. The AIM analysis has been performed at the Mp2/aug-cc-pVTZ level to examine the topological characteristics, confirming the coexistence of hydrogen bonds and one or two halogen bond for each complex.

Keywords: Halogen bond; hydrogen bond; interplay; electrostatic potential; AIM analysis.

1. Introduction

Halogen bond[1] is one of the most important intermolecular interactions which has been widely investigated both experimentally and theoretically, because of their great significance in molecular recognition,[2–4] crystal materials,[5–7] supermolecular chemistry,[8,9] and biological system.[10,11] Halogen bond is an attractive interaction between the covalent-bonded halogen atom and Lewis bases. The reason halogen atom can form halogen bond with an electronegative atom or group is the existence

[§]Corresponding author.

Spectrochimica Acta Part A: Molecular and Biomolecular Spectroscopy 133 (2014) 372–377

Contents lists available at ScienceDirect

Spectrochimica Acta Part A: Molecular and Biomolecular Spectroscopy

journal homepage: www.elsevier.com/locate/saa

Study on the interaction between carbonyl-fused N-confused porphyrin and bovine serum albumin by spectroscopic techniques

Xianyong Yu [a,b,c,*], Zhixi Liao [a], Bingfei Jiang [a], Lingyi Zheng [a], Xiaofang Li [a,*]

[a] Key Laboratory of Theoretical Organic Chemistry and Function Molecule, Ministry of Education, Hunan Province College Key Laboratory of QSAR/QSPR, School of Chemistry and Chemical Engineering, Hunan University of Science and Technology, Xiangtan 411201, China
[b] State Key Laboratory of Physical Chemistry of Solid Surfaces, Xiamen University, Xiamen 361005, China
[c] Key Laboratory of Computational Physical Sciences, Fudan University, Ministry of Education, Shanghai, China

HIGHLIGHTS

- The interaction between BSA and CF-NCP was studied.
- The fluorescence quenching mechanism is a static quenching procedure.
- The binding constants and binding sites were calculated.
- Electrostatic force played a major role in stabilizing the complex.
- The conformation of BSA was affected by CF-NCP.

GRAPHICAL ABSTRACT

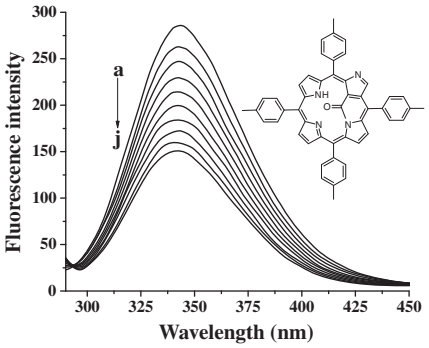

ARTICLE INFO

Article history:
Received 22 March 2014
Received in revised form 12 May 2014
Accepted 25 May 2014
Available online 11 June 2014

Keywords:
Interaction
Carbonyl fused N-confused porphyrin
Bovine serum albumin
Fluorescence spectroscopy
Ultraviolet–visible spectroscopy

ABSTRACT

The interaction between carbonyl-fused N-confused porphyrin (CF-NCP) and bovine serum albumin (BSA) was investigated by fluorescence and ultraviolet–visible (UV–Vis) spectroscopy. The results indicated that CF-NCP has strong ability to quench the intrinsic fluorescence of BSA by forming complexes. The binding constants (K_a), binding sites (n) were obtained. The corresponding thermodynamic parameters (ΔH, ΔS and ΔG) of the interaction system were calculated at three different temperatures. The results revealed that the binding process is spontaneous, and the acting force between CF-NCP and BSA were mainly electrostatic forces. According to Förster non-radiation energy transfer theory, the binding distance between CF-NCP and BSA was calculated to be 4.37 nm. What is more, the conformation of BSA was observed from synchronous fluorescence spectroscopy.

Introduction

The proteins are the most abundant macromolecules in biological cells, and meanwhile, they are also the fundamental substances that express various biological functions [1]. Serum albumins are the major soluble proteins in the circulatory system. The binding ability of drug–albumin in blood stream may have a significant impact on the distribution, free concentration, metabolism and toxicity of drugs [2,3]. Bovine serum albumin (BSA) has been one of the most extensively studied of this group of proteins, particularly because of its structural homology with human serum albumin (HSA) [4]. Besides, in this work, BSA is selected as our protein model because of its medical importance, stability, low cost, unusual ligand-binding properties [5,6].

* Corresponding authors. Address: Key Laboratory of Theoretical Organic Chemistry and Function Molecule, Ministry of Education, Hunan Province College Key Laboratory of QSAR/QSPR, School of Chemistry and Chemical Engineering, Hunan University of Science and Technology, Xiangtan 411201, China (X. Yu). Tel.: +86 731 58290187; fax: +86 731 58290509.
E-mail addresses: yu_xianyong@163.com (X. Yu), lixiaofang@iccas.ac.cn (X. Li).

http://dx.doi.org/10.1016/j.saa.2014.05.085
1386-1425/

Spectrochimica Acta Part A: Molecular and Biomolecular Spectroscopy 129 (2014) 314–319

Contents lists available at ScienceDirect

Spectrochimica Acta Part A: Molecular and Biomolecular Spectroscopy

journal homepage: www.elsevier.com/locate/saa

Interaction between pirenoxine and bovine serum albumin in aqueous solution

Zhixi Liao [a], Xianyong Yu [a,b,c,*], Qing Yao [a], Pinggui Yi [a,*]

[a] Key Laboratory of Theoretical Chemistry and Molecular Simulation of Ministry of Education, Hunan Province College Key Laboratory of QSAR/QSPR, School of Chemistry and Chemical Engineering, Hunan University of Science and Technology, Xiangtan 411201, PR China
[b] State Key Laboratory of Physical Chemistry of Solid Surfaces, Xiamen University, Xiamen 361005, PR China
[c] Key Laboratory of Computational Physical Sciences (Fudan University), Ministry of Education, Shanghai 200433, PR China

HIGHLIGHTS

- We explored the interaction between BSA and PRX by spectroscopic methods.
- The mainly binding forces are hydrophobic interactions.
- The fluorescence quenching mechanism is static quenching.
- The binding constants and binding sites were calculated.
- The conformation of BSA was changed due to the impact of PRX.

GRAPHICAL ABSTRACT

The interaction between prenoxine sodium (PRX) and bovine serum albumin (BSA) was studied by fluorescence, circular dichroism (CD) and UV–vis spectroscopy. The quenching mechanism, binding constants, and binding distance were determined. Conformation change of BSA was also observed.

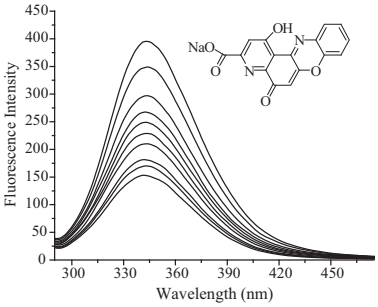

ARTICLE INFO

Article history:
Received 26 December 2013
Received in revised form 12 March 2014
Accepted 20 March 2014
Available online 1 April 2014

Keywords:
Bovine serum albumin
Prenoxine
Interaction
Spectroscopic means
Circular dichroism spectra

ABSTRACT

This work concerns the interaction of prenoxine sodium (PRX) and bovine serum albumin (BSA), which was conducted by spectroscopic means: fluorescence spectra, ultraviolet–visible spectra (UV–vis) and circular dichroism spectra (CD spectra) in physiological conditions. The results revealed the PRX can quench the fluorescence of BSA remarkably in aqueous solution. The quench mechanism has been obtained after corrected the fluorescence intensities for inner filter effects. The binding constants (K_a) were calculated according to the relevant fluorescence data at different temperatures. Moreover, from a series of analyses, we have obtained the binding sites, the binding distance and binding force. The effect of PRX on the conformation of BSA has been analyzed using synchronous fluorescence under experimental conditions. In addition, the CD spectra proved that the secondary structure of BSA changed in the presence of PRX in aqueous solution.

Introduction

Serum albumin, the major soluble protein in blood circulation, contributing many physiological functions of which most important are serving as a depot and a transport protein for many endogenous and exogenous drugs reversibly, has been one of the most

* Corresponding authors. Address: Key Laboratory of Theoretical Chemistry and Molecular Simulation of Ministry of Education, Hunan Province College Key Laboratory of QSAR/QSPR, School of Chemistry and Chemical Engineering, Hunan University of Science and Technology, Xiangtan 411201, PR China (X. Yu). Tel.: +86 731 58290187; fax: +86 731 58290509.
E-mail addresses: yu_xianyong@163.com (X. Yu), pgyi@hnust.cn (P. Yi).

http://dx.doi.org/10.1016/j.saa.2014.03.057
1386-1425/

Spectrochimica Acta Part A: Molecular and Biomolecular Spectroscopy 125 (2014) 285–289

Contents lists available at ScienceDirect

Spectrochimica Acta Part A: Molecular and Biomolecular Spectroscopy

journal homepage: www.elsevier.com/locate/saa

Visual determination of trace Cysteine based on promoted corrosion of triangular silver nanoplates by sodium thiosulfate

Xin Yan Hou, Shu Chen, Jian Tang, Yun Fei Long *

Key Laboratory of Theoretical Chemistry and Molecular Simulation of Ministry of Education of China, School of Chemistry and Chemical Engineering, Hunan University of Science and Technology, Xiangtan 411201, China

HIGHLIGHTS

- A new colorimetric strategy for Cysteine detection is demonstrated.
- The $Na_2S_2O_3$ improved the sensitivity for Cysteine detection.
- 0.025 μM Cysteine could be detected by naked eye.

GRAPHICAL ABSTRACT

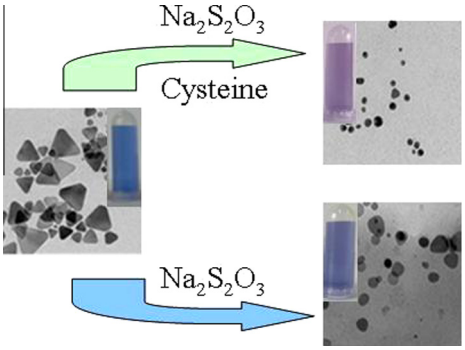

ARTICLE INFO

Article history:
Received 26 November 2013
Received in revised form 21 January 2014
Accepted 26 January 2014
Available online 5 February 2014

Keywords:
Triangular silver nanoplates
Cysteine
Sodium thiosulfate
Absorption spectrum

ABSTRACT

In this study, triangular silver nanoplates (TAg-NPs) were used to detect trace Cysteine concentration in the presence of sodium thiosulfate ($Na_2S_2O_3$). Study showed that the TAg-NPs could be gently etched by Cysteine with the concentration of 1.0×10^{-7} mol L^{-1} through forming Ag–S covalent bond at the three corners. However, in the presence of $Na_2S_2O_3$ (only 3.0×10^{-6} mol L^{-1}), the corrosion of Cysteine on TAg-NPs can be promoted significantly. It was also found that the color, morphology, and the maximum absorption wavelength of TAg-NPs change clearly with the concentrations of Cysteine as low as 2.5×10^{-8} mol L^{-1}. Furthermore, the wavelength shift values ($\Delta\lambda$) of TAg-NPs solution were proportional to the concentrations of Cysteine in the range of 1.0×10^{-9}–1.0×10^{-7} mol L^{-1}, and the linear regression equation is $\Delta\lambda = -0.89 + 319.94\,c$ (c, μM, $n = 5$) with the correlation coefficient of 0.990. At the same time, the color change of the TAg-NPs solution could be observed clearly by the naked eyes with increasing Cysteine concentrations in the range of 2.5×10^{-8}–1.0×10^{-7} mol L^{-1}. Thus, a novel method for the detection of Cysteine by either UV–vis spectrophotometry detection or naked eyes observation is established. It allows determination of Cysteine content in compound amino acid injection sample of 18AA-V.

Introduction

So far, many silver nanomaterials have applied to the detection of Cysteine successfully [1–3]. Silver nanoparticles in different shapes could display different optical properties and colors (like red, green, yellow, and blue respectively) [4,5]. Thus, the shape-controlled synthesis of silver nanoplates attracts many chemists attention. Recently, different morphologies and colors of silver nanomaterials with cubic [6], triangular [7,8], and hexagonal [9,10] shapes have been synthesized. In this study, the triangular silver nanoplates (TAg-NPs) with the color of blue was synthesized

* Corresponding author. Tel.: +86 731 58388503; fax: +86 731 58372324.
E-mail address: l_yunfei927@163.com (Y.F. Long).

http://dx.doi.org/10.1016/j.saa.2014.01.098
1386-1425/

Spectrochimica Acta Part A: Molecular and Biomolecular Spectroscopy 118 (2014) 765–775

Contents lists available at ScienceDirect

Spectrochimica Acta Part A: Molecular and Biomolecular Spectroscopy

journal homepage: www.elsevier.com/locate/saa

Chelating stability of an amphoteric chelating polymer flocculant with Cu(II), Pb(II), Cd(II), and Ni(II)

Lihua Liu *, Yanhong Li, Xing Liu, Zhihua Zhou, Yulin Ling

Key Laboratory of Theoretical Chemistry and Molecular Simulation of Ministry of Education and Hunan Province, Hunan Province College Key Laboratory of QSAR/QSPR, School of Chemistry and Chemical Engineering, Hunan University of Science and Technology, Xiangtan, Hunan 411201, PR China

HIGHLIGHTS

- Determination of the ultraviolet spectra of ACPF and its chelates with heavy metals.
- Determination of the compositions and stability constant of the chelates.
- The chelating precipitates are very stable at pH above 5.6.
- A chelating mechanism of ACPF with heavy metal ion was proposed.
- The stability mechanism of the chelating precipitates was explored at different pH.

GRAPHICAL ABSTRACT

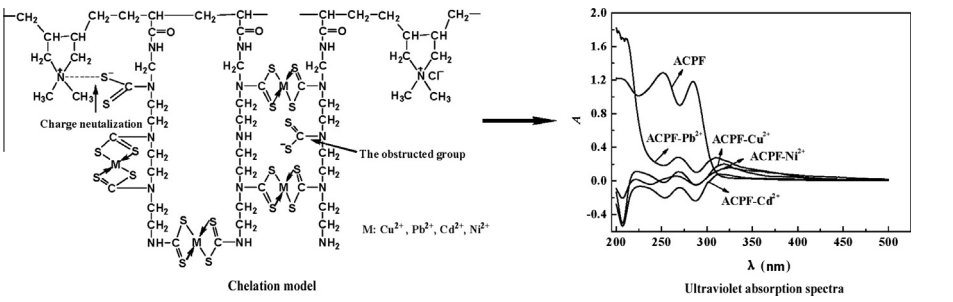

ARTICLE INFO

Article history:
Received 5 November 2012
Received in revised form 8 September 2013
Accepted 25 September 2013
Available online 4 October 2013

Keywords:
Stability constant
Amphoteric chelating polymer flocculant
Heavy metal ions
Ultraviolet spectrophotometric method
Leaching-out characteristics

ABSTRACT

The absorption spectra of Cu^{2+}, Pb^{2+}, Cd^{2+}, and Ni^{2+} chelates of an amphoteric chelating polymer flocculant (ACPF) were measured by ultraviolet spectrophotometry, and their compositions and stability constants (β) were calculated. ACPF exhibited three apparent absorption peaks at 204, 251, and 285 nm. The —CSS^- group of ACPF reacted with Cu^{2+}, Ni^{2+}, Pb^{2+}, and Cd^{2+} to form ACPF–Cu^{2+}, ACPF–Ni^{2+}, ACPF–Pb^{2+}, and ACPF–Cd^{2+} chelates, respectively, according to a molar ratio of 2:1. The maximum absorption peaks of ACPF–Cu^{2+}, ACPF–Ni^{2+}, ACPF–Pb^{2+}, and ACPF–Cd^{2+} appeared at 319, 326, 310, and 313.5 nm, respectively. The maximum absorption peaks of the chelates showed significant red shifting compared with the absorption peaks of ACPF. The β values of the ACPF–Cu^{2+}, ACPF–Pb^{2+}, ACPF–Cd^{2+}, and ACPF–Ni^{2+} chelates were $(1.37 \pm 0.35) \times 10^{12}$, $(3.26 \pm 0.39) \times 10^{11}$, $(2.05 \pm 0.27) \times 10^{11}$, and $(3.04 \pm 0.45) \times 10^{10}$, respectively. The leaching rate of heavy metal ions from the chelating precipitates decreased with increasing pH. ACPF–Cu^{2+}, ACPF–Ni^{2+}, ACPF–Pb^{2+}, and ACPF–Cd^{2+} were very stable at pH $\geqslant$ 5.6. Cu^{2+}, Ni^{2+}, Pb^{2+}, and Cd^{2+} concentrations in the leaching liquors were lower than the corresponding limits specified by the Integrated Wastewater Discharge Standard of China.

Introduction

The dangers posed by toxic heavy metals to the environment are an increasing global concern [1]. Heavy metal wastewater damages the ecological environment and seriously threatens human health. Thus, the exploration and development of effective removal methods and separation technologies for toxic heavy metal ions in wastewater has attracted significant research attention. Many heavy metal wastewater treatment methods, including chemical precipitation [2], ferrite method [3], chelation–precipitation method [4,5], ion exchange [6], adsorption [7], membrane separation [8], electrochemical method [9], and biological flocculation [10], have been developed. Among these methods, chelation–precipitation offers excellent results, lower costs, and better suitability for large-scale heavy metal wastewater treatment [4,5]. The treatment effects of chelation depend on the performance of the chelating flocculant. Chelating agents that have been recently developed

* Corresponding author. Tel.: +86 731 58291625.
E-mail addresses: llh213@163.com, liulihualj@sina.com.cn (L. Liu), lyh881205@163.com (Y. Li), 1249158985@qq.com (X. Liu), zhou7381@126.com (Z. Zhou), lyl931@126.com (Y. Ling).

1386-1425/$ - see front matter © 2013 Elsevier B.V. All rights reserved.
http://dx.doi.org/10.1016/j.saa.2013.09.066

ASIA-PACIFIC JOURNAL OF CHEMICAL ENGINEERING
Asia-Pac. J. Chem. Eng. 2015; **10**: 193–200
Published online 10 December 2014 in Wiley Online Library
(wileyonlinelibrary.com) DOI: 10.1002/apj.1862

Research article

Novel temperature-sensitive and pH-sensitive polyurethane membranes: preparation and characterization

Hu Zhou,[1]* *Bin Yu,*[1] *Ruiping Xun,*[1] *Ning Li,*[1] *Kejian Wu,*[1] *Hanzhou Sun*[2]** *and Zhihua Zhou*[1]

[1]*Key Laboratory of Theoretical Organic Chemistry and Function Molecule, Ministry of Education, School of Chemistry and Chemical Engineering, Hunan University of Science and Technology, Xiangtan, 411201, China*
[2]*College of Science, Central South University of Forestry and Technology, Changsha, 410004, China*

Received 20 July 2014; Revised 10 October 2014; Accepted 9 November 2014

ABSTRACT: The polyurethane (PU) membranes with temperature and pH double sensitivities for water permeation were designed and prepared from a two-step solution polymerization from the crystalline polycaprolactone diols (PCL), 4,4′-diphenylmethane diisocyanate (MDI) and pH-sensitive 2,2-dimethylol propionic acid (DMPA), etc. The structure and properties of PU membranes were characterized by differential scanning calorimetry meter, contact angle tester, mechanical tester, porosity tests, water flux tests, water absorption tests, etc. Results showed that all PU membranes had a similar crystalline melting transition in their soft segments. With increasing DMPA content, or −COOH group content, the mechanical property of PU membranes was decreased, but the surface wettability and porosity of PU membranes were increased, which were expected to improve the water flux and water absorption of PU membranes. When the environment temperature was raised above the temperature of crystal-melting transition (T_m) of the soft segments, the water fluxes across these PU membranes changed markedly, showing the temperature sensitivity. When pH varied around the dissociation constant (pKa) of DMPA contained in PU(2), PU(3) and PU(4) macromolecules, their water fluxes and water absorption were also obviously changed, showing the pH sensitivity. © 2014 Curtin University of Technology and John Wiley & Sons, Ltd.

KEYWORDS: polyurethane; membrane; temperature sensitivity; pH sensitivity; water flux; water absorption

INTRODUCTION

Now that the permeation of water is ubiquitous and momentous in agriculture, industry and all life forms,[1–5] more and more experts and scholars have set out to develop a new type of functional materials or advanced techniques for realizing the controllable water permeation with the goal to better understand biological processes and design and simulate some new apparatus based on micro-fluidics. Over the past decade, there have been many novel materials and technologies developed and reported for realizing controllable water permeation, like the zeolite molecular sieve membrane,[6] carbon nanotube film,[7] nanostructured copper mesh film,[5] etc. Nevertheless, all of these have turned out to be some of complicated, troublesome or exorbitant. Controllable water permeation can also be achieved by a stimuli-sensitive polymeric membrane. These membranes can reversibly change their pore size, surface wettability, etc. on receiving external stimulating signals, like temperature, pH, stress, ionic force, electric field, etc. in environmental conditions.[8] Thus, the mass transfer and permeability of these membranes can be easily regulated by adjusting external stimuli, which seems simpler, easier and lower cost in some cases. In particular, the membranes that can respond to dual or multiple external stimuli, for example, temperature and pH stimuli, are of particular interest and will have broader prospects in realizing the controllable water permeation.

Thermal sensitive polyurethane (TSPU) is one of the most popular and prominent temperature-responsive polymeric materials.[9–12] It has a typical block or segmented structure consisting of heat reversible phases and irreversible phases (or soft segments and hard segments).[13] The soft segment of TSPU often shows a phase transition temperature, i.e. crystal-melting transition or glass transition temperature. Soft segment softens or hardens when temperature is raised above or reduced below the temperature with sharp changes in some of physical performances of polymers, particularly the changes in free volume hole size or pore size, and micro-Brownian movement of

**Correspondence to*: Hu Zhou, Key Laboratory of Theoretical Organic Chemistry and Function Molecule, Ministry of Education, School of Chemistry and Chemical Engineering, Hunan University of Science and Technology, Xiangtan, 411201, China. E-mail: hnustchem@163.com
***Correspondence to*: Hanzhou Sun, College of Science, Central South University of Forestry and Technology, Changsha 410004, China. E-mail: sunhanzhou2013@163.com

Analytica Chimica Acta 825 (2014) 57–62

Contents lists available at ScienceDirect

Analytica Chimica Acta

journal homepage: www.elsevier.com/locate/aca

Silver nanoplates-based colorimetric iodide recognition and sensing using sodium thiosulfate as a sensitizer

Xinyan Hou, Shu Chen *, Jian Tang, Yuan Xiong, Yunfei Long **

Key Laboratory of Theoretical Chemistry and Molecular Simulation of Ministry of Education of China, School of Chemistry and Chemical Engineering, Hunan University of Science and Technology, Xiangtan 411201, China

HIGHLIGHTS

- A new colorimetric iodide detection strategy based on triangular Ag nanoplate.
- Sodium thiosulfate performed as a sensitizer.
- Formation of insoluble AgI on the surface of Ag nanoplate.
- This method has the advantages of good selectivity and high sensitivity.

GRAPHICAL ABSTRACT

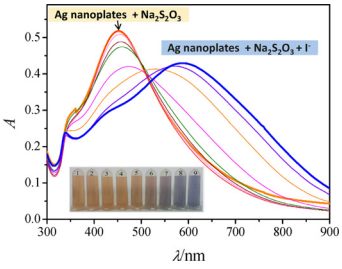

ARTICLE INFO

Article history:
Received 4 February 2014
Received in revised form 24 March 2014
Accepted 26 March 2014
Available online 29 March 2014

Keywords:
Triangular silver nanoplates
Iodide ions
Sodium thiosulfate
Colorimetric detection

ABSTRACT

A colorimetric method for the recognition and sensing of iodide ions (I^-) has been developed by utilizing the reactions between triangular silver nanoplates (TAg-NPs) and I^- in the presence of sodium thiosulfate ($Na_2S_2O_3$). Specifically, I^- together with $Na_2S_2O_3$ can induce protection of TAg-NPs owing to the formation of insoluble AgI, as confirmed by the high-resolution transmission electron microscopy (HRTEM). In the absence of $Na_2S_2O_3$, the etching reactions on TAg-NPs were observed not only by I^- but also other halides ions. The $Na_2S_2O_3$ plays as a sensitizer in this system, which improved the selectivity and sensitivity. The desired colorimetric detection can be achieved by measuring the change of the absorption peak wavelength corresponding to localized surface plasmon resonance (LSPR) with UV–vis spectrophotometer or recognized by naked eye observation. The results show that the shift of the maximum absorption wavelength ($\Delta\lambda$) of the TAg-NPs/$Na_2S_2O_3$/I^- mixture was proportional to the concentration of I^- in the range 1.0×10^{-9}–1.0×10^{-6} mol L^{-1}. Moreover, no other ions besides I^- can induce an eye discernible color change as low as 1.0×10^{-7} mol L^{-1}. Finally, this method was successfully applied for I^- determination in kelp samples.

1. Introduction

Silver nanostructures with different size and shape possess unique and tunable optical properties [1]. Well-defined structure includes nanocubes [2], nanodisks/nanoplates [3,4], nanoprisms [5], nanorods [6], nanowires [7], nanobelts [8], and branched nanocrystals [9]. Their fascinating surface plasmon features can be used for optical label [10], surface-enhanced Raman scattering (SERS) [11], chemical and biological sensing [12]. Among these structures, triangular silver naoplates (TAg-NPs) have attracted particular attention over the past decade due to their outstanding plasmonic features across visible-NIR regions. They exhibit intense and tunable localized surface plasmon resonance (LSPR) by controlling its ratio of edge length to thickness and the truncation degree of tips, which is not available for spherical Ag nanoparticles. Moreover, the LSRP induced unique colors ranging from yellow to

* Corresponding author. Tel.: +86 731 58388503; fax: +86 731 58372324.
** Corresponding author. Tel.: +86 73158372324; fax: +86 73158372324.
E-mail addresses: chenshumail@gmail.com (S. Chen), l_yunfei927@163.com, l_yunfei927@126.com (Y. Long).

http://dx.doi.org/10.1016/j.aca.2014.03.038
0003-2670/

Journal of Macromolecular Science®, Part B: Physics, 53:1145–1155, 2014

ISSN: 0022-2348 print / 1525-609X online
DOI: 10.1080/00222348.2014.895610

Influence of Nano-Bioactive Glass (NBG) Content on Properties of Gelatin-Hyaluronic Acid/NBG Composite Scaffolds

ZHIHUA ZHOU,[1,2,3] SILIANG HE,[3] BAOLI OU,[3] TIANLONG HUANG,[4] WENNAN ZENG,[3] LIHUA LIU,[3] QINGQUAN LIU,[3] JIAN CHEN,[3] YANMIN ZHAO,[3] ZHONGMIN YANG,[3] AND DAFU CAO[3]

[1]Key Laboratory of Theoretical Chemistry and Molecular Simulation of Ministry of Education, Hunan University of Science and Technology, Xiangtan, P. R. China
[2]Hunan Province College Key Laboratory of QSAR/QSPR, Hunan University of Science and Technology, Xiangtan, P. R. China
[3]School of Chemistry and Chemical Engineering, Hunan University of Science and Technology, Xiangtan, P. R. China
[4]Department of Orthopedics, the Second Xiangya Hospital, Central South University, Changsha, P. R. China

The development of three-dimensional (3-D) scaffolds with highly open porous structure is one of the most important issues in tissue engineering. A novel nanocomposite scaffold of gelatin (Gel), hyaluronic acid (HA), and nano-bioactive glass (NBG) was prepared by blending NBG with a Gel and HA solution followed by lyophilization. The effects of NBG content on the properties of the Gel-HA/NBG composite scaffolds, including the morphologies, porosity, compressive strength, swelling behavior, cell viability and alkaline phosphatase (ALP) activity, were investigated. Porous composite scaffolds with interconnected pores were obtained and the pores became cylindrical with increasing NBG content. The porosity percent and swelling ability decreased with increasing NBG content; however, the compressive strength, cell viability and ALP activity were enhanced. All the results showed the addition of NBG particles can improve the physicochemical and biological properties and the Gel-HA/NBG composite scaffolds exhibited good potential for tissue engineering applications.

Keywords composite scaffold, gelatin, hyaluronic acid, nano-bioactive glass, property

Introduction

Scaffolds developed from natural and synthetic polymers are commonly used in tissue engineering. These polymers mimic the chemical and physical properties of natural extracellular matrix (ECM).[1,2] Hydrogel-scaffolding materials have many different functions in

Received 17 March 2013; accepted 24 January 2014.
Address correspondence to Zhihua Zhou, Key Laboratory of Theoretical Chemistry and Molecular Simulation of Ministry of Education, Hunan University of Science and Technology, Xiangtan 411201, P. R. China. E-mail: zhou7381@126.com

Journal of Macromolecular Science®, Part B: Physics, 53:398–411, 2014

ISSN: 0022-2348 print / 1525-609X online
DOI: 10.1080/00222348.2013.845059

Preparation of Thermal and pH Dually Sensitive Polyurethane Membranes and Their Properties

HU ZHOU,[1,2] RUIPING XUN,[2] QINGQUAN LIU,[1,2]
HAOJUN FAN,[3] AND YUANSEN LIU[3]

[1]Key Laboratory of Theoretical Chemistry and Molecular Simulation of Ministry of Education, Hunan University of Science and Technology, Xiangtan, P.R. China
[2]School of Chemistry and Chemical Engineering, Hunan University of Science and Technology, Xiangtan, P.R. China
[3]National Engineering Laboratory for Clean Technology of Leather Manufacture, Sichuan University, Chengdu, P.R. China

With crystalline polycaprolactone diols (PCL) used as soft segments, and 1,4-butanediol (BDO), dimethylolpropionic acid (DMPA), and N-methyldiethanolamine (MDEA), respectively, used as different pH-sensitive components, *three types of thermal and pH-sensitive polyurethanes (PUs) were prepared by using the block copolymerization technique and are referred to as PU(a), PU(b), and PU(c), correspondingly. Fourier transform infrared (FTIR) spectroscopy, X-ray photoelectron spectroscopy (XPS), and differential scanning calorimetry (DSC) were used to study the distinct functional groups of the PUs and their segmented structures. Their thermal and pH stimuli sensitivity were measured by water permeability (WP) and water swelling (WS) tests. Fourier transform infrared analysis demonstrated that the $-COOH$ and $-N(CH_3)-$ groups were successfully introduced into the PU(b) and PU(c), respectively, and these acid–base groups did not change the basic structure of their main chains. X-ray photoelectron spectroscopy analysis showed that the O and N concentration increased on the surface of PU(b) and PU(c), respectively. Differential scanning calorimetry analysis indicated that all three PUs showed phase-separated structures and similar phase-transition temperatures of the soft segments (defined as the switch temperature, T_s), which showed that the introduction of the acid–base functional groups did not much affect the phase-separated structures and crystallization of the soft segments. The WP study indicated that all PUs showed thermal intelligent responses, i.e., the WPs were correspondingly changeable with change of the temperature. In particular, when the temperature varied near the T_s, e.g., from $T_s-10^\circ C$ to $T_s+10^\circ C$, the WPs changed markedly. In addition, due to PU(b) and PU(c) containing $-COOH$ and $-N(CH_3)-$ groups, respectively, they both showed a pH response in their WP and WS. When the pH changed from 4.0 to 5.5, the WP and WS of PU(b) were obviously changed. The same change also occurred for PU(c) in the pH range from 8.5 to 10.0. We thus conclude that the method utilized is an efficient way to prepare PUs that are dually responsive to both thermal and pH stimuli.*

Received 28 November 2012; accepted 2 July 2013.
Address correspondence to Hu Zhou, Key Laboratory of Theoretical Chemistry and Molecular Simulation of Ministry of Education, Hunan University of Science and Technology, Xiangtan 411201, P.R. China. E-mail: hnustchem@163.com

Synthetic Communications®, 44: 1012–1018, 2014

ISSN: 0039-7911 print/1532-2432 online
DOI: 10.1080/00397911.2013.841938

ASYMMETRIC SYNTHESIS OF NOVEL VICINAL AMINO ALCOHOLS VIA INTRAMOLECULAR KETONE-*N*-SULFINYLIMINE PINACOL-TYPE REDUCTIVE COUPLING PROMOTED BY SmI_2

Yun-Hui Zhao and Han-Wen Liu

Key Laboratory of Theoretical Chemistry and Molecular Simulation of Ministry of Education, Hunan Province College Key Laboratory of QSAR/QSPR, Hunan University of Science and Technology, Xiangtan, China

GRAPHICAL ABSTRACT

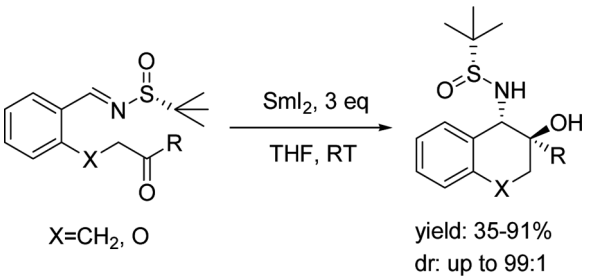

Abstract *A novel intramolecular asymmetric ketone-*N*-sulfinylimine pinacol-type reductive coupling reaction induced by SmI_2 was reported. A series of 1-amino-1,2,3,4-tetrahydronaphthalen-2-carbinols were obtained in moderate to good yields with excellent* ee *and high* dr.

[Supplementary materials are available for this article. Go to the publisher's online edition of Synthetic Communications® *for the following free supplemental resource(s): Full experimental and spectral details.]*

Keywords Asymmetric synthesis; *N*-sulfinylimine; samarium diiodide; vicinal amino alcohol

INTRODUCTION

Vicinal amino alcohols are common structures found in natural products.[1] The amino alcohols are also important building blocks for organic and pharmaceutical synthesis.[2] Moreover, 1,2-amino alcohols have been utilized as excellent chiral

Received July 4, 2013.

Address correspondence to Yun-Hui Zhao, Key Laboratory of Theoretical Chemistry and Molecular Simulation of Ministry of Education, Hunan Province College Key Laboratory of QSAR/QSPR, Hunan University of Science and Technology, Xiangtan 411201, China. E-mail: zyh00041130@163.com

Dalton Transactions

PAPER

View Article Online
View Journal | View Issue

Cite this: *Dalton Trans.*, 2014, **43**, 1524

A spectroscopic study on the coordination and solution structures of the interaction systems between biperoxidovanadate complexes and the pyrazolylpyridine-like ligands†

Xian-Yong Yu,*[a] Lin Deng,[a] Baishu Zheng,[a] Bi-Rong Zeng,[b] Pinggui Yi*[a] and Xin Xu*[c,d]

In order to understand the substitution effects of pyrazolylpyridine (pzpy) on the coordination reaction equilibria, the interactions between a series of pzpy-like ligands and biperoxidovanadate ($[OV(O_2)_2(D_2O)]^-$/$[OV(O_2)_2(HOD)]^-$, abbrv. bpV) have been explored using a combination of multinuclear (^1H, ^{13}C, and ^{51}V) magnetic resonance, heteronuclear single quantum coherence (HSQC), and variable temperature NMR in a 0.15 mol L^{-1} NaCl D_2O solution that mimics the physiological conditions. Both the direct NMR data and the equilibrium constants are reported for the first time. A series of new hepta-coordinated peroxidovanadate species $[OV(O_2)_2L]^-$ (L = pzpy-like chelating ligands) are formed due to several competitive coordination interactions. According to the equilibrium constants for products between bpV and the pzpy-like ligands, the relative affinity of the ligands is found to be pzpy > 2-Ester-pzpy ≈ 2-Me-pzpy ≈ 2-Amide-pzpy > 2-Et-pzpy. In the interaction system between bpV and pzpy, a pair of isomers (**Isomers A** and **B**) are observed in aqueous solution, which are attributed to different types of coordination modes between the metal center and the ligands, while the crystal structure of $NH_4[OV(O_2)_2(pzpy)]\cdot 6H_2O$ (**CCDC 898554**) has the same coordination structure as **Isomer A** (the main product for pzpy). For the N-substituted ligands, however, **Isomer A** or **B** type complexes can also be observed in solution but the molar ratios of the isomer are reversed (*i.e.*, **Isomer B** type is the main product). These results demonstrate that when the N atom in the pyrazole ring has a substitution group, hydrogen bonding (from the H atom in the pyrazole ring), the steric effect (from alkyl) and the solvation effect (from the ester or amide group) can jointly affect the coordination reaction equilibrium.

Received 22nd July 2013,
Accepted 21st October 2013

DOI: 10.1039/c3dt51986d

www.rsc.org/dalton

Introduction

In the last four decades, vanadium complexes, in particular, heteroligand peroxidovanadate complexes, have received increasing attention because they could act as an inorganic co-factor or a catalytic center involved in many enzymatic processes such as haloperoxidation, nitrogen fixation, *etc.*[1–4]

As peroxidovanadates and the corresponding complexes can inhibit protein tyrosine phosphatase (PTPase) and cause DNA cleavage both *in vitro* and *in vivo*, they have been tested as potential insulin-mimetic agents,[1–3,5] as well as anti-tumor drugs.[6] Being model compounds for haloperoxidases, peroxidovanadates could also oxidize organic or inorganic substrates to the corresponding products under mild conditions with high yield and remarkable selectivity. Therefore, the synthesis and characterization of peroxidovanadates and the investigation of their biological mechanisms have recently become the subject of extensive studies.[1–12] In these studies, the coordination chemistry of the peroxidovanadate complexes is

[a]*Key Laboratory of Theoretical Chemistry and Molecular Simulation of Ministry of Education, Hunan Province College Key Laboratory of QSAR/QSPR, School of Chemistry and Chemical Engineering, Hunan University of Science and Technology, Xiangtan 411201, China. E-mail: yu_xianyong@163.com, pgyi@hnust.cn; Fax: +86-731-58290509*

[b]*Department of Materials Science and Engineering, Key Laboratory for Fire Retardant Materials of Fujian Province, Xiamen University, Xiamen 361005, China*

[c]*Shanghai Key Laboratory of Molecular Catalysis and Innovative Materials, MOE Laboratory for Computational Physical Science, Department of Chemistry, Fudan University, Shanghai, 200433, China*

[d]*State Key Laboratory of Physical Chemistry of Solid Surfaces, College for Chemistry and Chemical Engineering, Xiamen University, Xiamen 361005, China. E-mail: xxchem@fudan.edu.cn*

†Electronic supplementary information (ESI) available: The experimental procedures and spectroscopic data of ligands **1–5** and complex **6**. CCDC 898554. For ESI and crystallographic data in CIF or other electronic format see DOI: 10.1039/c3dt51986d

CrystEngComm

COMMUNICATION

View Article Online
View Journal

Cite this: DOI: 10.1039/c4ce01165a

Received 8th June 2014,
Accepted 6th August 2014

DOI: 10.1039/c4ce01165a

www.rsc.org/crystengcomm

Enhanced water stability of a microporous acylamide-functionalized metal–organic framework *via* interpenetration and methyl decoration†

Baishu Zheng,*[a] Xiu Lin,[a] Zhaoxu Wang,*[a] Ruirui Yun,[b] Yanpeng Fan,[a] Mingsheng Ding,[a] Xiaolian Hu[a] and Pinggui Yi*[a]

A microporous acylamide-functionalized MOF with a 2-fold interpenetrated and methyl decorated framework (HNUST-4) has been designed and synthesized from $[Cu_2(COO)_4]$ motifs and a C_2-symmetric acylamide-linking tetracarboxylate, which exhibits good water stability, permanent porosity as well as high and selective CO_2 uptake at ambient temperature.

Metal–organic frameworks (MOFs) have become a leading class of porous crystalline materials due to their potential applications in gas storage,[1] gas separation[2] and catalysis.[3] These applications mainly hinge on two important properties of MOFs: porosity and stability. Currently, remarkable breakthroughs in the construction of MOFs with ultrahigh porosity have been reported and several landmark MOFs display large experimental BET surface areas with values exceeding 5000 $m^2\ g^{-1}$.[4] However, most of such highly porous MOFs are not robust enough and prone to collapse in humid environments, greatly hindering their practical gas storage/separation applications. Thus, how to design and address porous materials with high hydrostability is one of the key challenges we now face in MOF chemistry, and several strategies are envisaged to achieve this goal: (i) strengthening the metal–ligand coordination bonds by judicious choice of metal ions/clusters and organic ligands (*e.g.* high oxidation state metals such as Fe^{3+}, Cr^{3+}, Al^{3+}, Zr^{4+}, *etc.* for carboxylate-based MOFs[5] and nitrogen-containing linkers such as pyrazole, imidazole, pyridyl-carboxylate, *etc.* for transition-metal based MOFs or ZIFs[6]); (ii) utilizing interpenetration or catenation[7] to narrow the pore size; (iii) doping hybrid composites (*e.g.* carbon nanotubes and hetero-metals) into frameworks;[8] and (iv) decorating the pores with hydrophobic groups (*e.g.* methyl, ethyl ester, *etc.*).[9]

In pursuing new high-performance gas storage/separation materials, we are specially interested in the design and construction of porous MOFs from large multidentate carboxylate ligands with linking polar functional groups (*e.g.* acylamide, oxalamide, *etc.*) and a dicopper(II) paddlewheel cluster because such an approach may facilitate the generation of expanded MOFs with high surface area, open copper sites and pre-designed polar functionalities that are all beneficial to improve the gas (especially for CO_2) adsorption and separation properties of materials.[10] To extend our research in this area, herein we report a novel 2-fold interpenetrated microporous acylamide-functionalized MOF decorated with methyl groups, termed HNUST-4 (HNUST denotes the Hunan University of Science and Technology), designed from a nanosized flexible tetracarboxylate, 5,5′-[(5-methyl-1,3-phenylene) bis(carbonylimino)]diisophthalic acid (MPBD). Interestingly, HNUST-4 represents a rare example of water-stable MOFs constructed from paddlewheel SBUs and pure carboxylate ligands; its crystallinity can be sustained even after immersion in boiling water for a day. In addition, HNUST-4 exhibits a moderate BET surface area of 1136 $m^2\ g^{-1}$ as well as high and selective CO_2 uptake at ambient temperature.

Solvothermal reaction of MPBD and $Cu(NO_3)_2{\cdot}3H_2O$ in DMF–ethanol–H_2O (5 : 3 : 2 in volume) at 75 °C for 48 hours afforded pale blue block crystals of HNUST-4.‡ HNUST-4 crystallizes in the space group *I*4/*mmm* and the framework consists of $[Cu_2(COO)_4]$ paddlewheels linked by $MPBD^{4-}$ ligands. $MPBD^{4-}$ exhibits two crystallographically independent conformations (*syn*- and *anti*-) and the carbonyl moiety of the acylamide group is disordered over two positions with equal probability (Fig. S1†). Similar to the isostructural PMOF-3 and its analogues,[11] the overall structure of HNUST-4 exhibits 2-fold interpenetration and each single framework

[a] *Key Laboratory of Theoretical Organic Chemistry and Function Molecule of Ministry of Education, School of Chemistry and Chemical Engineering, Hunan University of Science and Technology, Xiangtan 411201, China. E-mail: zbaishu@163.com, hnust_chem@163.com, yipinggui@sohu.com*

[b] *College of Chemistry and Materials Science, Anhui Normal University, Wuhu 241000, China*

† Electronic supplementary information (ESI) available: Experimental details, TGA plots, heats of adsorption of H_2, CO_2 and CH_4, and sorption selectivity calculations. CCDC 1006012. For ESI and crystallographic data in CIF or other electronic format see DOI: 10.1039/c4ce01165a

Spectrochimica Acta Part A: Molecular and Biomolecular Spectroscopy 127 (2014) 231–236

Contents lists available at ScienceDirect

Spectrochimica Acta Part A: Molecular and Biomolecular Spectroscopy

journal homepage: www.elsevier.com/locate/saa

Spectroscopic studies on the interaction of Phacolysin and bovine serum albumin

Xianyong Yu [a,b,c,*], Zhixi Liao [a], Qing Yao [a], Heting Liu [a], Wenlin Xie [a,*]

[a] Key Laboratory of Theoretical Chemistry and Molecular Simulation of Ministry of Education, Hunan Province College Key Laboratory of QSAR/QSPR, School of Chemistry and Chemical Engineering, Hunan University of Science and Technology, Xiangtan 411201, China
[b] State Key Laboratory of Physical Chemistry of Solid Surfaces, Xiamen University, Xiamen 361005, China
[c] Key Laboratory of Computational Physical Sciences, Fudan University, Ministry of Education, Shanghai, China

HIGHLIGHTS

- We explored the interaction of BSA and PCL by spectroscopic methods.
- The fluorescence quenching mechanism is static quenching.
- The binding constants and binding sites were calculated.
- Hydrogen bonds and van der Waals forces were the main force in stabilizing the complex.
- The conformation of BSA was changed affected by PCL.

GRAPHICAL ABSTRACT

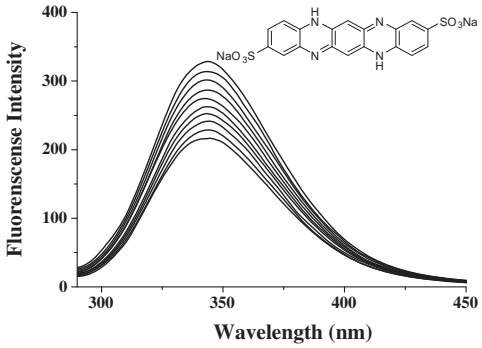

ARTICLE INFO

Article history:
Received 21 October 2013
Received in revised form 29 January 2014
Accepted 11 February 2014
Available online 27 February 2014

Keywords:
Interaction
Phacolysin
Bovine serum albumin
Spectroscopic techniques
Circular dichroism spectrum

ABSTRACT

The interaction between Phacolysin (PCL) and bovine serum albumin (BSA) under imitated physiological conditions was investigated by spectroscopic (fluorescence, UV–Vis absorption and Circular dichroism) techniques. The experiments were conducted at different temperatures (294 K, 302 K, 306 K and 310 K) and the results showed that the PCL caused the fluorescence quenching of BSA through a static quenching procedure. The binding constant (K_a), binding sites (n) were obtained. The corresponding thermodynamic parameters (ΔH, ΔS and ΔG) of the interaction system were calculated at different temperatures. The results revealed that the binding process was spontaneous and the acting force between PCL and BSA were mainly hydrogen bonding and van der Waals forces. According to Förster non-radiation energy transfer theory, the binding distance between PCL and BSA was calculated to be 2.41 nm. What is more, both synchronous fluorescence and Circular dichroism spectra confirmed the interaction, which indicated the conformational changes of BSA.

Introduction

As we all know, serum albumins (SA) contribute to colloid osmotic blood pressure and the maintenance of blood pH. They also play a dominant role in drug disposition and efficacy. Most drugs are transported as a complex with SA, which makes SA an important part of drug metabolism [1–3]. The serum protein used

* Corresponding authors. Address: Key Laboratory of Theoretical Chemistry and Molecular Simulation of Ministry of Education, Hunan Province College Key Laboratory of QSAR/QSPR, School of Chemistry and Chemical Engineering, Hunan University of Science and Technology, Xiangtan 411201, China (X. Yu). Tel.: +86 731 58290187; fax: +86 731 58290509.
E-mail addresses: yu_xianyong@163.com (X. Yu), xwl2000zsu@163.com (W. Xie).

http://dx.doi.org/10.1016/j.saa.2014.02.064
1386-1425/

Review

Wiley Online Library

ELECTROANALYSIS

Special Issue DIAGNOSTICS

DOI: 10.1002/elan.201400040

Electroanalytical Sensors and Methods for Assays and Studies of Neurological Biomarkers

Shu Chen,[a] Lin Zhang,[b, c] Yunfei Long,*[a] and Feimeng Zhou*[b, c]

Abstract: Diverse methods have been developed to reveal biochemical changes in neurological disorders and to detect biomarkers present in clinical samples. Electrochemical biosensors are attractive because of their low costs, high sensitivity, and easiness for miniaturization. They have the potential for both point-of-care and in vivo monitoring. With clever surface modification and effective immobilization of capture ligands, selective detection of neurological biomarkers can be achieved. This review covers select applications of electroanalytical methods/sensors for proteins, peptides, small molecules, metal ions, and neurotransmitters. Designs of various sensors and devices are reviewed and issues to be addressed for clinically viable sensors are discussed.

Keywords: Biosensors · Amyloidogenic proteins · Neurological biomarkers · Metal ions · Reactive oxygen species · Neurotransmitters

1 Introduction

Neurological disorders (NDs), such as Alzheimer's disease (AD), Parkinson's disease (PD), Creutzfeldt–Jakob disease (CJD), Huntington's disease (HD), Wilson's disease (WD), and many others, share similar neuropathology and account for a significant and increasing proportion of morbidity and mortality of the elderly in the world [1–3]. NDs are characterized by neuronal impairment that eventually leads to neuronal death [4]. A major hypothesis presumes that NDs are originated from misfolded or dysregulated proteins that accumulate into deleterious amyloid aggregates [5–7]. The process of forming amyloid-like aggregates or fibrils is also referred to as amyloidogenesis.

As the most prevalent form of dementia, AD affects about 35.6 million people world wide. With an aging population and no cures or even effective treatments, humankind is facing a dire situation: one in 85 persons worldwide is projected to suffer from one type of ND or a combination of several by 2050 [8]. As such, intense research has been undertaken to understand the etiology of NDs and to screen therapeutic drugs that target specific proteins responsible for the induction or aggravation of NDs. In such a formidable endeavor, reliable biochemical assays that can provide complementary information to other clinical methods (e.g., monitoring of behavioral changes) for accurate and reliable diagnoses of NDs are expected to contribute significantly. Identification and quantification of biomarkers in various types of samples (e.g., body fluids such as blood, urine, and cerebrospinal fluids) can provide vital information about the risk factors of NDs and severity of the diseases. Correlation of the disease biomarkers to the symptoms (or lack of) can also help guide the pre-market drug discovery and neurotoxicity screening. In this context, a biomarker is a target molecule that, when detected at unusual levels in biological samples or pathogenic processes, can be used to signal a specific type of ND or its prognosis [9,10]. While many traditional biomarkers are proteins, nucleic acids, or protein fragments (including peptides) in ND, species as diverse as neurotransmitters, lipids, and metal ions are found to be present at abnormal levels and hence should also be regarded as biomarkers. For example, imbalanced metabolism of neurotransmitters and excess production of reactive oxygen species (ROS) have been closely linked to a range of NDs [11]. ROS production in many cases is resulted from reactions of oxygen with redox-active metal complexes of proteins or peptides [12,13]. Metal ions can also affect neurodegeneration via pro-apoptotic biochemical signaling pathways, mediation of oxidative stress [14], and oxidative damages of neurotransmitters [15]. We should add that these processes are integral parts of the broadly defined "oxidative stress" hypothesis in the field. Another purported role of metal ions in ND etiology is the enhancement of protein-folding processes or stabilization of certain amyloid aggregate intermediates or conformations [1,16]. The premise that neuronal impairment/death is a direct result of amyloid genesis of proteins/peptides and/or metal-triggered forma-

[a] S. Chen, Y. Long
Key Laboratory of Theoretical Chemistry and Molecular Simulation of Ministry of Education of China, School of Chemistry and Chemical Engineering, Hunan University of Science and Technology
Xiangtan, 411201, P.R. China
*e-mail: l_yunfei927@163.com

[b] L. Zhang, F. Zhou
Department of Chemistry and Biochemistry, California State University, Los Angeles
Los Angeles, California 90032, United States
*e-mail: fzhou@calstatela.edu

[c] L. Zhang, F. Zhou
College of Chemistry and Chemical Engineering, Central South University
Changsha, Hunan 410083, P.R. China

Spectrochimica Acta Part A: Molecular and Biomolecular Spectroscopy 118 (2014) 331–336

Contents lists available at ScienceDirect

Spectrochimica Acta Part A: Molecular and Biomolecular Spectroscopy

journal homepage: www.elsevier.com/locate/saa

The investigation of the interaction between Tropicamide and bovine serum albumin by spectroscopic methods

Xianyong Yu [a,b,*], Zhixi Liao [a], Qing Yao [a], Heting Liu [a], Xiaofang Li [a], Pinggui Yi [a,*]

[a] Key Laboratory of Theoretical Chemistry and Molecular Simulation of Ministry of Education, Hunan Province College Key Laboratory of QSAR/QSPR, School of Chemistry and Chemical Engineering, Hunan University of Science and Technology, Xiangtan 411201, China
[b] State Key Laboratory of Physical Chemistry of Solid Surfaces, Xiamen University, Xiamen 361005, China

HIGHLIGHTS

- The interaction of bovine serum albumin (BSA) and Tropicamide (TA) was studied.
- The fluorescence quenching mechanism is static quenching.
- The binding constants and binding sites were calculated.
- Hydrogen binds and vander Waals interaction force played a major role in stabilizing the complex.
- The TA affects the conformation of BSA.

GRAPHICAL ABSTRACT

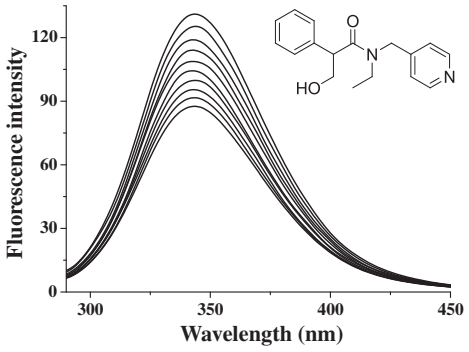

ARTICLE INFO

Article history:
Received 12 June 2013
Received in revised form 15 August 2013
Accepted 23 August 2013
Available online 31 August 2013

Keywords:
Fluorescence spectroscopy
Ultraviolet–visible spectroscopy
Interaction
Tropicamide
Bovine serum albumin

ABSTRACT

The fluorescence and ultraviolet–visible (UV–Vis) spectroscopy were explored to study the interaction between Tropicamide (TA) and bovine serum albumin (BSA) at three different temperatures (292, 301 and 310 K) under imitated physiological conditions. The experimental results showed that the fluorescence quenching mechanism between TA and BSA was static quenching procedure. The binding constant (K_a), binding sites (n) were obtained. The corresponding thermodynamic parameters (ΔH, ΔS and ΔG) of the interaction system were calculated at different temperatures. The results revealed that the binding process is spontaneous, hydrogen binds and vander Waals were the main force to stabilize the complex. According to Förster non-radiation energy transfer theory, the binding distance between TA and BSA was calculated to be 4.90 nm. Synchronous fluorescence spectroscopy indicated the conformation of BSA changed in the presence of TA. Furthermore, the effect of some common metal ions (Mg^{2+}, Ca^{2+}, Cu^{2+}, and Ni^{2+}) on the binding constants between TA and BSA were examined.

Introduction

Fluorescence studies on protein–ligand interaction with characteristic fluorescence properties of the drug (ligand) have gained enormous interest in recent times [1,2]. It is well known that the serum albumin is a major soluble protein constituent in the circulatory system, which plays an important role in the transportation and deposition of many drug molecules in the blood [3–5]. In this work, bovine serum albumin (BSA) is selected as our protein model because of its medical importance, stability, low cost, unusual ligand-binding properties. It displays approximately 76% sequence homology, and the 3D structure of BSA is believed to be similar to that of HSA [6–8]. However, they differ in the number of tryptophans: BSA has two tryptophans, but HSA has only one [9–10].

* Corresponding authors. Address: Key Laboratory of Theoretical Chemistry and Molecular Simulation of Ministry of Education, Hunan Province College Key Laboratory of QSAR/QSPR, School of Chemistry and Chemical Engineering, Hunan University of Science and Technology, Xiangtan 411201, China. Tel.: +86 731 58290187; fax: +86 731 58290509 (X. Yu).
E-mail addresses: yu_xianyong@163.com (X. Yu), pgyi@hnust.cn (P. Yi).

1386-1425/$ - see front matter © 2013 Elsevier B.V. All rights reserved.
http://dx.doi.org/10.1016/j.saa.2013.08.103

Synthetic Communications®, 44: 1414–1421, 2014

ISSN: 0039-7911 print/1532-2432 online
DOI: 10.1080/00397911.2011.557850

ONE-POT SYNTHESIS OF NOVEL SPIRO PYRANO[2,3-*d*][1,3]THIAZOLO[3,2-*a*]PYRIMIDINE DERIVATIVES

Xiaofang Li, Haochong Liu, Aiting Zheng, Zhikui Li, Xianyong Yu, and Pinggui Yi

Key Laboratory of Theoretical Chemistry and Molecular Simulation of Ministry of Education, Hunan Province College Key Laboratory of QSAR/QSPR, School of Chemistry and Chemical Engineering, Hunan University of Science and Technology, Xiangtan, Hunan, China

GRAPHICAL ABSTRACT

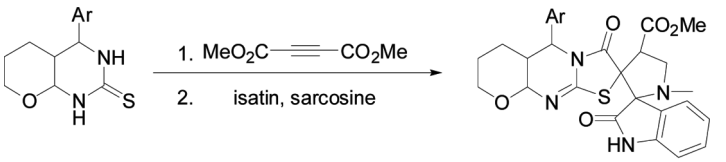

1a-1i **2a-2i**

Ar: **a**, 4-ClC_6H_4; **b**, 4-$OCH_3C_6H_4$; **c**, 2,4-$Cl_2C_6H_3$; **d**, 3,4,5- $(CH_3O)_3C_6H_2$; **e**, 4-FC_6H_4; **f**, 4-$SCH_3C_6H_4$; **g**, 4-$CH_3C_6H_4$; **h**, 4-$COOCH_3C_6H_4$; **i**, C_6H_5

Abstract *In a one-pot synthesis, 1′-methyl-2,3″-dioxo-5″-aryl-1,2,5a″,7″,8″,9a″-hexahydro-5″H,6″H-dispiro[indole-3,2′-pyrrolidine-3′,2″-pyrano[2,3-d][1,3]thiazolo[3,2-a]pyrimidine]-4′-carboxylic acid methyl ester was prepared via the sequential reaction of 4-aryl-octahydro-pyrano[2,3-d]pyrimidine-2-thione, dimethyl acetylenedicarboxylate (DMAD), and a mixture of isatin and sarcosine. All the novel spiro compounds, in moderate yields, were characterized thoroughly by infrared, NMR, mass spectromentry, and elemental analysis together with x-ray crystallographic analysis.*

Keywords Azomethine ylide; 1,3-dipolar cycloaddition; one-pot reaction; pyrano[2,3-*d*]-[1,3]thiazolo[3,2-*a*]pyrimidine; pyrano[2,3-*d*]pyrimidine

INTRODUCTION

One-pot multicomponent reactions are the processes that trigger the conversion of three or more starting materials in a single operation without the need to isolate intermediates. These strategies are used to improve the efficiency of chemical reactions whereby multiple carbon–carbon and carbon–heteroatom and stereocenters are formed.[1–3]

Received October 13, 2010.

Address correspondence to Pinggui Yi, School of Chemistry and Chemical Engineering, Hunan University of Science and Technology, Xiangtan, Hunan 411201, China. E-mail: pgyi@hnust.edu.cn

Journal of Macromolecular Science, Part A: Pure and Applied Chemistry (2014) **51**, 271–278

ISSN: 1060-1325 print / 1520-5738 online
DOI: 10.1080/10601325.2014.882683

A Novel Route to Prepare Cationic Polystyrene Latex Particles with Monodispersity

QINGQUAN LIU[1,2*], ZHE TANG[2], ZHIHUA ZHOU[1,2*], HU ZHOU[1,2], BAOLI OU[1,2], BO LIAO[1,2], SHAOHUA SHEN[1,2], and LIJUAN CHEN[1,2]

[1]*Key Laboratory of Theoretical Chemistry and Molecular Simulation of Ministry of Education, Hunan University of Science and Technology, Xiangtan 411201, China*
[2]*School of Chemistry and Chemical Engineering, Hunan University of Science and Technology, Xiangtan 411201, China*

Received and Accepted October 2013

Relatively clean cation-charged polystyrene (PS) latex particles were prepared via a novel and simple route in the absence of steric stabilizers. The reaction system only included medium, styrene, and initiator with quaternary ammonium moiety. The influences of initiator concentration, and medium composition on the diameter and size distribution of PS latex particles were systematically investigated. The particle morphology and size, the surface N content, and the particle size distribution were respectively determined by SEM, XPS, and laser particle size analyzer. The results indicated that monodisperse and cation-charged PS latex particles with diameter of 0.45–0.95 μm could be successfully produced via the simple reaction system, and cationic initiator concentration played a key role in the preparation of uniform PS latex particles. Finally, a plausible mechanism was proposed for explaining nucleation, growth, and stabilization of PS latex particles.

Keywords: polystyrene, latex particles, monodispersity

1 Introduction

Cationic polymer latex particles not only had the common features of general polymer latex particles such as small size and high specific surface area, but also had some unique properties like positive charge on the surface, good mechanical stability, chemical stability, low surface tension, high hydrophobic, etc. Consequently, cationic polymer latex particles were employed in a wide range of fields including drug delivery, chromatographic separation, enzyme encapsulation, medical diagnosis and many other fields (1-3). For example, in the papermaking and wastewater treatment, the cationic latex particles could be used as flocculant and displayed higher treatment efficiency than anionic and non-ionic polymer latex particles (4).

Conventional emulsion (5), emulsifier-free emulsion (6), and dispersion (7) polymerization are often used for preparing monodisperse cationic PS latex particles. The first route can generate nanosized cationic latex particles by using cationic surfactants such as cetyltrimethylammonium bromide (CTAB), dodecyltrimethylammonium bromide (DTAB) (5), and 1-[-(4-methoxy-4-biphenylyloxy)alkyl] pyridinium bromides (PCX) (8). However, this approach has a disadvantage that charges are not covalently bound to the particles. The second technique can solve this problem by using a cationic azo initiator like 2,2′-Azobis(2-methylpropionamide) dihydrochloride (AIBA) (9). Decomposition of this type initiator forms cation-charged radicals, which is capable of generating one or two cations in each polymer chain. The copolymerization of quaternary ammonium functionalized monomers like (vinylbenzyl)trimethyl- ammonium chloride (VBTMAC), [(2-(acryloyloxy)ethyl] trimethylammonium chloride (AETMAC), diallyldimethylammonium chloride (DADMAC), and (3-(methacryloylamino) propyl) trimethyl ammonium chloride (MAPTAC) with hydrophobic monomer during emulsifier-free emulsion can also produce cation-charged latex particles (10, 11). There is no problem of removing stabilizers, but this process often leads to coagulum formation. Nevertheless, hydrophilic amino comonomers like VBTMAC, AETMAC, DADMAC, and MAPTAC often result in a broad size distribution and formation of water-soluble polyeletrolytes.

The third technique was originated from the 1970's. It is well known that dispersion polymerization can generate

*Address correspondence to: Qingquan Liu and Zhihua Zhou, Institute of Chemistry and Chemical Engineering, Hunan University of Science and Technology, Xiangtan 411201, China. Fax: (86-731)5829-0045; E-mail: qqliu@hnust.edu.cn or zhou7381@126.com

Color versions of one or more of the figures in the article can be found online at www.tandfonline.com/lmsa.

[Article] doi: 10.3866/PKU.WHXB201512291 www.whxb.pku.edu.cn

超分子作用对2-(2-氨基苯基)苯并噻唑分子内质子转移的影响

向俊峰 易平贵* 任志勇 于贤勇 陈 建 刘 武 李桃梅
(湖南科技大学化学化工学院，理论有机化学与功能分子教育部重点实验室，
分子构效关系湖南省普通高校重点实验室，湖南 湘潭 411201)

摘要：采用稳态荧光、瞬态荧光及量子化学计算等手段对2-(2-氨基苯基)苯并噻唑(APBT)在不同溶剂中的质子转移进行了研究。结果表明，溶剂的极性及质子化对APBT的质子转移有较大的影响，通过对超分子作用的考察，发现七元瓜环(CB[7])的加入对APBT质子转移起到了一定的抑制作用，APBT与CB[7]能形成化学计量比为1∶1的主客体包合物，同时测定了包合物的结合常数等热力学参数。此外，核磁共振氢谱和包合物的理论计算表明APBT分子进入了CB[7]的疏水空腔。

关键词：质子转移；七元瓜环；极化连续介质模型；热力学；主客体化学
中图分类号：O641

Effect of Supra-Molecular Interaction on the Intramolecular Proton Transfer of 2-(2-Aminophenyl)benzothiazole

XIANG Jun-Feng YI Ping-Gui* REN Zhi-Yong YU Xian-Yong
CHEN Jian LIU Wu LI Tao-Mei
(*Hunan Province College Key Laboratory of QSAR/QSPR, Key Laboratory of Theoretical Chemistry and Molecular Simulation, Ministry of Education, School of Chemistry and Chemical Engineering, Hunan University of Science and Technology, Xiangtan 411201, Hunan Province, P. R. China*)

Abstract: The excited-state intramolecular proton transfer of 2-(2-aminophenyl)benzothiazole (APBT) in different environments was detected by steady-state and transient fluorescence spectral measurements and quantum chemical calculations. The results showed that the polarity and protonation of the solution strongly affect the proton transfer of APBT. When APBT and cucurbit[7]uril (CB[7]) were mixed with each other, we found that the proton transfer process of APBT was restrained by the formation of a complex with a stoichiometric ratio of 1 : 1. The association constant and thermodynamic parameters of this complex were calculated. ^{1}H NMR spectroscopy and quantum chemical calculation data indicated that a 1 : 1 APBT@CB[7] complex of the amine or imine tautomer of APBT formed.

Key Words: Proton transfer; Cucurbit[7]uril; Polarizable continuum model; Thermodynamics; Host-guest chemistry

1 引 言

质子转移[1−3]在化学和生物领域中都广泛存在[4,5]。质子转移化合物在光、电或者是热的作用下，其酸性基团上的质子通过分子内氢键转移到相对应的N、O或S等能够接受质子的基团上，这一过程就是激发态质子转移(ESIPT)。激发态质子

Received: August 28, 2015; Revised: December 28, 2015; Published on Web: December 29, 2015.
*Corresponding author. Email: yipinggui@sohu.com; Tel: +86-731-58290187; Fax: +86-731-58290187.
The project was supported by the National Natural Science Foundation of China (21172066, 20971041) and Hunan University of Technology Team Projects , China ([2012]318).
国家自然科学基金(21172066, 20971041)和湖南省高校科技创新团队项目(湘教通[2012]318)资助

Research Article

Journal of Physical Organic Chemistry

Received: 7 June 2014, Revised: 9 July 2014, Accepted: 16 July 2014, Published online in Wiley Online Library: 11 August 2014

(wileyonlinelibrary.com) DOI: 10.1002/poc.3341

An attempt of molecular design and synthesis of 3,4′/4,3′-disubstituted benzylideneanilines with specified UV–Vis absorption maximum wavelength

Linyan Wang[a,b,c], Chaotun Cao[b,c] and Chenzhong Cao[b,c]*

Thirty-one samples of 3,4′/4,3′-disubstituted benzylideneanilines (XBAY) with specified UV–Vis absorption maximum wavelength (λ_{max}) were designed and synthesized by applying the equation (Eqn (1)) which was abstracted from the UV–Vis absorption maximum wavelength energy ($\nu_{max} = 1/\lambda_{max}$) of 4,4′-disubstituted benzylideneanilines. Then, the UV–Vis data (λ_{max}) of the designed compounds were measured in anhydrous ethanol. The predicted UV–Vis data of designed compounds are in agreement with the experimental ones, in which the mean absolute error is 2.9 nm. The results show that Eqn (1) is applicative for the prediction of UV–Vis absorption λ_{max} values of both 4,4′-disubstituted benzylideneanilines and 3,4′/4,3′-disubstituted benzylideneanilines. For a same pair of groups (X and Y), one can at least get four disubstituted benzylideneaniline compounds which have different λ_{max} values. It perhaps provides a convenient method to design an optical material for benzylideneaniline compounds. Copyright © 2014 John Wiley & Sons, Ltd.

Keywords: disubstituted benzylideneaniline; UV spectrum; molecular design; synthesis

INTRODUCTION

In recent years, optoelectronic materials have attracted extensive attention as a new type of function material. In the field of optoelectronic materials, the liquid crystal and nonlinear optical (NLO) material are the hot topics and have been studied deeply, which involve inorganic materials and organic materials.[1–3] Compared with inorganic materials, organic materials have vaster application prospects because their molecules are easy to be designed and assembled. Some organic compounds containing classical π conjugate system are applied well in many fields of optical function materials due to their potential optoelectronic properties.[4–7] The benzylideneanilines are a kind of typical compounds that have π conjugate system; their polymers and coordination compounds are important optical functional compounds and have been applied extensively in the fields of liquid crystal and NLO material.[3,8–10] For example, Ramamurthi[11,12] et al. have made many linear and nonlinear studies deeply about the compounds of 4-bromo-4′-chloro benzylideneaniline and 4-bromo-4′-dimethylamino benzylideneaniline, and attained meaningful results. The previous studies of benzylideneanilines mostly focus on the synthesis, photoelectric performance and quantitative molecular structure–performance relationship.[10,13–15] As we know, luminescent materials and filters have particularly a close connection to their UV–Vis absorption maximum wavelength energy; if a designed optoelectronic material can be put into a practical application, its molecular UV–Vis absorption maximum wavelength energy (ν_{max}) must be predicted accurately in advance. Therefore, to design and synthesize a series of target compounds with the specified UV–Vis absorption ν_{max} values is a key and an important work for getting the optoelectronic materials with the desired performance.

In our previous research,[15–20] the excited-state substituent constants have been proposed to quantify the influence of substituent on the UV–Vis absorption ν_{max} values and were applied successfully in quantifying the UV–Vis absorption ν_{max} values of compounds, such as XPh, XPhY, XPh(CH = CH)$_n$PhY (n = 0, 1, 2), XPhCH = NPhY and XPh(CH = CHPh)$_n$Y (n = 0, 1, 2). Moreover, a general equation of quantifying the UV–Vis absorption ν_{max} values of 4,4′-disubstituted benzylideneanilines (XBAY) has been proposed,[15] which is rewritten as shown in Eqn (1).

$$\nu_{max} = 32119.79 - 718.51\sigma(X) + 1197.18\sigma(Y) - 1017.23\Delta\sigma^2 + 1632.49\sum\sigma_{cc}^{ex} - 229.53\Delta\sigma_{cc}^{ex2} \quad (1)$$

* *Correspondence to: Chenzhong Cao, School of Chemistry and Chemical Engineering, Hunan University of Science and Technology, Xiangtan 411201, China. E-mail: czcao@hnust.edu.cn*

a *L. Wang*
School of Chemistry and Chemical Engineering, Central South University, Changsha 410083, China

b *L. Wang, C. Cao, C. Cao*
School of Chemistry and Chemical Engineering, Hunan University of Science and Technology, Xiangtan 411201, China

c *L. Wang, C. Cao, C. Cao*
Key Laboratory of Theoretical Organic Chemistry and Function Molecule (Hunan University of Science and Technology), Ministry of Education, Hunan Provincial University Key Laboratory of QSAR/QSPR, Hunan University of Science and Technology, Xiangtan 411201, China

Vol. 35 高等学校化学学报 No. 6
2014 年 6 月 CHEMICAL JOURNAL OF CHINESE UNIVERSITIES 1219 ~ 1223

doi: 10.7503/cjcu20130996

光谱法研究七元瓜环作用下 2-(2-羟苯基)咪唑并[1,2-a]吡啶的质子转移

易平贵，刘 金，陈 建，于贤勇，李筱芳，郑柏树，陶洪文，郝艳雷

(湖南科技大学化学化工学院，理论化学与分子模拟省部共建教育部重点实验室，
分子构效关系湖南省普通高等学校重点实验室，湘潭 411201)

摘要 采用荧光发射光谱法、瞬态荧光光谱法和紫外-可见光谱法考察了七元瓜环(CB7)与 2-(2-羟苯基)咪唑并[1,2-a]吡啶(HPIP)的相互作用，结果表明二者发生了相互作用. 瞬态荧光光谱结果表明，CB7 的加入使荧光寿命下降而量子产率逐渐增加，在 1,4-二氧六环溶液中，CB7 的加入限制了 HPIP 的质子转移过程，而在环己烷溶液中则有利于 HPIP 的激发态质子转移. 采用 Benesi-Hildebrand 方程对所测数据进行了线性拟合，结果表明形成了化学计量比为 1∶1 的复合物.

关键词 七元瓜环；2-(2-羟苯基)咪唑并[1,2-a]吡啶；质子转移；相互作用

中图分类号 O621.1；O641.3 **文献标志码** A

激发态分子内质子转移(ESIPT)是指荧光分子受到激发后，在分子内部相邻位置的质子供体和质子受体之间发生的质子转移过程. 近年来，对于 ESIPT 的实验和理论研究已有大量报道[1~9]. 瓜环[10~12](葫芦脲 Cucurbit[n]uril)是由甘脲单元连接成的大环化合物，由于具有纳米尺寸的疏水空腔、亲水的端口、刚性的结构和极强的主客体相互作用能力，已成为广泛用于主客体相互作用研究的主体化合物[13~18]. 由于具有生物活性，咪唑并[1,2-a]吡啶及其衍生物近年来备受关注[19~21]. 2-(2-羟苯基)咪唑并[1,2-a]吡啶(HPIP)是在咪唑并[1,2-a]吡啶的咪唑环的 3 位上连接了邻羟基苯基的衍生物，Douhal 等[22]首次报道了 HPIP 的分子内质子转移过程. Mutai 等[23]合成了一系列 HPIP 衍生物，并研究了取代基效应对其在液体介质和刚性介质中 ESIPT 的影响. Shigemitsu 等[24]通过量子化学计算的方法研究了 HPIP 在固体状态下荧光的增强和荧光对不同异构体的依耐性. 迄今，将 HPIP 作为受体小分子，与瓜环相互作用的激发态质子转移的研究尚未见报道. 本文以七元瓜环(CB7)作为主体分子，对 HPIP 在 CB7 作用下的质子转移过程进行了研究，为进一步研究纳米介质中质子转移的规律以及生物体系中质子转移过程的研究提供了参考.

1 实验部分

1.1 试剂与仪器

七元瓜环(CB7)由贵州大学陶朱教授课题组提供；2-氨基吡啶购自国药集团化学试剂有限公司；邻氨基苯乙酮购自上海达瑞精细化学品有限公司；1,4-二氧六环和无水乙醇购自天津科密欧试剂有限公司；所用试剂均为分析纯；实验用水为二次蒸馏水.

Bruke AVⅡ 500 MHz 核磁共振仪；Shimadzu RF-5301 PC 荧光光谱仪；Shimadzu UV-2501 PC 紫外-可见分光光度计；FLSP920 稳态瞬态荧光光谱仪；Q-Tof Premier 液相色谱-四极柱飞行时间质谱仪.

1.2 实验过程

1.2.1 HPIP 的合成 参照文献[25]方法合成 HPIP，ESI-HRMS($C_{13}H_{10}N_2O$ 文献值[25])，*m/z*:

收稿日期：2013-10-12.

基金项目：国家自然科学基金(批准号：21172066，20971041)、湖南省自然科学基金(批准号：11JJ2007)和湖南省高校科技创新团队项目(批准号：湘教通[2012]318)资助.

联系人简介：易平贵，男，博士，教授，主要从事功能分子设计合成与理论计算研究. E-mail：pgyi@hnust.cn

Chinese Chemical Letters 25 (2014) 1271–1274

Contents lists available at ScienceDirect

Chinese Chemical Letters

journal homepage: www.elsevier.com/locate/cclet

Original article

Using unmodified Au nanoparticles as colorimetric probes for TNT based on their competitive reactions with melamine

Xiao-Dong Xia *, Hao-Wen Huang

Key Laboratory of Theoretical Chemistry and Molecular Simulation, Minister of Education, School of Chemistry and Chemical Engineering, Hunan University of Science and Technology, Xiangtan 411201, China

ARTICLE INFO

Article history:
Received 14 January 2014
Received in revised form 16 February 2014
Accepted 28 February 2014
Available online 12 March 2014

Keywords:
Electron donor–acceptor interaction
Gold nanoparticles
Melamine
Trinitrotoluene
Colorimetry

ABSTRACT

Gold nanoparticles (Au NPs) can serve as visualized colorimetric probes for various targets and modification-free sensing strategies are preferred. The donor–acceptor interaction between the electron-rich melamine (MA) and the electron-deficient trinitrotoluene (TNT) allows formation of a supramolecule in aqueous solution. Melamine alone makes the initially individual reddish Au NPs aggregate into gray/blue Au NP assemblies due to melamine forming multiple ligand sites toward the Au NPs. Interestingly, the preformed supramolecule of MA–TNT disenables aggregation of the Au NPs. Therefore the unmodified Au NPs provide facile colorimetric probes for TNT detection in aqueous solution. Rapid identification of TNT is established by naked eye inspection. By using spectrophotometer tools, quantification of TNT is accomplished with a linear range of 80 μmol L^{-1} to 1.2 mmol L^{-1} and a limit of detection (LOD) of 27 μmol L^{-1}. In contrast to previous strategy with surface-modified Au NPs, here a modification-free sensing strategy for TNT assay has been developed with greater convenience, rapidity, and cost-effectiveness.

1. Introduction

2,4,6-Trinitrotoluene (TNT), a leading example of a nitroaromatic explosive, detrimentally affects the environment and human health, and threatens the safety of society. Traditional assays for TNT detection, such as gas chromatography and mass spectroscopy (MS), are accurate. However, these assays cannot be field-deployed and need bulky and expensive instruments, time-consuming sample preparation, and well-trained technicians [1–3]. For on-the-spot detection of TNT, dramatic improvements in detection methods are essential.

Recently, nanomaterials with various functionalities have been widely employed as reliable analytical platforms for TNT. For example, nanomaterial-based optical sensors for TNT detection exhibit improved sensitivity and selectivity [4–9]. A cysteine-modified Au nanoparticle (Au NPs) can serve as a surface-enhanced Raman probe for TNT recognition based on the formation of a Meisenheimer complex between TNT and cysteine [9], and amine group-functionalized mesoporous silica nanocomposites containing fluorescent polymers have been used as sensors to detect TNT by emission quenching [10]. Also, nanostructures containing fluorescent Ag nanoclusters (NCs) have been employed to sense and image TNT [11], and various quantum dots (QDs) have been exploited to detect TNT [7,12,8]. However, most of these strategies involve time-consuming nanomaterial preparation and functionalization and require special instruments. For promoting safety and environmental conscientiousness, visualized colorimetric probes enabling on-the-spot detection of TNT are preferred.

Visual colorimetric methods are extremely attractive because the detection results can be easily read out by the naked eye. The surface plasmon absorption band of gold nanoparticles, which is located in the visible region with a very high extinction coefficient (2.7×10^8 L mol^{-1} cm^{-1} at 520 nm for 13 nm Au NPs), provides promising visualized colorimetric platforms [13–16]. All these colorimetric sensors are based on the color change of Au NPs caused by their controllable dispersion/aggregation states. Au NP-based colorimetric probes are often achieved by carefully tailoring the surface chemistry of the Au NPs for identification of specific analytes. Particularly, cysteamine-functionalized Au NPs has been developed into a colorimetric sensor for determination of TNT [17]. The electron donor–acceptor (D–A) interaction between the primary amine of cysteamine and TNT allows aggregation of the initially dispersed Au NPs, resulting in color change from red to blue. Also, ethylenediamine (EDA)-capped Au NPs can serve as

* Corresponding author.
E-mail address: xxdwork@126.com (X.-D. Xia).

http://dx.doi.org/10.1016/j.cclet.2014.03.008

Cu^{2+} 印迹壳聚糖/Al_2O_3 的制备及动态吸附性能

曾坚贤，陈华俊，刘国清，喻 谢，钱朝辉
(湖南科技大学 化学化工学院 理论化学与分子模拟省部共建教育部重点实验室
分子构效关系湖南省普通高等学校重点实验室，湖南 湘潭 411201)

摘要: 以表面接枝和表面印迹技术为基础，采用正硅酸乙酯改性的 Al_2O_3 为载体，壳聚糖为功能单体，制备了一种新型 Cu^{2+} 印迹壳聚糖/Al_2O_3 复合材料(IIP/Al_2O_3) ，以傅里叶变换红外表征了 IIP/Al_2O_3，发现 Cu^{2+} 印迹壳聚糖被有效接枝到 Al_2O_3 表面。考察填充柱入口 Cu^{2+} 质量浓度、柱高、流速和 pH 值对 IIP/Al_2O_3 柱动态吸附性能的影响，研究动态吸附模型，结果表明: 当填充柱入口 Cu^{2+} 质量浓度为 100 mg/L、柱高为 37.25 mm、流速为 1.0 mL/min 和 pH 值为 5 时，IIP/Al_2O_3 柱穿透吸附量和平衡吸附量分别为 4.03 和 15.68 mg/g，吸附平衡时间为 215 min，穿透时间为 31 min，吸附行为符合 Thomas 模型，理论平衡吸附量为 15.76 mg/g，Thomas 常数为 $0.342\ 9\times10^{-3}$ L/(mg·min) 。研究 IIP/Al_2O_3 柱的选择性分离特性和稳定性，发现 IIP/Al_2O_3 柱对 Cu^{2+} 吸附率远高于竞争离子 Ni^{2+} 和 Zn^{2+}，经 5 次吸附-洗脱后，穿透吸附量及平衡吸附量仅分别下降 5.2% 和 3.0% 。

关键词: 表面印迹; 动态吸附; 铜离子; 壳聚糖; 三氧化二铝
中图分类号: TQ 028.8 **文献标识码:** A **文章编号:** 1005-9954(2014) 07-0022-06
DOI: 10.3969/j.issn.1005-9954.2014.07.005

Preparation and dynamic adsorption performance of copper (Ⅱ) -imprinted chitosan/Al_2O_3 composite material

ZENG Jian-xian, CHEN Hua-jun, LIU Guo-qing, YU Xie, QIAN Zhao-hui
(Hunan Province College Key Laboratory of QSAR/QSPR; Key Laboratory of Theoretical Chemistry and Molecular Simulation of Ministry of Education; School of Chemistry and Chemical Engineering, Hunan University of Science and Technology, Xiangtan 411201, Hunan Province, China)

Abstract: Taking Al_2O_3 modified with tetraethylorthosilicate as carrier material, and chitosan as functional monomer, a novel copper ion imprinted chitosan/aluminium oxide (IIP/Al_2O_3) was prepared based on the surface-grafted and surface imprinting technologies. The IIP/Al_2O_3 was characterized by using the Fourier transform infrared spectroscopy. The results show that copper ion imprinted chitosan is grafted successfully on the surface of Al_2O_3. The effects of Cu^{2+} inlet mass concentration, column height, flow rate and pH value on the dynamic adsorption of Cu^{2+} on IIP/Al_2O_3 were investigated. The model for dynamic adsorption of Cu^{2+} on IIP/Al_2O_3 was studied. The results indicate that when Cu^{2+} inlet mass concentration is 100 mg/L, column height is 37.25 mm, flow rate is 1.0 mL/min and pH value is 5, the breakthrough capacity and dynamic adsorption capacity of the IIP/Al_2O_3 are 4.03 mg/g and 15.68 mg/g, respectively, and equilibrium time and breakthrough time are 215 min and 31 min, respectively. Thomas model is suitable for the description of dynamic adsorption of the IIP/Al_2O_3. The theoretical adsorption capacity of the IIP/Al_2O_3 is 15.76 mg/g, and Thomas constant is $0.342\ 9\times10^{-3}$ L/(mg·min) . The selectivity and stability of IIP/Al_2O_3 were studied further. The IIP/Al_2O_3 showed good characteristics, such as high selectivity and good reusability. The adsorption percentage of Cu^{2+} on IIP/Al_2O_3 was higher than that of Ni^{2+} or Zn^{2+} on IIP/Al_2O_3. After the adsorption-desorption cycles were repeated 5 times, the breakthrough capacity and dynamic adsorption capacity were decreased only by 5.2% and 3.0%, respectively.

收稿日期: 2013-11-29
基金项目: 国家自然科学基金资助项目(20976040) ; 湖南省自然科学基金资助项目(13JJ3086)
作者简介: 曾坚贤(1970—) ，男，博士，教授，主要从事新型分离技术研究，E-mail: zengjianxian@163.com。

doi:10.13582/j.cnki.1672-9102.2014.04.020

分子结构对羧酸酯亲核取代反应速率的定量影响规律

袁华,卢永志

(湖南科技大学 理论有机化学与功能分子教育部重点实验室,分子构效关系湖南省普通高校重点实验室,
化学化工学院,湖南 湘潭 411201)

摘 要:羧酸酯的亲核取代反应速率受羧酸酯的离去基团(LG)、非离去基团(NLG)和亲核试剂(Nu)结构的影响.从文献整理了大量结构多样的羧酸酯与各种亲核试剂发生亲核取代反应的表观二级速率常数 k_N,基于亲核取代反应机理,用非离去基团的极化效应指数 PEI(NLG)和基团体积参数 GVI(NLG),亲核试剂与离去基团的体积参数之比 GVI(Nu)/GVI(LG),以及亲核试剂与离去基团共轭酸的 pK_a 之差(pK_a(Nu)-pK_a(LG))分别表征非离去基团、离去基团和亲核试剂的结构特征及亲核试剂与离去基团的相互竞争,并用上述参数对 73 组亲核取代反应的 $\log k_N$ 建立多元线性回归模型,得到较好的结果.该模型所用参数简便,物理意义明确,为从分子结构特征定量估算羧酸酯亲核取代反应的速率提供了理论依据.

关键词:羧酸酯;亲核取代;反应速率;定量结构-性质相关

中图分类号:O647 **文献标志码**:A **文章编号**:1672-9102(2014)04-0098-06

The quantitative influence of molecular structure on the nucleophilic substitution reaction rate of carboxylic esters

YUAN Hua, LU Yongzhi

(Key Laboratory of Theoretical Organic Chemistry and Function Molecule, Ministry of Education,
Key Laboratory of QSAR/QSPR of Hunan Provincial University, School of Chemistry and Chemical Engineering,
Hunan University of Science and Technology, Xiangtan 411201, China)

Abstract: The nucleophilic substitution reaction rate of carboxylic ester is influenced by the structures of leaving group (LG), non-leaving group (NLG) of carboxylic ester and the nucleophile (Nu). A large number of apparent second-order rate constants (k_N) were colletcd and analyzed, which of nucleophilic substitution reactions between structurally diverse carboxylic esters and a variety of nucleophiles. Based on the mechanism of nucleophilic substitution reaction, the polarizability effect index PEI(NLG) and group volume index GVI(NLG) of non-leaving group, the ratio of group volume index of nucleophile to that of the leaving group GVI(Nu)/GVI(LG), the difference between pK_a of the conjugate acid of nucleophile and that of leaving group (pK_a(Nu)-pK_a(LG)), were employed to characterize the structures of non-leaving group, leaving group and nucleophile. $\log k_N$ of 73 nucleophilic substitution reactions were correlated to the structural descriptors mentioned above, and multiple linear regression model was established with good performances. The parameters used in the model were simple and had clear physical meanings. This study provided a theoretical basis for quantitatively estimating the nucleophilic substitution reaction rate of carboxylic esters from molecular structures.

Key words: carboxylic ester; nucleophilic substitution; reaction rate; quantitative structure-property relationship

收稿日期:2014-11-19

基金项目:湖南省自然科学基金资助项目(14JJ3112);理论有机化学与功能分子教育部重点实验室开放基金(E21205)

通信作者:袁华(1976-),女,湖南邵阳人,博士,副教授,主要从事物理有机化学研究. E-mail: yh_cathy@163.com

DOI:10.19342/j.cnki.issn.1009-9212.2014.04.009

医药及中间体

邻氨基苯甲醇烷基化合成 2-(2-羟甲基苯基氨基)乙酰芳胺

王 恋[1]，唐子龙[1,2*]，王宏清[3]，王岭帅[1]，焦银春[1,2]
(1. 湖南科技大学 化学化工学院，湖南 湘潭 411201；2. 湖南科技大学 理论有机化学与功能分子教育部重点实验室，湖南 湘潭 411201；3. 南华大学 化学化工学院，湖南 衡阳 421001)

摘 要：研究了 2-溴乙酰芳胺对邻氨基苯甲醇的烷基化反应，反应主要发生在 *N* 原子上，并由此合成了一系列新型芳胺基取代乙酰芳胺类化合物（**4a~4e**）。对反应溶剂、碱的种类及用量、反应温度、时间、反应物的量之比等条件对反应的影响进行了研究，获得优化反应条件。在优化条件下化合物 **4a~4e** 的收率为 68.9%~72.8%。对反应影响比较大的因素主要是溶剂，采用 *v*(*N*,*N*-二甲基甲酰胺):*v*(四氢呋喃)=1:2 的混合溶剂可使反应收率从 36.1%（THF 中）提高到 70.3%。用 IR、^{1}H NMR 和 ^{13}C NMR 对化合物 **4a~4e** 的结构进行了分析与表征。

关键词：邻氨基苯甲醇；烷基化反应；2-(2-羟甲基苯基氨基)乙酰芳胺；合成
中图分类号：TQ246 **文献标志码**：A **文章编号**：1009-9212(2014)04-0035-05

Synthesis of 2-(2-Hydroxymethylphenylamino)acetyl Arylamides by Alkylation of 2-Aminobenzyl Alcohol

WANG Lian[1], *TANG Zi-long*[1,2*], *WANG Hong-qing*[3], *WANG Ling-shuai*[1], *JIAO Yin-chun*[1,2]
(1. School of Chemistry and Chemical Engineering, Hunan University of Science and Technology, Xiangtan 411201, China; 2. Key Laboratory of Theoretical Organic Chemistry and Function Molecules, Ministry of Education, Xiangtan 411201, China; 3. School of Chemistry and Chemical Engineering, University of South China, Hengyang 421001, China)

Abstract: The alkylation of 2-aminobenzyl alcohol with 2-bromoacetyl arylamines was studied. The alkylation reaction dominantly gave *N*-alkylation product. The effects of solvent, the sort and the amount of bases, temperature, reaction time and the ratio of the reactants on the yield of the product were investigated and the target products (**4a~4e**) were obtained in yield of 68.9%~72.8% under optimum conditions. The results showed that the solvent impacted great influence on the yield. The reaction yield was raised from 36.1% in THF to 70.3% in the mixture solvent of *v*(DMF):*v*(THF)=1:2. The structures of **4a~4e** were characterized by IR, ^{1}H NMR and ^{13}C NMR spectra.

Key words: 2-aminobenzyl alcohol; alkylation; 2-(2-hydroxymethylphenylamino)acyl arylamide; synthesis

1 前 言

烷基化反应在有机合成中占有重要地位，特别是胺的 *N*-烷基化反应，在药物、阳离子表面活性剂、染料等领域发挥着重要作用[1-5]。如药物分子中的氨基经烷基化后可提高其脂溶性和对人体的渗透性[4]。染料分子中的氨基经烷基化后可加深染料的颜色等，故胺的烷基化反应在染料工业有着极为重要的意义[5]。

另一方面，酰胺类化合物具有广泛的生物活性，如杀菌活性[6]，商品化的杀菌剂有酰芳胺类杀

基金项目：国家自然科学基金（21372070），湖南省高校创新平台开放基金（13K089），理论有机化学与功能分子教育部重点实验室开放基金（LKF1302）。
作者简介：王 恋（1989-），女，湖南邵阳人，硕士研究生，主要从事有机合成化学研究（491862259@qq.com）。
联 系 人：唐子龙，教授，博士，主要从事有机合成、农药化学和药物化学研究（E-mail：zltang67@aliyun.com）。
收稿日期：2014-06-27

DOI: 10.13595/j.cnki.issn1000-0720.2014.0291

电化学法制备电还原的氧化石墨烯 - 铁氰化镍修饰电极检测亚硝酸根

李春香,邱喜阳,周建红,邓克勤*
(湖南科技大学化学化工学院理论有机化学与功能分子教育部重点实验室,湘潭 411201)

摘 要: 通过静电作用,在氧化石墨烯(GO)表面吸附一层均匀分散的 Ni^{2+} 形成 GO-Ni^{2+} 复合物,利用循环伏安法,把 GO-Ni^{2+} 修饰电极上的 Ni^{2+} 转化为铁氰化镍(NiHCF),再通过电还原制备电还原的氧化石墨烯 - 铁氰化镍修饰的玻碳电极(ERGO-NiHCF/GCE)。采用扫描电子显微镜(SEM)对其表面结构进行了表征。研究了 NO_2^- 在不同修饰电极上的电化学行为,ERGO-NiHCF/GCE 对 NO_2^- 的氧化反应有很好的电催化活性,NO_2^- 的浓度与其氧化峰电流呈良好的线性关系。

关键词: 氧化石墨烯; 铁氰化镍; 亚硝酸根; 电化学
中图分类号: O657.1 **文献标识码:** A **文章编号:** 1000-0720(2014)11-1241-04

亚硝酸盐,具有防腐性,可防止肉毒梭状芽孢杆菌的产生,提高食用肉制品的安全性,还可与肉品中的肌红素结合而更稳定,在食品加工业作为保色剂。但是,人体吸收过量亚硝酸盐,会影响红细胞的运作,引起俗称的"蓝血病";它还可与氨基酸反应,生成有强致癌性的亚硝胺[1]。目前,测定 NO_2^- 的方法主要有分光光度法[2]、离子色谱法[3]、化学发光法[4],毛细管电泳法[5]和电化学分析法[6,7]等。

氧化石墨烯(GO)作为化学合成石墨烯的前驱物,其表面具有相当数量的活性基团,能与多种有机和无机材料通过非共价键、共价键或离子键方式相互作用,合成功能化的混合物和复合物,可弥补功能缺陷或提高石墨烯的性能[8]。本文通过静电作用,在 GO 表面吸附一层均匀分散的 Ni^{2+} 形成 GO-Ni^{2+} 复合物,利用循环伏安法,把 GO-Ni^{2+} 修饰电极上的 Ni^{2+} 转化为铁氰化镍(NiHCF),再通过电化学还原 GO 制备电还原的氧化石墨烯 - 铁氰化镍修饰的玻碳电极(ERGO-NiHCF/GCE),该电极 NO_2^- 的氧化表现出了良好的电催化活性,据此建立了测定 NO_2^- 的新方法。

1 实验部分

1.1 仪器与试剂

CHI 760C 电化学工作站(上海辰华公司);JSM-5610L 扫描电子显微镜(日本 JEOL 公司);三电极系统:修饰的玻碳电极为工作电极,饱和甘汞电极为参比电极,铂电极为对电极。

$NaNO_2$,$NiCl_2$,铁氰酸钾($K_3Fe(CN)_6$)、高纯石墨粉均购于上海化学试剂厂。其他试剂均为分析纯,水为二次蒸馏水。

1.2 GO-Ni^{2+} 的合成

GO 采用 Hummers 和 Offeman 法制备[9],后将其分散于水中透析纯化 3 次,每次 24 h,之后超声处理 60 min,取上层液离心分离,并在 40 ℃ 真空条件下干燥,即得 GO。充分混合等体积的 0.5 mg/mL 的 GO 分散液与 0.2 mmol/L 的 $NiCl_2$ 溶液,磁力搅拌 3 h,离心分离掉过量的 Ni^{2+} 后,分散沉降物到二次水中。再次离心并分散,得到吸附 Ni^{2+} 的 GO-Ni^{2+} 溶液。

1.3 修饰电极的制备

将玻碳电极(GCE)表面抛光,并依次用 8 mol/L HNO_3,0.2 mol/L NaOH、丙酮、水各超声洗涤 5 min,干燥。在洁净的电极表面滴加 5 μL

收稿日期: 2014-06-29
基金项目: 国家自然科学基金(21471052)、湖南省科技计划项目(2014F53048)与教育部重点实验室开放课题(LKF1306)资助
E-mail: keqindeng@hnust.edu.cn

综合评述

锂离子电池电极材料磷酸氧钒锂的研究进展

贺冬华[a] 唐安平[a,b*] 申 洁[a] 徐国荣[a,b] 刘立华[a,b] 令玉林[b]
([a]湖南科技大学化学化工学院;[b]理论化学与分子模拟省部共建教育部重点实验室 湘潭 411201)

摘 要 介绍了磷酸氧钒锂(α-$LiVOPO_4$、β-$LiVOPO_4$和α_1-$LiVOPO_4$)电极材料的结构和电化学性能;综述了现有的$LiVOPO_4$电极材料的合成方法(包括高温固相法,化学还原法,溶胶-凝胶法,溶剂热法,离子交换法等)及其改性研究现状。最后对其未来的发展趋势进行了展望。

关键词 锂离子电池,磷酸氧钒锂,正极材料,合成方法
中图分类号:O646.2 文献标识码:A 文章编号:1000-0518(2014)10-1115-08
DOI:10.3724/SP.J.1095.2014.30632

锂离子电池具有工作电压高、能量密度大、循环性能好、自放电小、无记忆效应和工作温度范围宽等优点,已成为目前综合性能最好的二次电池体系,因而广泛应用于许多便携式电子设备上,如移动手机、笔记本电脑和小型摄像机等。近年来新一代电子产品及电动汽车的开发与应用对二次电源系统的能量密度和功率密度提出了更高要求,而新型高容量电极材料特别是正极材料的开发是获得高性能锂离子电池的关键。以$LiFePO_4$为代表的聚阴离子型化合物作为锂离子电池正极材料具有良好的性能[1-5],可望成为下一代锂离子电池正极。

钒是价态丰富的过渡金属元素,它既可以与锂和磷酸根等结合生成聚阴离子型化合物,也可先与氧结合,再以钒氧离子的形式与锂和磷酸根等结合,因此,钒的聚阴离子型化合物电池材料具有很大的研究空间。目前,研究发现的具有储锂性能的含钒磷酸盐体系正极材料主要有$LiVPO_4F$[6-8]、$Li_3V_2(PO_4)_3$[9-11]和$VOPO_4$[12-13]或$LiVOPO_4$[14]等。相对钒的氧化物而言,PO_4^{3-}对O^{2-}的取代,使化合物的三维结构发生了变化,增加了化合物的结构稳定性,并使Li^+扩散通道变大,有利于Li^+的嵌脱。此外,离子取代还能够从两个方面改变电位,即通过诱导效应改变离子对和金属离子的能级以及通过提供较多的电子来改变Li^+的浓度,从而有利于氧化还原反应的发生。其中$LiVOPO_4$中P—O共价键的存在不仅能够提高$LiVOPO_4$动力学和热力学稳定性,而且还能削弱V—O共价键(即诱导效应),降低V^{4+}/V^{5+}反键轨道能,从而提高V^{4+}/V^{5+}的氧化还原能级,使得$LiVOPO_4$具有比V_2O_5更高的放电平台(前者约为3.9 V *vs* Li/Li^+,后者约为3.5 V)。尽管$Li_3V_2(PO_4)_3$的理论比容量高达197 mA·h/g,但在放电过程中出现多个电压平台,这样不利于它在锂离子电池中的实际应用;其次,它的第三个电子的脱嵌[$LiV_2(PO_4)_3(V_2(PO_4)_3$]电位值高达4.5 V以上,易造成电解液的氧化分解。因此,$LiVOPO_4$的放电平台较为理想,因为它不至于高到分解电解液,又不至于低到牺牲能量密度。此外,尽管$LiVOPO_4$的理论比容量(158 mA·h/g)稍低于$LiFePO_4$的理论比容量(170 mA·h/g),但它具有更高的放电平台(3.9 V *vs* Li/Li^+)以及更高的理论能量密度(616 Wh/Kg)。再者,与$LiFePO_4$、$LiVPO_4F$、$Li_3V_2(PO_4)_3$相比,$LiVOPO_4$的制备相对简易,可以在空气气氛下进行制备反应,避免了还原性气体或惰性气体的使用。基于以上优点,$LiVOPO_4$正极材料引起了人们的关注。

本文重点对锂离子电池正极材料$LiVOPO_4$的结构、合成方法及电化学性能的研究现状进行综述。

2013-12-11 收稿,2014-01-20 修回,2014-03-21 接受
湖南省自然科学基金(12JJ2022,06JJ50078)资助项目

通讯联系人:唐安平,副教授; Tel:0731-58290683; Fax:0731-58290187; E-mail:anpingxt@126.com; 研究方向:新型化学电源及其电极材料

文章编号：1000-1190(2014)03-0360-06

$FeCl_3 \cdot 6H_2O$ 催化合成 2,3-二取代-1,3-苯并噁嗪及其杀菌活性

唐子龙[1,2*]，夏赞稳[2]，陆良秋[1,3]

(1. 湖南科技大学 理论化学与分子模拟省部共建教育部重点实验室，湖南 湘潭 411201；
2. 湖南科技大学 化学化工学院，湖南 湘潭 411201；3. 华中师范大学 化学学院，武汉 430079)

摘 要：以 2-(胺甲基)苯酚和取代苯甲醛为原料，首次以 $FeCl_3 \cdot 6H_2O$ 为催化剂合成了一系列 2,3-二取代-1,3-苯并噁嗪，所合成化合物的结构用 IR、^1H NMR、^{13}C NMR 进行了分析与鉴定. 采用离体法初步测试了目标化合物的杀菌活性，大部分化合物具有良好的杀菌活性，化合物 3c 对灰霉病菌的抑制率为 86.8%，3f 对纹枯病菌的抑制率为 87.7%.

关键词：2,3-二取代-1,3-苯并噁嗪；催化；合成；杀菌活性

中图分类号：O626 **文献标识码**：A

3,4-二氢-1,3-苯并噁嗪(简称 1,3-苯并噁嗪)类化合物通常具有抗病毒、抗癌、杀菌等生物活性[1-7]. 2-芳酰基-1,3-苯并噁嗪类化合物，具有很好的抗 HIV 病毒的活性，可用来治疗 AIDS[3]. 3,4-二烷基-1,3-苯并噁嗪类化合物既具有杀虫活性又具有杀菌活性[4]；N-酰基-1,3-苯并噁嗪类化合物对金黄色葡萄球菌、大肠杆菌、枯草杆菌和病原菌具有良好的活性[5]. 吡啶基取代 1,3-苯并噁嗪类化合物具有抑制 DNA 依赖性蛋白激酶 (DNA-PK) 和抗血小板的生物活性[6]. 含环酮基的 1,3-苯并噁嗪类化合物对人体乳腺癌细胞 (MCF-7) 具有抑制活性[7]. 含 1,3-苯并噁嗪环的喜树碱衍生物对胰腺癌、肺癌、乳腺癌、肝癌和结肠癌等癌细胞具有一定的抑制作用[2]. 此外，1,3-苯并噁嗪类化合物还是合成苯并噁嗪树脂的重要单体[8-9]. 近年来，发现螺 1,3-苯并噁嗪类化合物具有光致变色的特性，成为一类新型光致变色材料[10-11].

1,3-苯并噁嗪类化合物的合成一直受到广泛关注. Mannich 反应是最早用来合成 1,3-苯并噁嗪的方法，也是用得最多的方法[12-13]. 另一种常见的方法就是利用邻氨基甲基苯酚与醛或酮的缩合成环反应[14-15]，这一反应通常需要对甲苯磺酸等作催化剂. 近年来，本课题组报道了 $SnCl_4$、$(CH_3)_3SiCl$ 催化邻氨基甲基苯酚与芳醛反应合成 2,3-二芳基-1,3-苯并噁嗪类化合物的方法[16-17]，利用相转移催化法合成了一系列 3-噻二唑基-1,3-苯并噁嗪类化合物[18]，并且发现这些化合物具有良好的杀菌活性.

$FeCl_3$ 和 $FeCl_3 \cdot 6H_2O$ 具有对环境友好、腐蚀性小、价格低廉等特点而日益受到重视，作为催化剂在有机合成中的应用已有大量报道，如能催化加成、取代、偶联、环化、羟醛缩合和氧化-还原等反应[19-21]. 但是，目前还未见 $FeCl_3$ 和 $FeCl_3 \cdot 6H_2O$ 用于 1,3-苯并噁嗪类化合物合成的报道. 因此，为了进一步研究 1,3-苯并噁嗪类化合物，以期发现活性更高的化合物，同时也为了获得合成 1,3-苯并噁嗪类化合物的新方法，本文以 $FeCl_3 \cdot 6H_2O$ 为催化剂，邻胺基甲基苯酚(1)和取代苯甲醛为原料，合成了一系列 2,3-二取代-1,3-苯并噁嗪类化合物，并对其杀菌活性进行了初步研究，合成路线如图 1 所示.

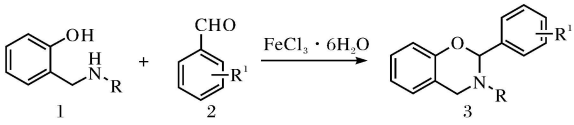

图 1 2,3-二取代-1,3-苯并噁嗪的合成

Fig. 1 Synthesis of 2,3-disubstituted-1,3-benzoxazines

收稿日期：2014-01-15.

基金项目：国家自然科学基金项目(21372070)；湖南省高校创新平台开放基金项目(13K089)；理论化学与分子模拟省部共建教育部重点实验室开放基金项目(LKF1102).

* 通讯联系人. E-mail：zltang67@aliyun.com.

doi:10.13582/j.cnki.1672-9102.2014.03.020

溶胶-凝胶自蔓延燃烧法制备铜铬黑颜料及表征

刘立华,李波,唐安平,徐国荣

(湖南科技大学 化学化工学院,理论有机化学与功能分子教育部重点实验室,
分子构效关系湖南省普通高等学校重点实验室,湖南 湘潭 411201)

摘　要:以硝酸铜和硝酸铬为原料,硬脂酸为胶凝剂,采用溶胶-凝胶自蔓延燃烧法合成了铜铬黑颜料.考察了原料配比对凝胶的制备,煅烧温度和保温时间对铜铬黑颜料晶型形成的影响,并用热重-差热分析和红外光谱对前驱体,以及扫描电镜、能谱分析和 X-射线衍射对产物结构进行表征.结果表明,当硝酸铜和硝酸铬的摩尔比为 1∶2,硬脂酸与金属盐的摩尔比为 1.25~1.50∶1,煅烧温度为 800 ℃,保温时间为 3 h 时,制备的铜铬黑颜料纯度高、晶型规整、粒度较小且分布较窄,其平均粒径为 60~80 nm.比以柠檬酸为胶凝剂的成本低,比高温固相法和醇-水共沉淀法的煅烧温度和能耗低.

关键词:铜铬黑颜料;溶胶-凝胶;自蔓延燃烧;硬脂酸

中图分类号:TQ 621.2　　**文献标志码**:A　　**文章编号**:1672-9102(2014)03-0091-07

Synthesis and structural characterization of copper chromite black pigment by sol-gel self-propagating combustion

LIU Lihua, LI Bo, TANG Anping, XU Guorong

(Key Laboratory of Theoretical Organic Chemistry and Function Molecule, Ministry of Education, Hunan Province College Key Laboratory of QSAR/QSPR, School of Chemistry and Chemical Engineering, Hunan University of Science and Technology, Xiangtan 411201, China)

Abstract: Copper chromite black pigment was prepared from copper nitrate and chromic nitrate using stearic acid as a gelling agent by sol-gel self-propagating combustion. The effects of raw material ratio on the sol preparation, and calcining temperature and holding time on the formation of copper chromite black crystal were investigated. The precursors prepared were characterized by thermogravimetry-differential thermal analysis (TG-DTA) and infrared spectroscopic analysis (IR), and the production structures were characterized by scanning electron microscope (SEM), energy spectrum analysis (ESA) and X-ray diffraction (XRD). The results show that, when the molar ratio of copper nitrate to chromic nitrate is 1∶2, the molar ratio of stearic acid to metal slats is 1.25~1.50∶1, and the calcination temperature is 800 ℃ and the holding time is 3 h, the copper chromite black pigment is of high purification, regular crystal form, and smaller particle size and narrow distribution. Its average particle size is about 60~80 nm. The cost of this method is lower than that using citric acid as a gelling agent, and the calcination temperature and energy consumption are lower than the solid-state method and the alcohol-water co-precipitation method.

Key words: Copper Chromite black pigment; sol-gel; self-propagating combustion; stearic acid

铜铬黑($CuCr_2O_4$)是一种具有尖晶石型晶体结构的黑色混相金属氧化物,由于具有优良的遮盖力、耐化学品性能,卓越的耐高温、耐候性能、户外稳定和不扩散等性能,在陶瓷、搪瓷、室外用的钢卷

收稿日期:2014-02-06
基金项目:国家自然科学基金资助项目(51078141);湖南省科技计划项目(2010FJ3030)
通信作者:刘立华(1969-),男,湖南隆回人,博士,教授,主要从事功能高分子和污染治理技术研究. E-mail: llh213@163.com

doi:10.13582/j.cnki.1672-9102.2014.03.021

咪唑啉季铵盐与 fsDNA 作用的共振光散射光谱分析及应用

石顺存,龙云飞, 邓春凤,喻娟娟,康玉佳

(湖南科技大学 化学化工学院 理论化学与分子模拟省部共建教育部重点实验室,
分子构效关系湖南省普通高等学校重点实验室, 湖南 湘潭 411201)

摘　要:利用环烷酸、二乙烯三胺或三乙烯四胺、硫酸二乙酯为原料合成了 2 种咪唑啉季铵盐 M_1 和 M_2,M_1,M_2 分别在 pH=2.36 和 pH=3.78 的 Britton-Robinson 缓冲溶液中与 fsDNA 相互作用后,体系的共振光散射(RLS)强度明显增强.研究了它们与 fsDNA 作用的影响因素,在优化条件下,RLS 强度增加值与 fsDNA 浓度之间呈良好的线性关系,拟定了新的测定 fsDNA 的 RLS 法.该法具有灵敏度高,操作简单,准确度好,线性范围宽等特点,用于合成样的测定,结果满意.

关键词:咪唑啉;咪唑啉季铵盐;fsDNA;共振光散射(RLS)

中图分类号:O657.3　　**文献标志码**:A　　**文章编号**:1672-9102(2014)03-0098-05

The interaction between imidazolinyl-quaternary-ammonium-salt and fsDNA and its analytical applications using resonance light scattering spectroscopy

SHI Shuncun, LONG Yunfei, DENG Chunfeng, YU Juanjuan, KANG Yujia

(Key Laboratory of Theoretical Chemistry and Molecular Simulation of Ministry of Education,
Hunan Province College Key Laboratory of Quantitative Structure-Activity or Structure-Property Relationship,
School of Chemistry and Chemical Engineering, Hunan University of Science and Technology, Xiangtan 411201, China)

Abstract: Two imidazolinyl-quaternary-ammonium-salt M_1 and M_2 were synthesised using naphthenic acid, diethylene triamine (or triethylene tetramine), and diethyl sulfate. The interaction between fsDNA respectively with M_1 and M_2, enhanced the intensities of resonance light scattering (RLS) significantly in Britton- Robinson buffer solution of the pH 2.36 for M_1 and 3.78 for M_2. Also, it was studied the effect factors on the reaction between imidazolinyl-quaternary-ammonium-salt and fsDNA. Under the optimum conditions, the enhanced intensities of RLS had good linear relationship with the concentration of fsDNA. Thus, a new RLS method for determination of fsDNA was established. The method has the properties of high sensitivity, simple operation, good accuracy and the wide range of linear. It can be used to the determination of fsDNA contain in the synthesized samples with the result of satisfying.

Key words: imidazoline, imidazolinyl-quaternary-ammonium-salt, fsDNA, resonance light scattering

咪唑啉类化合物,因对碳钢等金属具有良好的缓蚀性能而在工业上得到了较广泛的应用[1],本文工作发现,新合成的两种咪唑啉类化合物能和 DNA 发生强烈的相互作用并引起强烈的 RLS 强度增强现象,利用这一现象不仅能建立 fsDNA 的定量分析新方法,还可为继续研究合成的两种咪唑啉类化合物对细菌的抑制作用提供重要的指导.

DNA 分析在临床及生物化学分析中具有十分

收稿日期:2013-10-31
基金项目:湖南省教育厅资助项目(12k102);湖南省大学生研究性学习和创新性实验计划项目(KDCX0804)
通信作者:石顺存(1964-),男,湖南湘潭人,教授,主要从事水处理缓蚀剂研究. E-mali: shishuncun@163.com

doi:10.13582/j.cnki.1672-9102.2014.02.019

2-(2-羟苯基)苯并咪唑-碱(土)金属离子π复合物的电子结构及其分子内质子转移的理论研究

徐百元,易平贵,汪朝旭,于贤勇,刘峥军,侯博,郝艳雷

(湖南科技大学 化学化工学院,理论化学与分子模拟省部共建教育部重点实验室,
分子构效关系湖南省普通高等学校重点实验室,湖南 湘潭 411201)

摘 要:对碱(土)金属离子(Li^+, Na^+, K^+, Be^{2+}, Mg^{2+}和Ca^{2+})与2-(2-羟苯基)苯并咪唑(HBI)所形成阳离子-π复合物进行密度泛函B3LYP/6-311++G(d,p)水平的理论研究. 结果显示其有强阳离子-π作用. 并分析了复合物分子内氢键临界点的性质,相对能量和核磁计算结果显示碱(土)金属离子和溶剂化作用能增加或降低HBI分子内质子转移过程的能垒,可反转优势构型.

关键词:溶剂化效应;阳离子-π作用;分子中的原子(AIM);分子内质子转移;密度泛函理论(DFT)

中图分类号:O641.1;O621.1 **文献标志码**:A **文章编号**:1672-9102(2014)02-0089-05

Theoretical investigation on the electronic structure and intramolecular proton transfers of cation-π complexes of 2-(2-Hydroxyphenyl) benzoimidazole with alkali (alkali earth) metal ions

XU Bai-yuan, YI Ping-gui, WANG Zhao-xu, YU Xian-yong, LIU Zheng-jun, HOU Bo, HAO Yan-lei
(Key Laboratory of Theoretical Chemistry and Molecular Simulation of Ministry of Education, Hunan Province College Key Laboratory of QSAR/QSPR, School of Chemistry and Chemical Engineering, Hunan University of Science and Technology, Xiangtan 411201, China)

Abstract: The geometrical models of 2-(2-Hydroxyphenyl)benzoimidazole with alkali(or alkaline earth) metal ions were fully optimized by using B3LYP density functional theory at the 6-311++G(d, p) level. Results indicate that the cation-π interaction between metal ions and HBI compounds are strong, some of these even reach a chemical bond strength. The energy barrier of the intramolecular proton transfer increased or decreased by Cation-π interaction and injection solvent effects and these show in the relative energies display.

Key words: injection solvent effects; cation-π interaction; atoms in molecules(AIM); intramolecular proton transfer; density functional theory(DFT)

阳离子借助其正电荷与芳环中的π电子所形成的阳离子-π作用及分子内或分子间质子转移作用,在生物体中系普遍存在. 这些作用对分子识别,蛋白质核酸的结构功能及其稳定性,蛋白质与配体相互作用等有重要影响,其相关研究已被关注. 陈凯先等[1]系统研究了阳离子与苯分子或芳环基团间形成的阳离子-π复合物的物理机制,Vyas等[2]理论计算了Be^{2+}, Mg^{2+}, Ca^{2+}与苯丙氨

收稿日期:2013-11-08

基金项目:国家自然科学基金资助项目(21172066);湖南省自然科学基金资助项目(11JJ2007);湖南省高校科技创新团队支持计划资助项目([2012]318-17)

通信作者:易平贵(1961-),男,湖南邵阳人,博士,教授,主要从事分子构效与计算化学研究. E-mail: pgyi@hnust.cn

doi:10.13582/j.cnki.1672-9102.2014.04.022

一步 RAFT 聚合法合成两亲性嵌段共聚物 PEG-*b*-P(St-*co*-VBC)

黄富华,陈建,李亚,曾志强,侯庆杨,丁勇,刘胜利

(湖南科技大学 化学化工学院,理论化学与分子模拟省部共建教育部重点实验室,
分子构效关系湖南省普通高等学校重点实验室,湖南 湘潭 411201)

摘 要:采用一步可逆加成-断裂链转移(RAFT)聚合法合成了一系列分子量可控、分子量分布较窄的两亲性嵌段共聚物 PEG-*b*-P(St-*co*-VBC),并通过凝胶渗透色谱(GPC)、核磁共振谱(NMR)、傅立叶变换红外光谱(FT-IR)和示差扫描量热仪(DSC)对所合成的嵌段共聚物进行了相关表征.结果表明,通过控制聚合单体中对氯甲基苯乙烯(VBC)和苯乙烯(St)的摩尔比,可以实现对两亲性嵌段共聚物 PEG-*b*-P(St-*co*-VBC)中 VBC 重复单元的精确控制.随着嵌段共聚物中 VBC 含量的增加,PEG-*b*-P(St-*co*-VBC)的玻璃化转变温度逐渐升高.

关键词:聚乙二醇;可逆加成-断裂链转移聚合;对氯甲基苯乙烯;嵌段共聚物
中图分类号:TQ31;063 **文献标志码**:A **文章编号**:1672-9102(2014)04-0108-06

Synthesis of amphiphilic block copolymer PEG-*b*-P(St-*co*-VBC) via one-step RAFT polymerization method

HUANG Fuhua, CHEN Jian, LI Ya, ZENG Zhiqiang, HOU Qingyang, DING Yong, LIU Shengli
(School of Chemistry and Chemical Engineering, Key Laboratory of Theoretical Chemistry and Molecular Simulation of Ministry of Education, Hunan Province College Key Laboratory of QSAR/QSPR, Hunan University of Science and Technology, Xiangtan 411201, China)

Abstract: Amphiphilic block copolymers PEG-*b*-P(St-*co*-VBC) with controllable molecular weight and low polydispersity were synthesized by one-step reversible addition-fragmentation transfer(RAFT). The structure and property of the synthesized amphiphilic copolymers were characterized by GPC, NMR, FT-IR and DSC. The results showed that the number of vinylbenzyl chloride (VBC) units in amphiphilic block copolymers PEG-*b*-P(St-*co*-VBC) can be well tuned by controlling the mole ratio of VBC and Styrene (St). Moreover, the glass transition temperature of PEG-*b*-P(St-*co*-VBC) is gradually increased with the addition of VBC units in block copolymers.

Key words: polyethylene glycol; reversible addition-fragmentation transfer; vinylbenzyl chloride; block copolymers

两亲性嵌段共聚物是由亲水段和亲油段组成,它能在水中自组装形成具有“核-壳”结构的纳米级胶束[1-2].因此,两亲性嵌段共聚物在功能型高分子材料研究方面及生物医药学等多重领域有着远大的发展前景,因而受到越来越多的广泛关注,该研究也得到了不断的发展与进步.两亲性嵌段共

收稿日期:2013-11-10
基金项目:国家自然科学基金资助项目(51003026,51373002);湖南省教育厅资助科研项目(12B041);湖南科技大学研究生创新基金资助项目(S120026);湖南省高校创新平台开放基金项目(09K082)
通信作者:陈建(1980-),男,湖南沅江人,博士,副教授,主要从事荧光功能聚合物材料研究. E-mail:cj0066@gmail.com

DOI:10.14133/j.cnki.1008-9357.2014.04.011

温度和 pH 双重敏感聚氨酯膜材料的制备及其性能

周 虎， 寻瑞平， 吴科建， 周智华， 余 斌， 唐友新
（湖南科技大学化学化工学院，理论有机化学与功能分子教育部重点实验室，湖南 湘潭 411201）

摘 要： 以 4，4'-二苯基甲烷二异氰酸酯（MDI）、聚己内酯二元醇（PCL）、*N*-甲基二乙醇胺（MDEA）等为主要原料，通过两步溶液聚合法和湿法转相技术成功制备了一种对温度和 pH 具有双重响应功能的聚氨酯膜材料。采用 FT-IR、DSC、SEM、水滴角测试仪、电子拉力机以及孔隙率和水通量测试对聚氨酯膜材料的结构和性能进行了表征。研究结果表明：MDEA 已经成功嵌入到了聚氨酯分子链中；4 种聚氨酯膜都显示了一个相似的结晶熔融峰，分别对应于各自的软段结晶熔融转变；聚氨酯膜截面呈现了皮层、指状大孔层和海绵状层的 3 层结构；随着易离子化基团（—N(CH_3)—）引入量的增加，聚氨酯膜的孔隙率增大，膜表面水接触角减小，力学性能降低；当温度从低温提高到各自的软段结晶熔融温度以上时，聚氨酯膜的水通量明显变大，显示了温度敏感性。当 pH 从 8.5 升高到 10 时，聚氨酯膜的水通量明显变大，显示了 pH 敏感性。

关键词： 聚氨酯；温度敏感性；pH 敏感性；结晶熔融；亲水性；水通量
中图分类号： TQ323.8 **文献标志码：** A **文章编号：** 1008-9357(2014)04-0419-07

Preparation and Properties of Temperature- and pH-Sensitive Polyurethane Membranes

ZHOU Hu, XUN Rui-ping, WU Ke-jian, ZHOU Zhi-hua, YU Bin, TANG You-xin
(Key Laboratory of Theoretical Organic Chemistry and Function Molecule of Ministry of Education, School of Chemistry and Chemical Engineering, Hunan University of Science and Technology, Xiangtan 411201, Hunan, China)

Abstract: Using crystalline polycaprolactone diols (PCL), 4, 4′-diphenylmethane diisocyanate (MDI), *N*-methyldiethanolamine (MDEA) as main raw materials, a new type of temperature- and pH-sensitive polyurethane (PU) membranes were prepared from a two-step solution polymerization and a wet phase inversion method. The structure and properties were characterized by FT-IR, DSC, SEM, water contact angle tester, mechanical tester, and measurements of porosity and water flux. Results showed that the MDEA was successfully embedded into the PU macromolecules. All four PU membranes had a similar crystalline melting transition in their soft segments. The section of PU membrane was composed of skin layer, finger-like pores layer and sponge-like structure layer. With the increasing of —N(CH_3)— group content, the porosity of PU membranes was increased, but the water contact angle and mechanical property of PU membranes were decreased. When temperature varied near the crystalline melting transition temperature, their water fluxes changed markedly, showing the temperature sensitivity. When the pH changed from 8.5 to 10, their water fluxes were also obviously changed, showing the pH sensitivity.

Key words: polyurethane; temperature sensitivity; pH sensitivity; crystalline melting; hydrophily; water flux

---

收稿日期：2014-07-21
基金项目：国家自然科学基金(51443002)；湖南省自然科学基金(14JJ5013)；湖南省教育厅青年项目(14B064)
作者简介：周 虎(1981-)，男，江苏徐州人，博士，副教授，研究方向为功能和智能高分子。E-mail：hnustchem@163.com